Kathrin Bretterebner BSc

# Bacteriophage Induction by Bacterial Genotoxicity and Promoter Identification in *Klebsiella spp.*

**MASTERARBEIT**

zur Erlangung des akademischen Grades
Master of Science

Masterstudium
Molekulare Mikrobiologie

eingereicht an der
**Technischen Universität Graz**

**Betreuerin**
Ao. Univ.-Prof. Dr. rer. nat. Ellen L. Zechner
Institute of Molecular Biosciences

Graz, November 2023

# Contents

# Abstract

*Klebsiella oxytoca* is a toxin-producing bacterium that inhabits the human gut as an opportunistic pathogen. Since the bacterium encodes a beta-lactamase it can lead to overgrowth during beta-lactam treatments which can result in antibiotic-associated hemorrhagic colitis (AAHC). The two toxins *K. oxytoca* produces, tilimycin and tilivalline, have been identified as small non-ribosomal peptides of the class of pyrrolobenzodiazepines. Tilivalline is known to disrupt the epithelial barrier integrity by inducing apoptotic cell death and tilimycin is a genotoxin that damages DNA and shows antimicrobial activity.

This study focuses on two topics involving the toxicity of *K. oxytoca.* The first part focuses on the effect of *K. oxytoca* on bacteriophages. Phages are omnipresent in the human gut and a common vector for antibiotic resistances to be transferred from one bacterial species to another. Bacterial toxins have been proven to induce phage releases [19]. The study showed that when treated with 85 µM tilimycin, *Escherichia coli* strains carrying phage λ showed reduced growth compared to a control strain carrying a non-inducible phage λ. To characterize the correlation between the toxin and phage release in depth, further studies must be done.

The second aspect of this work was focused on the pathogenicity island (PAI) of *K. oxytoca* which consists of the *aroX* and the NRPS operon. The two genes *aroX* and *npsA* are connected by a sequence that was suspected to have promoter activity. This study shows via fluorescence assays that both orientations of the promoter region show activity in both *E. coli* and *K. oxytoca*. This confirms that the sequence is a low-activity promoter region. It could also be shown that the *aroX* orientation has a higher promoter activity in *K. oxytoca* than the *npsA* orientation in *K. oxytoca.*

# Zusammenfassung

**Bakteriophagen Induktion durch bakterielle Genotoxizität und Promotor Identifizierung in *Klebsiella spp.***

*Klebsiella oxytoca* ist ein Toxin produzierendes Bakterium, das als opportunistisches Pathogen, den menschlichen Darm besiedelt. Das Bakterium trägt eine Ampicillin Resistenz, was zu einem übermäßigen Bewuchs während einer Beta-Lactam Therapie führen kann. Dies kann wiederum eine Antibiotika-assoziierte hämorrhagische Colitis (AAHC) verursachen. Die zwei Toxine, die von *K. oxytoca* produziert werden, Tilimycin und Tilivalline, sind kleine nicht-ribosomale Peptide, aus der Klasse der Pyrrolobenzodiazepine. Tilivalline verursacht apoptotischen Zelltod und zerstört damit die epitheliale Barriere des Darms und Tilimycin ist ein DNA schädigendes Genotoxin, das auch antimikrobiell wirkt.

Der Schwerpunkt dieser Studie liegt auf zwei Themen, die sich mit der Toxizität von *K. oxytoca* beschäftigen. Der erste Teil befasst sich mit der Auswirkung von *K. oxytoca* auf Bakteriophagen. Phagen sind ein allgegenwärtiger Faktor im menschlichen Darm und eine verbreitete Art Antibiotikaresistenzen von einem Bakterium auf ein anderes zu übertragen. Es wurde bereits gezeigt, dass bakterielle Toxine ein Auslöser für Phagen Freisetzung sein können [19]. Diese Arbeit konnte zeigen, dass bei einer Behandlung mit 85 µM Tilimycin, *Escherichia coli* Stämme, die den Phagen λ tragen, ein vermindertes Wachstum im Vergleich zu einem Stamm, der einen nicht-induzierbaren Phagen λ trägt, zeigen. Um den Zusammenhang zwischen Toxin und Phagen-Freisetzung besser zu verstehen, muss dieser noch weiter erforscht werden.

Der zweite Aspekt dieser Arbeit befasst sich mit der Pathogenitätsinsel (PI) von *K. oxytoca*, die aus dem AROX und NRPS Operons besteht. Die zwei Gene *aroX* und *npsA* sind durch eine Sequenz, in welcher Promotoraktivität vermutet wurde, miteinander verbunden. Diese Studie zeigt durch Fluoreszenzassays, dass beide Orientierungen dieser Sequenz in *E. coli* und in *K. oxytoca* Promotoraktivität vorweisen. Das bestätigt, dass diese Sequenz tatsächlich eine Promotorregion mit zwei schwachen Promotoren ist, wobei die *aroX* Ausrichtung in *K. oxytoca* eine stärkere Aktivität zeigt als die *npsA* Ausrichtung.

# Acknowledgements

I would like to thank Professor Dr. Ellen Zechner for allowing me to work on this interesting topic for my master's thesis and for always encouraging me to think critically.

Furthermore, I'm very thankful to Dr. Sabine Kienesberger-Feist, for always offering me great advice and being supportive and patient.

I would also like to thank Sandra Raffl for sharing her knowledge and teaching me important techniques in the lab.

Many thanks to Nina Fasching for being the best bench mate and making long lab days fun, as well as Amar Cosic, who always had motivating words for me and was always very helpful and supportive.

I would also like to thank my parents Bruni and Günter Bretterebner, my brother Martin Bretterebner, as well as my partner Michael Erhart for supporting me in every possible way and always believing in me.

# Introduction

## Bacteriophages

Bacteriophages, also known as phages, are viruses that infect bacteria and use bacterial cells to replicate. They have a vast diversity in size, genomic organization, and morphology [1,2]. Phages were first discovered in 1929 and are known to be the most abundant biological agent present in the environment [3,4]. They have an immense impact on bacterial communities, which can be either negative by killing them or positive by inducing horizontal gene transfer and therefore transferring antibiotic resistances for example.

There are two different forms of bacteriophages that show different life cycles within the cell. The lytic cycle is practiced in virulent phages, where the virus uses the cell and its components to generate a vast number of new bacteriophages which eventually kills the bacterial cell. The lysogenic cycle occurs in temperate phages, where the virus becomes a temporarily inactive prophage but can also be induced to go over into the lytic cycle (Figure 1).

Prophages are temporarily inactive forms of phages that are usually integrated into the bacterial genome, but they can also occur as an extrachromosomal structure. Most bacterial genomes contain prophages and different tools to detect them are available [5,6].

Prophages can be induced and therefore switched back to the lytic cycle. This happens in case of the occurrence of DNA damage which results in a SOS response within the cell [7]. Many bacterial toxins, e.g. cholera, diphtheria, and Shiga-toxin are encoded on temperate phages and can be transferred to different bacteria by them [8].

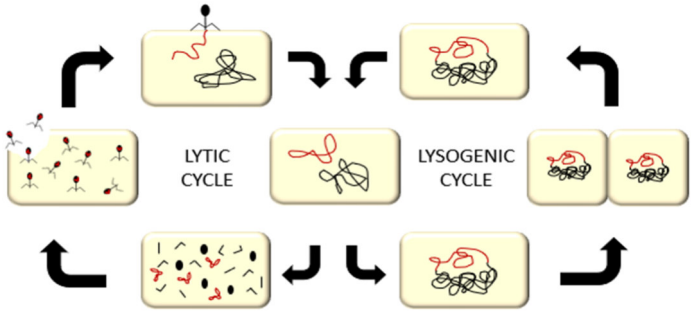


*Figure 1 The life cycles of temperate bacteriophages*

Temperate phages can occur in different life cycles. Usually after the infection, the phage DNA stays in the cell as a prophage. In this case, the bacteriophage DNA is integrated into the chromosomal genome. If the bacterial cells grow and divide the inactive prophage is spread throughout the population. In case of DNA damage, the prophages convert into the lytic cycle and use the bacterial cell to generate new infectious temperate phages.

## Bacteriophage λ

Phage λ was discovered in 1951 by Esther Lederberg when she observed that it was released by an *Escherichia coli* K-12 strain after its exposure to UV radiation [9]. Its DNA was one of the first models for researching the physical characteristics of DNA and genes. The genome has 48,5 kbp and lies within the head of the bacteriophage, which is called capsid, in linear form [10]. The capsid has an isometric, icosahedral structure and is placed on top of the tube fragment which forms the tail of the phage. The capsid and tail are connected via the portal protein B and tail terminator protein U. The tip of the tail is used for the infection of bacterial cells, and it also contains side tail fibers which are used to ensure a stable binding to the target. In the process of the infection, the tail tip protein J interacts with the bacterial porin LamB, which enables the injection of phage DNA. A negatively stained electron micrograph of a lambda virion can be seen in Figure 2.

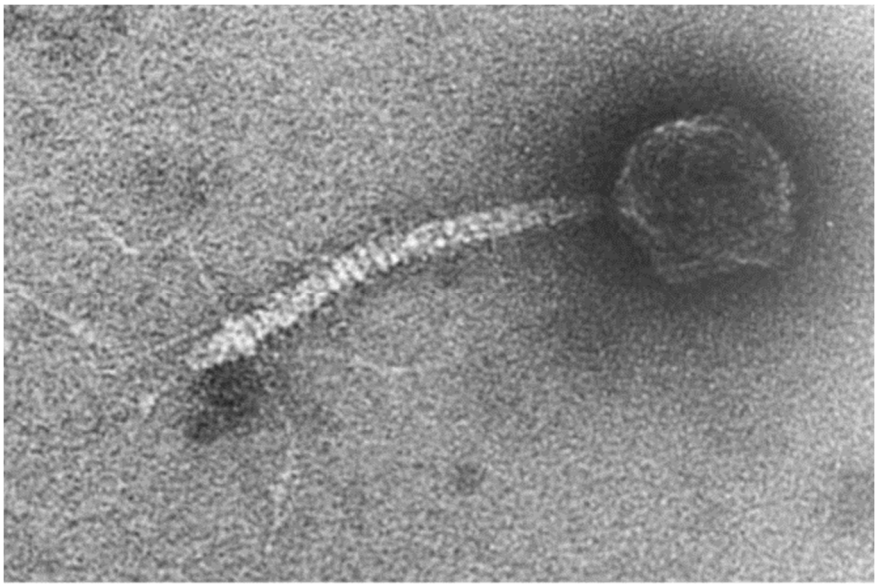

*Figure 2 Lambda virion [11]*

The negatively stained electron micrograph of the lambda virion shows the icosahedral, isometric structure of the capsid as well as the tube fragment of the tail. The tail tip and tail fibers can also be seen.

After the infection of the cell, the linear DNA circularizes within the cell at cos sites. The ends are ligated via the host DNA ligase. After the infection, the host RNA polymerase starts with the expression of the early genes. The early delayed genes follow and in combination with the early genes determine whether the phage starts a lytic or lysogenic cycle. The lytic cycle occurs with the expression of late genes and the lysogenic cycle occurs if the λ repressor (*cI*) is present. Once the phage DNA entered the lysogenic cycle the DNA is integrated into the genome and it stays there until the cell experiences stress i.e., DNA damage. In that instance, the prophage gets induced, and the lytic cycle begins.

## Prophages in the gut

A prophage is the form of a temperate phage that is integrated into the bacterial host genome. The prophage DNA can be beneficial to the host as it can encode antibiotic resistance. Bacteriophages therefore can transfer antibiotic resistances, which is especially critical within the gut. Not only does this apply to antibiotics but to toxins as well, as prophages encode the Shiga and cholera toxins for example which grant the infected population a selective advantage over other species, while affecting the human negatively. Prophages can also be beneficial to their host in other ways, for example prophages in *E. coli* carry genes like the *sitABCD* operon that encodes an iron transporter that actively improves the iron uptake of the host [12]. The persistence of a prophage in the genome can also avert infections of the bacterial carrier by another related phage [13]. The release of phage particles grants the host species a selective advantage over neighboring bacterial species [14,15].

Nevertheless, extreme prophage induction can take a toll on the fitness of the bacterial host. Lysogeny in λ only provides an advantage in the mouse gut if infectible bacteria are present. Without susceptible competitors, the prophage is detrimental to the host [15]. This means that a prophage can negatively affect both its host through phage release and other neighboring species as well. Prophages can even potentially affect the whole microbiome. Whole-virome analysis has shown, that human hosts with inflammatory bowel disease show specific changes to the virome and Crohn's disease patients show an increased number of temperate phages whereas healthy humans carry predominately a stable population of virulent phages (Figure 3) [16].

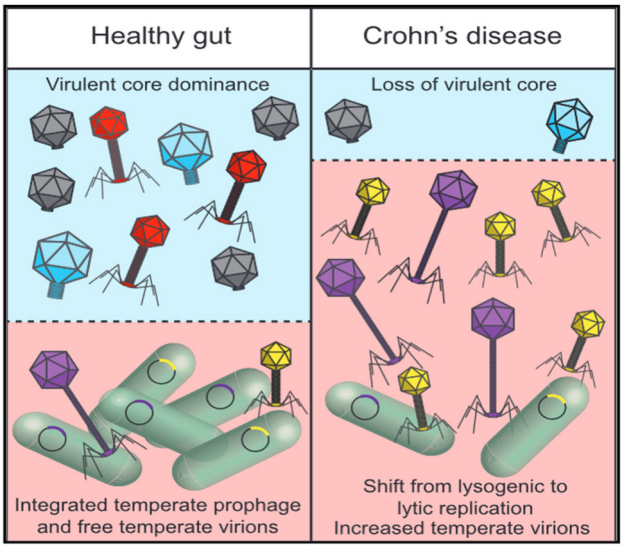


*Figure 3 Virome Shift in Crohn's disease patients [16]*

In human hosts with Crohn's disease the virome shows an increased number of temperate virions as opposed to the healthy virome which is dominated by virulent phages.

Prophages can be induced spontaneously or initiated by certain factors. One of the triggers can be an SOS response of the cell, which is caused by external factors, like reactive oxygen species, UV radiation, or even antibiotics like fluoroquinolones [7,17]. Those factors are DNA-damaging and therefore trigger the SOS response of the cell. The λ repressor cI is cleaved and therefore inactivated by RecA, which is a direct product of the SOS response [18].

Since bacterial toxins can have a DNA damaging effect, the question is, whether those toxins can trigger prophage induction in other bacterial species. It has been shown that this is the

case for colibactin, which is a genotoxin that is produced by various bacterial species of the gut microbiome [19,20]. Colibactin is an unstable molecule encoded on the *pks* gene cluster that triggers the bacterial SOS response (Figure 4), which induces the lytic cycle in bacteria that carry prophages [19].

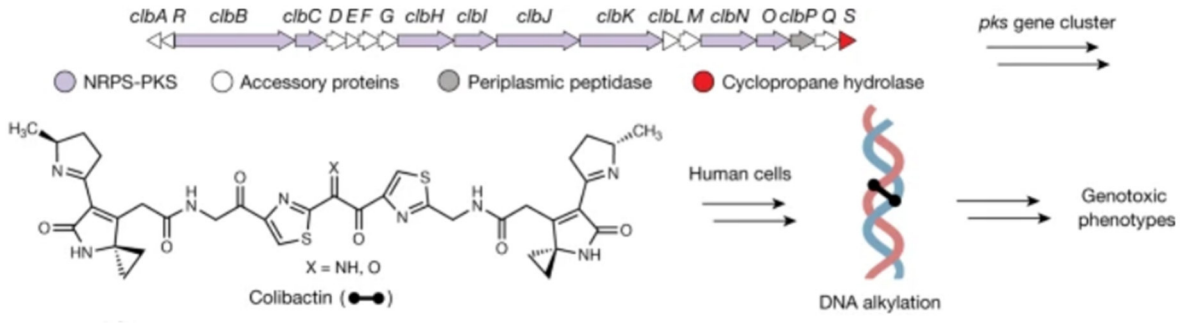


*Figure 4 Colibactin has DNA damaging properties [19]*

The *pks* gene cluster encodes the genotoxic molecule colibactin that is produced by various bacterial species. It has DNA-damaging properties as it leads to DNA alkylation when it reaches the cells of the human host. This leads to genotoxic phenotypes.

Bacteria that produce a colibactin resistance protein (ClbS) are protected from this process [19]. This means that the production of certain toxins in the gut not only influences the human host, by causing disease, but also alters the microbiome.

## Medical use of bacteriophages

Antibiotic resistances are on the rise in bacterial species and only a few backup antibiotic substances to treat multi-resistant strains are available [21]. The rate of resistance occurrence tops the rate of antibiotic detection and development by far and an estimate of up to 10 million people could die every year by bacterial infection with multi-resistant strains until the year 2050 [22].

Research is focusing on different ways to treat bacterial infections. Evolving as natural antagonists of bacteria, bacteriophages have returned to the focus [23]. The first successful studies using bacteriophages to treat bacterial infections were performed over 80 years ago [24, 25]. With the rise of antibiotics, phage therapy ceased to be further developed and was only used in certain parts of Eastern Europe [23]. The use of lytic phages to treat bacteria is convenient since they are self-amplifying and potentially kill cells more efficiently than antibiotics that cannot self-amplify [26]. There are various receptors on the bacterial cell for bacteriophage binding. Some phages bind to protein structures of the bacterium such as flagella [27], porins [28], pili [29], or efflux pumps [30].

In 1982 Smith and Huggins [31] were able to address many of the previously stated criticisms of phage therapy. They were able to show that phage effectiveness in vitro correlates with in vivo efficacy and they chose phage R for treatment which they identified as the bacteriophage with the greatest in vitro virulence [31]. They also showed that bacterial lysate, without phages, resulted in no therapeutic effect. In the same paper, they were able to show that one dose of phage R resulted in the same effectiveness as eight doses of streptomycin, which leads to the conclusion that phage therapy could potentially be more effective than chemical antibiotics [31]. Phage R however seems to have a limited host range as it only infects $K1^+$ *E. coli* and probably uses the K1 capsule as its receptor [31]. To combat the emergence of phage-resistant *E. coli* mutants they utilized a multi-phage approach, where they used a combination of lytic phages B44/1 and B44/3. The latter one was chosen for its capability to infect bacteria that were resistant to the first one [32]. In further examinations, which focused on the stability of orally administered phages, Smith and Huggins were able to show that administering calcium carbonate before the phage can combat the poor phage stability in the acidic stomach environment [33]. With the mentioned studies Smith and Huggins were able to eradicate certain criticisms of phage therapy and lay the foundations for new approaches to phage therapy.

One question that remains open is whether phage therapy will ever replace antibiotics. In theory, phage therapy has many advantages over chemical antibiotic therapy. Bacteriostatic antibiotics can enable the emergence of antibiotic resistance easily, as well as persistor cells that are genetically equivalent to wild-type strains but physiologically able to defy the antibiotics [34]. Another point is that common broad-spectrum antibiotics disrupt the natural balance of the microbiome, which can otherwise have a protective effect by occupying niche sites that hinder bacterial pathogens from inhabiting the body [35]. A distinct advantage of phage therapy is that it can be specific to species and single strains of bacteria, which means they can be used to selectively target and kill occurring pathogens [36]. Additionally, contrary to chemical antibiotics that must be continually administered, phages can self-amplify at the target site and will exit the body when the infectible bacteria are gone. While phage therapy is not immune to emerging resistances in bacteria [37], bacteriophages can co-evolve with the bacteria in an arms race which means the phage population can evolve to infect the resistant bacteria. This is not possible with chemical antibiotics. Phage therapy may be a better treatment of biofilms than common antibiotics [38]. However, this advantage varies with the target bacterium and the beneficial effect of phages in biofilm treatment calls for further research [39].

Even though phage therapy shows many advantages over common antibiotic treatment, phages still have limitations. Bacteriophages inhabit everything including the human microbiome, which means that neutralizing antibodies against phages may be an obstacle in phage therapy [26]. Another point is that antibiotics and their interactions with the human immune system have been studied for decades, as opposed to phage therapy, for which

research of this magnitude is yet to be performed [36,40]. Another point is that phages cannot be used to treat all infections. Antibiotics can be used to treat intracellular bacterial pathogens; phages however do not have a dependable entry mechanism into eukaryotic cells [26].

Since both phage therapy and antibiotic therapy have strengths and weaknesses, a combination of both will likely be the best path to take. A perfect example is a combination treatment of phage and antibiotics, which has been proven effective in the past to treat a *K. pneumoniae* biofilm [41]

## The human microbiome

It is estimated that the microbiota that inhabits the human body reach a 10-fold higher number than human germ and somatic cells [42]. Research of the human microbiome has been of scientific interest since the first half of the 20$^{th}$ century when the studies consisted of culture-based surveys of the oral cavity of periodontitis simplex patients [43]. However, it was the Human Microbiome Project that took a big step in characterizing the microbes of a healthy human body and they did so at five major sites, including the gastrointestinal tract, via 26S and metagenomic shotgun sequencing [42]. The main goal of the Human Microbiome project was to distinguish the factors that impact the composition and evolution of the microbiome as well as identify the organisms that make up the microbiota [42]. Metagenomic analysis and bioinformatics are the keys to further categorize and characterize the microorganisms native to the human organism.

### Colonization of the human gut

The human gut microbiota forms a vital component of human health. The microbiome not only consists of different bacterial species but also eukaryotes, archaea, and bacteriophages [44]. The colonization of the human gut influences the host's health through their entire life span. Factors such as the delivery mode, diet, hospitalization and prematurity, antibiotic use, and even the presence of older siblings influence the colonization and diversity of a baby's microbiome. For example, neonates born via cesarean section have lower numbers of bifidobacterial and *Bacteroides* than vaginally born infants, and formula-fed babies showed colonization with *E. coli, C. difficile, Bacteroides,* and lactobacilli more often than breastfed infants. The use of antibiotics leads to fewer bifidobacteria and *Bacteroides* in the infants and babies with older siblings showed an increased number of bifidobacteria, in comparison to infants without any siblings [45].

## Dysbiosis of the human gut

Dysbiosis can be defined as a disrupted microbiome, which is characterized by a reduction in diversity of microbiota and a decrease in beneficial microbiota. Dysbiosis of the gut microbiome can occur through the oral use of drugs such as antibiotics i.e., azithromycin [46], non-steroidal anti-inflammatory drugs i.e., aspirin [47], or proton pump inhibitors [48]. It has also been shown that chemotherapy negatively alters the gut microbiome and induces dysbiosis [49]. The other way around it has been shown that a lack in bacterial species abundance within the microbiome heavily relates to the occurrence of diseases like ulcerative colitis or Crohn's disease [50]. However, the species abundance of the gut microbiome is not only a necessity for gut health, as it also influences other diseases in the human body for example asthma [51], allergic airway disease [52], Parkinson's disease, and depression [53].

Another example of how gut dysbiosis can impact the whole human body is obesity. In mice, a high-fat diet reduces the gut microbiota diversity, while a high-sucrose diet modifies the bacterial composition related to obesity. It has been shown that probiotics supplementation can improve gut microbiome dysbiosis and slow down weight gain in mice fed with high-fat and high-sucrose diets. The reduction of diet-induced obesity using probiotics could especially be seen in high-sucrose diet-induced obesity [54]. Since gut dysbiosis is linked to so many diseases, the treatment of dysbiosis is potentially a way to treat the disease itself. Probiotics have been shown to reduce the development of Alzheimer's disease in transgenic mice [55]. Another way of treating microbiome dysbiosis in the gut is fecal microbiota transplantation. The transplantation of fecal matter containing healthy gut microbiota into a patient's gastrointestinal tract has been successfully used for the treatment of ulcerative colitis [56].

## *Klebsiella oxytoca*

*Klebsiella oxytoca* is a gram-negative, non-motile rod-shaped bacterium that acts as an opportunistic pathogen. It is a member of the family Enterobacteriaceae and lives as a facultative anaerobe. In an oxygen-free environment, the bacterium can ferment glucose and fixate atmospheric nitrogen [57]. As a part of the *Klebsiella* genus *K. oxytoca*, like *Klebsiella pneumoniae*, is pervasive in various habitats not only in the environment for example in soil and water but can also be detected on parts of the human body, like skin, mucosal surfaces, and gut. *Klebsiella spp.* are known to cause nosocomial infections, like urinary tract infections, pneumonia, wound infections, or septicemia. In the US and Europe about 8 % of nosocomial bacterial infections are due to *Klebsiella spp.* where most of the infections are caused by *K. pneumoniae* and some, at a much lesser degree caused by *K. oxytoca* [58].

*Klebsiella* spp. Express various virulence factors, such as the polysaccharide capsule that protects the bacterial cells from phagocytosis by leucocytes [59]. The capsule also protects from bactericidal serum factors. As it is common in gram-negative bacteria, *Klebsiella spp.* produce type 1 and type 3 fimbriae to enable initial attachment to host surfaces [58].

*K. oxytoca* among other *Klebsiellae* can form biofilms [60]. An essential pathogenicity factor in all *Klebsiella spp.* is the expression of β-lactamases, which grant resistance to carboxypenicillins and aminopenicillins [61]. In addition to penicillin resistant *Klebsiella* spp., multidrug-resistant strains, that express extended spectrum β-lactamases (ESBL), have emerged [58]. The increase of ESBL-producing strains amongst clinical *Klebsiella* isolates results in limitations of therapeutic options to manage the occurring hospital infections. While running out of therapeutic methods, Klebsiella pathogenicity factors like lipopolysaccharides or capsules are considered targets for the development of vaccinations to gain immunological infection control [58].

## Antibiotic-associated hemorrhagic colitis (AAHC)

In the case of dysbiosis in the human intestine (e.g. caused by antibiotics) an overgrowth of *K. oxytoca* occurs which can lead to Antibiotic-associated hemorrhagic colitis. antibiotic-associated hemorrhagic colitis (AAHC) is a special form of antibiotic-associated colitis (AAC). Other than AAC, which is usually caused by *Clostridium difficile* after antibiotic treatment, AAHC is caused by *Klebsiella oxytoca* [62,63]. Patients with AAHC show symptoms of bloody diarrhea and abdominal pain after receiving antibiotic treatment and often require hospitalization. The characteristics of AAHC are mucosal hemorrhage and mucosal edema, typically affecting the ascending colon as well as the cecum [63]. The causative agents behind the symptoms of AAHC are the cytotoxins produced *by K. oxytoca* tilimycin (TM) and tilivalline (TV) [64,65,66].

TM can be produced by pathogenic *K. oxytoca* strains in the human intestine and spontaneously reacts to TV in the presence of indole [67]. This reaction including the structures can be seen in Figure 5. TM is a DNA-damaging agent and has specific target bases for DNA alkylation. The diazepine ring in its structure interacts with the minor groove of the DNA and therefore stabilizes the double strand [68].

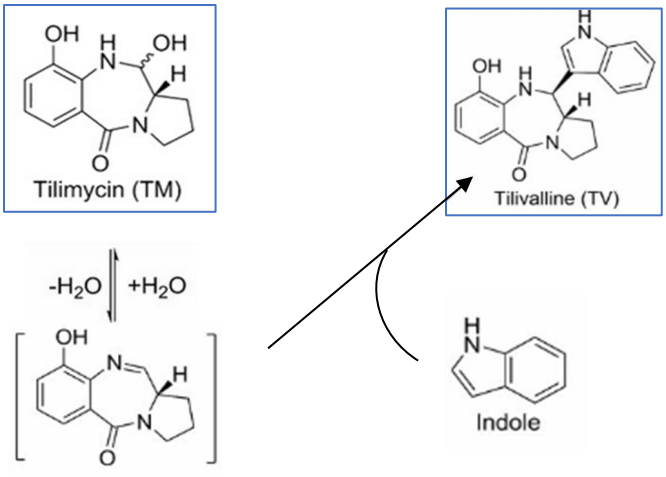


*Figure 5 Tilivalline Synthesis from tilimycin and indole*
Tilimycin, which can be produced by toxin-producing *K. oxytoca* strains, reacts to tilivalline spontaneously in the presence of indole in the human gut. Modified from [67].

Stool samples of patients with active AAHC show *K. oxytoca* in vast amounts of over $10^6$ CFU/ml [69]. The stool of AAHC patients contains both enterotoxins during the active phase [66]. The fecal content of patients carrying *K. oxytoca* without symptoms exhibit amounts of $10^2$ CFU/g [66]. Examining the stool of one AAHC patient showed that after 3 days TM and TV could still be detected in stool samples whereas after 5 days the toxins could no longer be detected. At this point, the presence of K. oxytoca in the stool was also reduced to $10^4$ cfu/g [66]. This only represented one patient and cannot universally be applied to all AAHC patients.

Since the incidence of AAHC is minimal, the number of samples from patients, which are available for studies is very low. In a murine disease model, the relevant concentrations of TM and TV for the active phase of AAHC could be determined. TM showed a higher concentration of 136 ± 40 nmol/g feces whereas TV measured a concentration of 19 ± 6 pmol/g feces [66]. Since the abundance of *K. oxytoca* in the fecal samples of the murine model is much higher than in human patients ($10^{10}$ cfu/g), the enterotoxin concentrations to cause AAHC in humans are expected to be lower [66].

## Necrotizing Enterocolitis (NEC)

Necrotizing Enterocolitis (NEC) is a disease that has been observed in preterm infants since their treatment in neonatal intensive care units (NICU) began. The inflammatory disease of the gut is characterized by abdominal distension, bloody stool, and bilious vomiting [70]. Preterm infants with NEC with a very low birth weight show a mortality rate of 10-30% and preterm infants with an extremely low birth weight (<1000 g) even show a mortality rate between 30 and 50%. Surviving infants are at a higher risk of morbidity, like short bowel syndrome [71]. Other complications that can occur at increased risk include microcephaly and neurodevelopmental impairment as well as delays in mental development and psychomotor development [72,73]. It has been shown that infants receiving initial empirical antibiotic

treatment for an extended time are at greater risk of experiencing NEC [74]. However, breastfeeding infants has proven to reduce the risk of infection [75]. Probiotics have shown the capacity to prevent NEC, however, their efficiency is chiefly observed in infants with a birth weight of >1000 g, whereas birthweights <1000 g are the ones more likely to develop NEC [76].

In recent years NEC has been associated with cytotoxin-producing *K. oxytoca* since the species has been detected in affected patients' stool samples using next-generation 16S rRNA sequencing in combination with a specialized system to select for *K. oxytoca* [77]. The system comprised selective and differential culturing in combination with PCR. The cultures made with the isolates that were retrieved from the patients showed the presence of the toxins TM and TV. Toxin-producing *K oxytoca* strains could be isolated from 6 out of 10 patients suffering from NEC from two different NICUs [77]. The presence of toxin-producers could also be confirmed in healthy individuals, however at a lower abundance. It has been proposed that an outgrowth of *K. oxytoca* might cause NEC however it may have been overlooked by previous detection methods since 16S sequencing is not sufficient to identify the pathobiont indefinitely and a combination of other identification methods is needed [77].

Even though NEC is one of the leading causes of death in newborns [78], the pathogenesis of the disease is not completely understood, and further studies are needed.

## Pathogenicity of *Klebsiella oxytoca*

Toxin-producing *K. oxytoca* strains have genetic elements that are specific to them. The genes that are responsible for toxin production are organized within a pathogenicity island (PAI) and were characterized by Schneditz *et al*. [65]. They discovered four toxin-deficient mutants which grew normally compared to the clinical AAHC isolate AHC-6 which was their wild-type strain. They identified the genes as *aroX* which encodes a 2-keto-3-deoxy-D-arabino-heptulosonate-7-phosphate (DAHP) synthase, *npsA*, and *npsB* which are nonribosomal peptide synthetase (NRPS) genes and *aroB* which is a 3-dehydroquinate-synthase gene [65]. They also showed that *npsA* and *npsB* are part of an operon and both gene products are necessary for toxin production. Three of the four genes are clustered in a 7 kb region on the genome. The region is flanked by asparagine tRNA genes (Figure 6). The location of the gene cluster is in a high-plasticity locus in the core genome which characteristically holds mobile DNA elements. Those factors suggest that the identified toxin genes are part of a PAI. Since the *aroB* gene has a role in the general metabolism with an essential role in the shikimate pathway, it is not found within the PAI [65,79].

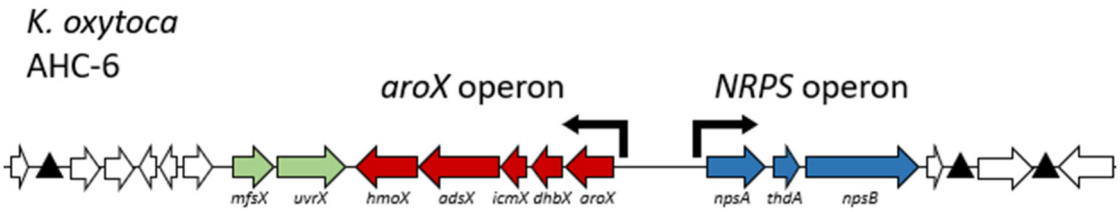


*Figure 6 Pathogenicity Island of Klebsiella oxytoca AHC-6*
The toxin-producing gene cluster of *K. oxytoca* contains the *arox* operon and the NPRS operon. The two operons are connected by a sequence that potentially holds a promoter function in both operon orientations. The figure was modified from [65].

The product of the gene cluster on the PAI encodes a nonribosomal peptide with a similar pathway to pyrrolobenzodiazepine production in actinomycetes. First, only tilivalline (TV) was identified as a *K. oxytoca* toxin. TV induces apoptotic cell death and disrupts the epithelial barrier integrity in cultured human cells in vitro, which aligns with *K. oxytoca* pathogenicity symptoms observed in human AAHC [66]. However, Dornisch *et al.* [67] were able to show that the toxin gene cluster delivers three secondary metabolites, out of which two are cytotoxic. They discovered that TV is not a direct product of the nonribosomal peptide synthetase. The product is an N-acylprolial, which reacts spontaneously to two other secondary metabolites, one of them being tilimycin (TM) and the other one being culdesacin [67]. In the presence of indole, TM reacts to TV (Figure 5). Both TM and TV are known to be cytotoxic to human cells. Culdesacin however has no apparent bioactivity [67].

TM is a genotoxin and causes cellular DNA damage in vitro as well as in vivo but contrary to TV, TM also shows antibacterial activity [67]. Knowing that TM influences bacteria, the question that formed was how this affects the other bacterial species in the gut when produced by *K. oxytoca* inside the human gut. Kienesberger *et al.* [80] were able to show via mouse model that TM alters the diversity of the gut microbiome. They also showed that TM introduces mutations into other bacteria. They monitored the appearance of rifampicin-resistant *E. coli* B13Sm colonies, which developed at a higher rate in mice that were co-colonized with toxin-producing *K. oxytoca* AHC-6 compared to a mutant non-producer strain [80]. This means that toxin-producing *K. oxytoca* can alter the gut microbiota and enable the appearance of mutations in present opportunistic pathogens. [80]. This is especially important in children since carriage rates for *K. oxytoca* in infants delivered vaginally are at 9 % and in cesarian sections at 20 % in the UK [81].

## Gene Expression and Regulation

Gene expression is defined as the procedure in which the information contained in a gene is used to form RNA molecules that are used to generate proteins or non-coding RNA molecules that have different cellular functions. Gene expression is thoroughly regulated and adapted to changing conditions. Location, point in time, and quantity of an expressed gene can be determined by tracking the functional activity of the gene's product or by monitoring a certain phenotype that correlates with the gene. [82]. For this study, we tracked the production of GFP (gene's product) to assess whether the region we cloned upstream of the *gfp* gene is a functional promoter.

Gene regulation, the molecular control mechanism of gene expression, defines whether, how, and when a gene is expressed [83]. There are intra and extracellular triggers of gene expression. Regulators can be programmed within the cell or occur as a reaction to a change in environment, i.e., cell stress. Within the cell, there are different checkpoints at which regulation can occur. These points can be on DNA, RNA, or protein level. Basic components of gene regulation within the cell are short DNA sections with a defined sequence and regulatory proteins that can identify and bind those sequences. Gene regulation is one of the essential steps that a cell needs to be able to generate transcripts that are used to create proteins. As it is a fundamental function of the cellular mechanism, a vast amount of the cell's energy is used for gene regulation. The cellular genome might consist largely of sequences to regulate so that the cell will respond appropriately in case of stress or repair [83].

Genes in prokaryotic cells are organized in operons. Those operons are DNA sequences that usually contain an operator and various structural genes that are controlled by a promoter. The operon model was proposed by the French scientists Jacob and Monod in 1960 [84]. One operon that is used in genetic research frequently and was also the first operon to be described is the lactose operon or short lac operon [85]. It consists of the structural genes *lacZ, lacY,* and *lacA* as well as the lac operator and lac promoter. The operator allows the lac operon to bind the lac repressor and is located downstream of the promoter and upstream of the structural genes (Figure 7). The lac operon contains three operators that result in the formation of a loop in case of a repressor binding, which causes an active closure of the regulated region including the promoter. The promoter sequence is located upstream of the operator and the structural genes and in the absence of repression it allows the RNA polymerase to bind and initiate transcription. The *lacI* gene that encodes the lac repressor is located upstream of the promoter. The lac repressor is not part of the operon.

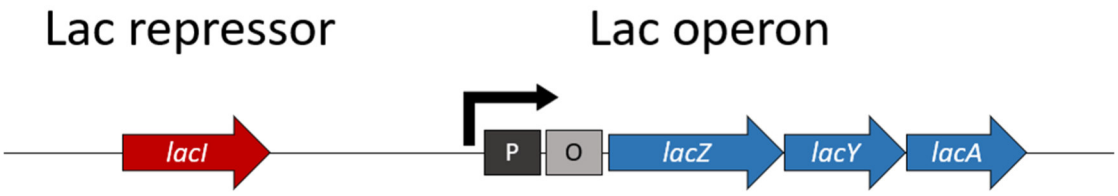


*Figure 7 Lac operon and lac repressor*

The lac operon consists of a promoter (P) an operator (O) and the three structural genes *lacZ, lacY,* and *lacA.* The lac repressor gene *lacI* is located upstream of the lac operon and is not an active part of the operon.

Since promoters are essential for the initiation and transcription of genes, current bioinformatics is focusing on generating tools to accurately identify and predict promoters in prokaryotes as well as eukaryotes [86].

## Green Fluorescent Protein as a Reporter

Green fluorescent protein (GFP) from jellyfish is a stable fluorescent reporter which is a staple in cloning and tagging. After its discovery it became popular as a reporter for gene expression and protein localization in *Caenorhabditis elegans* because the transparency of the worm enables the tracking of in vivo dynamics [87]. However, GFP is also a popular tool used in bacteria, as it is a reporter for the identification of promoters. For this the supposed promoter region is cloned upstream of the *GFP* gene and if GFP shows a signal under the specific conditions tested, the cloned region is a promoter [88]. The intensity of the GFP signal also gives insight into whether the sequence contains a strong or a weak promoter.

Using GFP as a reporter for promoter activity is limited to being able to tell if the promoter is on or not. Since GFP is a stable molecule there is no signal as to whether the promoter is turned off again. For gaining this data a different reporter system with a less stable reporter must be used for example the lux reporter system which is based on the oxidation of an aldehyde substrate that is catalyzed by the bacterial luciferase enzyme.

## Aim and Hypothesis

The thesis is split into two major projects. One aspect of this work focuses on the hypothesis that if tilimycin causes a DNA damage SOS stress response in *E. coli* it will result in prophage induction in vitro and in vivo. To test this hypothesis the goal was to establish a system using phage λ that can be used in in vitro and in the mouse model. To achieve this the *E. coli* strains carrying phage λ that we received from De Paepe *et al*. [15] had to be tested in cocultivation with *K. oxytoca* and pure tilimycin at a concentration that has previously been shown to influence bacteria (85 µM). Additionally, an ampicillin resistance had to be introduced into the

*E. coli* strains, so they could be used in cocultivation with ampicillin-resistant *K. oxytoca* in the murine model.

For the second part of the thesis, the focus lies on the PAI which all toxin-producing *K. oxytoca* strains have in common [89]. The aim was to characterize the region between the *aroX* and *npsA* genes and to potentially identify the region as a promoter region. To execute this, the potential promoter region was amplified and cloned in both orientations upstream of a *gfp* gene located on a cloning vector and tested in different bacterial strains. This work hypothesizes that if the region on the PAI of *K. oxytoca* is a promoter region the *gfp* gene downstream of the sequence in both orientations will be transcribed and this will result in a fluorescence signal.

# Material & Methods

## Strains, Plasmids and Oligonucleotides

For this study the following bacterial strains were used (Table 1).

**Table 1 Bacterial strains used in this study**, with relevant description and number (#IMB) in the AG Zechner Strain Collection Database

| # | Strain | Description | Plasmid | #IMB | Reference |
|---|---|---|---|---|---|
| 1 | *Klebsiella oxytoca* AHC6 | Isolated from stool of AAHC patient (acute phase), AmpR | | 2042 | Database AG Zechner [63] |
| 2 | *Klebsiella oxytoca* AHC6 Mut89 | AmpR, KanR, npsB::Tn5 | | 2043 | Database AG Zechner [65] |
| 3 | *Escherichia coli* DH5α | Cloning strain | | 37 | Database AG Zechner |
| 4 | *Escherichia coli* MG1655 | K12 strain | | 1440 | Database AG Zechner |
| 5 | *Klebsiella oxytoca* AHC6 Δ*tnaA* | ΔtrpA, AmpR, TetR | | 2127 | Database AG Zechner |
| 6 | *Escherichia coli* Top 10 | Cloning strain | | 1414 | Database AG Zechner |
| 7 | *Escherichia coli* DH5α | AmpR | pBluescript-II-KS(-) | 1085 | Database AG Zechner |
| 8 | *Escherichia coli* DH5α | CmR | pAR181_gfpmut3b | 2263 | Database AG Zechner |
| 9 | *Escherichia coli* DH5α | CmR | pAR181_PrnpsA _gfpmut3b | 2273 | Database AG Zechner |
| 10 | *Escherichia coli* DH5α | CmR | pAR181_PraroX _gfpmut3b | 2275 | Database AG Zechner |
| 11 | *Klebsiella oxytoca* AHC6 | AmpR, CmR | pAR181_gfpmut3b | 2060 | Database AG Zechner |
| 12 | *Escherichia coli* E239 | CmR, TetR | pACYC184 | 980 | Database AG Zechner |

| | | | | | |
|---|---|---|---|---|---|
| 13 | *Escherichia coli* MS614 | KmR, TetR | pAR183 | 935 | Database AG Zechner |
| 14 | *Escherichia coli* DH5α | AmpR, TetR | pBlue_A_TetRA_mono | 2024 | Database AG Zechner |
| 15 | *Escherichia coli* DH5α | AmpR | pKD46 | 1700 | Database AG Zechner |
| 16 | *Escherichia coli* DH5α | TetR | pKD46-tet | 2291 | Database AG Zechner |
| 17 | *Escherichia coli* XL1 | TetR, AmpR | pBR322 | 862 | Microbiology strain collection |
| 18 | *Escherichia coli* MD5 | MG1655 Δ*fliC* Δ*ompF hsdR::KanR* | | 2258 | De Paepe *et al.* [15] |
| 19 | *Escherichia coli* MD6 | MG1655 Δ*fliC* Δ*ompF stfR::cat (*λ *ble)* | | 2259 | De Paepe *et al.* [15] |
| 20 | *Escherichia coli* MD47 | MG1655 Δ*fliC* Δ*ompF lamB*::KanR | | 2260 | De Paepe *et al.* [15] |
| 21 | *Escherichia coli* MD56 | MG1655 Δ*fliC* Δ*ompF lamB*::FRT *stfR::cat* (λ *ble*) | | 2261 | De Paepe *et al.* [15] |
| 22 | *Escherichia coli* MD74 | MG1655 Δ*fliC* Δ*ompF lamB*::FRT *stfR::cat* (λ *ble* $cI^{ind-}$) | | 2262 | De Paepe *et al.* [15] |

*E. coli* MG1655 and *K. oxytoca* AHC6 as well as *K. oxytoca* AHC6 Δ*tnaA* were transformed with the plasmids pAR181_gfpmut3b, pAR181_PrnpsA _gfpmut3b, pAR181_PraroX _gfpmut3b and pACYC184 and subsequently used for assays of this study. Due to the limited amount of storage and the relatively easy procedure to transform the strains anew with the plasmids if needed in the future, not all of them were frozen and stored in the strain collection. However, the relevant plasmids were stored in the plasmid collection as documented below.

The following plasmids were used for this study (Table 2).

**Table 2 Plasmids used in this study,** with relevant description and number (#IMB) in the AG Zechner Plasmid Collection Database

| # | Plasmid | Description | #IMB | Reference |
|---|---|---|---|---|
| 1 | pAR181_gfpmut3b | CmR, p15A, gfpmut3b, pACYC184 backbone | 1129 | Database AG Zechner E. Dornisch |
| 2 | pAR181_PrnpsA _gfpmut3b | CmR, p15A, gfpmut3b, *npsA* oriented promoter, pACYC184 backbone | 1192 | This study |
| 3 | pAR181_PraroX _gfpmut3b | CmR, p15A, gfpmut3b, *aroX* oriented promoter, pACYC184 backbone | 1194 | This study |
| 4 | pKD46 | AmpR | 220 | Database AG Zechner |
| 5 | pKD46-tet | TetR | 1207 | This study |
| 6 | pAR183 | TetR, KmR, R1 backbone | 217 | Database AG Zechner A. Reisner |
| 7 | pACYC184 | CmR, TetR | 375 | Database AG Zechner |
| 8 | pBluescript-II-KS(-) | AmpR | 454 | Database AG Zechner |
| 9 | pBlue_A_TetRA_mono | AmpR, TetR | 1110 | Database AG Zechner M. Hiesinger |
| 10 | pBR322 | AmpR, TetR | - | Microbiology strain collection |

The following two bacteriophage strains were used in this study (Table 3).

**Table 3 Bacteriophage strains used in this study,** with relevant description

| # | Bacteriophages | Description | #IMB | Reference |
|---|---|---|---|---|
| 1 | λ *ble* (WT) | Urλ, BleR | - | De Paepe *et al.* [15] |
| 2 | λ $cI^{ind-}$ | Urλ, *cIA111T,* BleR | - | De Paepe *et al.* [15] |

For this study the following oligonucleotides were used. Underlined nucleotides indicate complementary sequences to the target and bold sequences are target sequences for restriction enzymes or homologous regions for the λ RED recombination (Table 4).

**Table 4 Oligonucleotides used in this study,** with number (#IMB) in the AG Zechner Oligonucleotide Collection Database, underlined nucleotides indicate complementary sequences to the template, bold nucleotides mark the sequences of restriction enzymes or homologous overhangs for the λ RED recombination.

| # | Oligonucleotide | Sequenz (5'-3') | Position* | Template | #IMB |
|---|---|---|---|---|---|
| 1 | PrnpsA_SacI | TTA**GAGCTC**TTCTAATCTCTCACTC GAAATTTAACAG | -1 .. -28 | *npsA* promoter region (AHC6) | 2644 |

| | | | | | |
|---|---|---|---|---|---|
| 2 | PrnpsA_SphI | TAT**GCATGC**CACTCTCTCCTGGAGAATTAGG | -436 .. -457 | *npsA* promoter region (AHC6) | 2645 |
| 3 | PraroX_SphI | TAT**GCATGC**TTCTAATCTCTCACTCGAAATTTAACAG | -430 .. -457 | *aroX* promoter region (AHC6) | 2646 |
| 4 | PraroX_SacI | TTA**GAGCTC**CACTCTCTCCTGGAGAATTAGG | -1 .. -22 | *aroX* promoter region (AHC-6) | 2647 |
| 5 | Seq_Prom_gfp_fw | ATAACCTTCGGGCATGGCACTCT | 254 .. 276 | gfpmut3b (pAR181_gfpmut3b) | 2073 |
| 6 | Pms5 | TATAGTCCTGTCGGGTTTCGCCAC | 191 .. 214 | Ori(p15a) (pAR181_gfpmut3b) | 862 |
| 7 | PvuI-tetfw | TAT**CGATCG**CAAGAATTGCCGGCGGATC | 682 .. 705 | *tetRA* (R) | 2648 |
| 8 | PvuI-tetrev | ATA**CGATCG**GGTATTTCACACCGCATAGC | 1284 .. 1308 | *tetRA* (A) | 2649 |
| 9 | 1_StfR_down_homol_P_AmpR | **TGGCCTTTGTTGATGCCGTTCCTGCGCTGGAAGACGCTGACTGAGCCGACG**TACATTCAAATATGTATCCGCTC | -52 .. -74 | *bla* (pBluescript-II-KS(-)) | 2659 |
| 10 | 2_StfR_homol_AmpR_stop_AmpR | **GGAAGGATTCCCGCCGTCACATGCCGGGACCATTACCGTGTATGAAGATTC**TTACCAATGCTTAATCAGTGAGG | 839 .. 861 | *bla* (pBluescript-II-KS(-)) | 2660 |
| 11 | 3_hsdR_down_homol_P_AmpR | **CTTTAGTGACCAGACGGTAGTACCAGACAGCCAGGCGGAACCCGAGTCGC**TACATTCAAATATGTATCCGCTC | -52 .. -74 | *bla* (pBluescript-II-KS(-)) | 2661 |
| 12 | 4_hsdR_up_homol_stop_AmpR | **TGACAACATCCTCTCTGTATTTCACAAATTACGCCGCATTGGTAACCAG**GTTACCAATGCTTAATCAGTGAGG | 839 .. 862 | *bla* (pBluescript-II-KS(-)) | 2662 |
| 13 | TetR seq1 | CTTATTCGGCCTTGAATTG | 561 .. 579 | *tetRA* (R) (pKD46-tet) | 2411 |
| 14 | check1 | CTAAATACATTCAAATATG | -61 .. -79 | *bla* (pKD46) | 1988 |
| 15 | pT18agowa4 | ATGATACCGCGAGACCCACG | 712 .. 731 | *bla* (pKD46) | 2000 |
| 16 | Ftet | AT**CGATCG**TTCTCATGTTTGACAGCTTATC | -64 .. -85 | *tetR* (pBR322) | 2676 |
| 17 | Rtet | AT**CGATCG**TCAGGTCGAGGTGGCCCGGCT | 1171 .. 1191 | *tetR* | 2677 |

| | | | | | |
|---|---|---|---|---|---|
| | | | | (pBR322) | |
| 18 | T7 promotor primer | TAATACGACTCACTATAGGG | 172 .. 191 | *lacZ* | 910 |
| 19 | lacPromotorprimer | TTTACACTTTATGCTTCCGGCTCG | -51 .. -74 | *lacZ* | 1972 |
| 20 | Pms7 | ATGGAGGCGGATAAAGTTGCAGG | 625 .. 647 | *bla* | 864 |
| 21 | stfR_fw | TCAGTACAGCGTTATTCTGTTGGT | 168 .. 191 | *stfR* (MG1655) | 2686 |
| 22 | sftR_rv | GCGGCAGCACTTTTTGATGCTTCA | 543 .. 566 | *stfR* (MG1655) | 2687 |
| 23 | hsdR_fw | ACCTACCGTACCGCGGTTATCGAC | 1963 .. 1986 | *hsdR* (MG1655) | 2688 |
| 24 | hsdR_rev | CACTTTGCGCGCGTCTTTATCGGC | 2353 .. 2376 | *hsdR* (MG1655) | 2689 |

*relative to open reading frame

## In Silico Cloning

All in silico cloning was done using SnapGene 6.0.4. Vector maps were made using SnapGene 6.0.4. The remaining graphics were made with Microsoft PowerPoint. Graphs and diagrams were made with Graphpad Prism.

## Growth Conditions

*E. coli* strains were grown in LB broth or on LB agar plates (Table 5). *K. oxytoca* strains were cultured in CASO bouillon or on CASO agar plates. The *E. coli* strains containing the thermosensitive plasmid pKD46 and pKD46-tet were incubated at 30°C while all other strains were incubated at 37°C. Liquid cultures were incubated under aerobic conditions while shaking at 180 rpm. Bacterial strains that were carrying plasmids or other selection markers were grown under the respective conditions with the needed antibiotics at fixed concentrations (*Table 6*).

**Table 5 LB broth and agar recipe used in this study**

| LB medium/ agar | | Final volume |
|---|---|---|
| Bacto™ Tryptone | 10 g | 1000 ml |
| Yeast Extract | 5 g | |
| NaCl | 5 g | |
| Agar | 15 g | |

For the CASO medium 30 g of CASO bouillon powder from Carl Roth were used for 1000 ml medium and for CASO agar 40 g of CASO agar powder from Carl Roth were used for 1000 ml agar.

**Table 6 Concentrations of Antibiotics used in this study**

| Antibiotics | Concentration [µg/ml] |
|---|---|
| Chloramphenicol (Cm) | 10 (*E. coli)* / 20 (*K. oxytoca)* |
| Ampicillin (Amp) | 100 |
| Tetracycline (Tet) | 15 |

The tilimycin concentration used in the experiments was 85 µM and Glucose was used at a concentration of 0.25 g/L.

# DNA Methods

## Polymerase Chain Reaction (PCR)

To amplify the DNA fragments required for cloning Phusion High-Fidelity Polymerase by NEB was used according to the company's protocol. For control PCRs the Taq DNA Polymerase by NEB was used. The PCR was done in a BIORAD thermocycler. For colony PCR a single colony was suspended in 30 µl of dd$H_2O$ and lysed at 100°C for 10 min. 2 µl of the suspension was used as a template in the PCR reaction.

## Enzymatic Reactions

Restriction high-fidelity enzymes by NEB were used to perform digestions for the cloning experiments. They were inactivated and loaded on an agarose gel using NEB purple loading dye. Shrimp Alkaline Phosphatase (rSAP) by NEB was used for vector-dephosphorylation. For the Ligation reaction, the T4-DNA Ligase by LifeTech Austria was used. After ligation, the ligation products were desalted using microfilters for 1 hour. The protocols of the manufacturers were followed for the reactions.

## Agarose Gel Electrophoresis

Agarose gels with 1x TAE Buffer and a concentration of 0.05 µg/ml ethidium bromide were used. Gels with a final concentration of 1 % agarose were used for control gels and a final concentration of 0.8 % agarose was used for gel purification of PCR products or enzymatic reaction products. The electrophoresis was run at 5-10 V/cm and 1x TAE Buffer was utilized as a running buffer. The 1 kb Ladder by GeneRuler from Thermo Scientific was applied as a marker.

## Purification of DNA and Preparation of Plasmids

QIAquick® PCR purification and Gel extraction Kit by Qiagen (Ref. 28506) was used to purify PCR products and extract DNA from fragments excised from agarose gels. QIAprep® Spin

Miniprep Kit by Qiagen (Ref. 27106) was utilized for plasmid preparations according to the manufacturer's protocol. For low-copy plasmids, the NucleoBond® PC00 (Ref. 740573) kit was used according to the manufacturer's protocol.

### Chromosomal DNA Isolation

Qiagen DNeasy Blood & Tissue Kit (Ref. 69504) was used for the isolation of chromosomal DNA. For *K. oxytoca* 3 ml overnight cultures (ONC) were used. The remaining steps were performed according to the manufacturer's protocol.

### DNA sequencing

Sequencing was performed by the company MicroSynth with Sanger Sequencing. The sequences were analyzed in SnapGene 6.0.4.

## Electrocompetent cells

### Generation of electrocompetent *E. coli* cells

A 5 ml ONC was prepared and 50 µl were used to inoculate 50 ml of LB. The culture was incubated at 37°C and shaking at 180 rpm to a final OD600 of 0,5-0,7. The cells were then cooled on ice for 10 min. After that the culture was split and the cells were pelleted in 50 ml Sarstedt tubes at 5000 rpm for 10 min at 4°C in an Eppendorf centrifuge. The pellet was resuspended in a total volume of 2 ml in 10% glycerin and transferred to an Eppendorf tube. The glycerin needs to be ice-cold. The suspension was then pelleted and resuspended in 10% glycerin 2 more times. After the second time, the pellet was suspended in 400 µl of 10% glycerin. The final suspension was either used for transformation directly or portioned and frozen at -80°C.

### Transformation of electrocompetent *E. coli* cells

To transform electrocompetent *E. coli* cells 40 µl of the cells were thawed on ice for 10 minutes or used directly after generating and combined with 10-200 ng of plasmid DNA (cloning product). Using precooled electroporation cuvettes, the mixture was electroporated with 1800 Volt. Instantly, 1 ml of LB medium was added and subsequently, the cells were regenerated at 37°C for 1 hour (strains with thermosensitive plasmids were regenerated at 30°C). Afterward, appropriate dilutions were plated on LB agar plates with the desired antibiotics and incubated at 37°C (strains with thermosensitive plasmids were incubated at 30°C) overnight. If using a cloning product, a positive control using 10 ng of the wild type vector plasmid was used to transform the cells. Negative controls using 1 µl of water were performed as well.

## Generation of electrocompetent *K. oxytoca* cells

An ONC is used to inoculate 100 ml CASO medium with 0.7 mM EDTA to a starting OD600 of 0.05. The culture is incubated at 37°C with shaking at 180 rpm to an OD600 of 0.6-0.7. At that point, the culture was split into two 50 ml Greiner tubes and cooled on ice. Subsequently, the cells were pelleted at 5000 rpm for 20 min at 4°C. Then the pellets were resuspended in 50 ml of 10 % glycerin. The glycerin needs to be ice-cold. The suspensions were centrifuged again under the same conditions and the pellets were resuspended in 10 ml of 10 % glycerin. Once again, the suspensions were centrifuged like before and the pellets were resuspended in 2.5 ml 10% glycerin. After one last time of centrifuging the pellets were resuspended together in 100 µl 10% glycerin. The cells are either portioned and stored at -80°C or used for transformation directly.

## Transformation of electrocompetent *K. oxytoca* cells

To transform electrocompetent *K. oxytoca* cells 80 µl of the cells were thawed on ice for 10 minutes or used directly after generating and combined with 20-60 ng of plasmid DNA (cloning product). Using precooled electroporation cuvettes, the mixture was electroporated with 2000 Volt. Instantly, 1 ml of CASO medium with 0.7 mM EDTA was added and the cells were regenerated at 37°C for 1 hour. Afterward, appropriate dilutions of 100 µl in volume were plated on LB agar plates with the desired antibiotics and incubated at 37°C overnight. If using a cloning product, a positive control using 10 ng of the wild type vector plasmid was used to transform the cells. Negative controls using 1 µl of water were performed as well.

## Lambda RED Recombination System

The λ RED recombination system is an effective method for performing gene knockouts and introducing new genes in Enterobacteriaceae like *E. coli.* To use this method a linear DNA fragment had to be constructed. The linear fragment must contain the sequence of the gene that we are trying to introduce into the strain flanked by regions that are homologous (50 bp) to the gene of interest we want to replace on the chromosomal DNA. The linear fragment is amplified by PCR and transformed into an *E. coli* strain that carries the pKD46 plasmid. This plasmid is essential for the system since it expresses the bacteriophage ʎ components *exo, bet,* and *gam.* The expression of those genes is controlled by an *araB* promoter which means it must be induced with arabinose. When induced the components of the system stimulate the homologous recombination between the chromosomal DNA and the 50 bp overhangs of the linear DNA fragment

To perform the recombination *E. coli* MD strains were transformed with pKD46-tet. ONCs of the strains were made and 500 µl of them were used to inoculate 50 ml of LB medium with tetracycline which were then incubated. When reaching an OD600 of 0.1 500 µl of 15% arabinose were added. The cultures were then incubated to an OD600 of 0.5-0.8. All

incubation steps with pKD46-tet are performed at 30°C. After reaching the desired OD600 the cells were put into a 42°C water bath with a shaker for 15 min. Subsequently, the flasks with the cultures were lightly shaken by hand in an ice water bath for 3 min. The cells were then centrifuged at 5.000 rpm in a 50 ml Greiner tube. After that, the pellet was resuspended in 2 ml ice-cold 10% glycerin and transferred into two Eppendorf tubes with 1 ml each. The cells were pelleted at 10.000 rpm and resuspended in 1 ml ice-cold 10% glycerin two more times. After the cells were pelleted for the last time, they were resuspended in 200 µl ice-cold 10% glycerin and put on ice.

For the transformation setup, 60 µl of the cells were used and mixed with at least 200 ng of the linear DNA fragment with homologous overhangs in precooled electroporation cuvettes. The mixture was then electroporated at 1800 V. Right after 1 ml LB was added to the cuvette and the cells were transferred to an Eppendorf tube, which was then incubated for 1,5 hours at 30°C. After that 100 µl of the cells were plated on LB agar plated with Ampicillin and incubated at 30°C overnight.

## GFP assay

The plasmids pAR181_PrnpsA_gfpmut3b and pAR181_PraroX_gfpmut3b as well as pAR181_gfpmut3b (PrrnB) as a positive control and pACYC184 as a negative control were used to transform different bacterial strains. ONCs of the strains containing the plasmids were prepared and diluted with medium including Chloramphenicol to an OD600 of 0.2. Then 24 well plates for fluorescence application from Greiner were loaded with 1 ml of the dilutions and put into the Omega plate reader. The fluorescence was measured using an excitation of 485 and an emission of 520. Shaking was performed at a frequency of 300 rpm and the temperature was 37°C. The OD600 and fluorescence values were measured subsequently every 2 minutes.

One assay was performed for which cultures of 5 ml CASO were made with *K. oxytoca* AHC6 pAR181_PrnpsA_gfpmut3b, pAR181_PraroX_gfpmut3b as well as pAR181_gfpmut3b (PrrnB) and pACYC184 after 20 hours one ml of the culture was used for a measurement in the plate reader for OD600 and fluorescence, as described above.

## MD TM OD600 assay

*K. oxytoca* AHC6 wild type (Tox+) and a toxin-deficient mutation AHC6 Mut89 (Tox-) were cultured in 50 ml of Caso medium for 17 hours and the supernatant was harvested via centrifuging the cells (3000 rpm, 30 min) and transferring the supernatant via pipette to a 50 ml glass bottle. Since the supernatant was still very turbid the cultures were centrifuged for another 30 min. The supernatant is then sterile filtered (0,45 nm) and stored in a 50 ml glass bottle. The supernatants were used to treat MD strains that carry phage lambda (MD6, MD56, MD74), so overnight cultures of all 3 strains were prepared (3 ml LB). Since tilimycin sticks to

plastic, we tried to use as few plastic vessels as possible. As controls, the cells were treated with 85 µM TM and LB medium. The MD strains with their treatments were added to 24 well plates at a total of 1 ml per well and the OD600 was measured in the Omega plate reader for 8 hours at 37°C while shaking at 300 rpm. The supernatants were then transferred to Eppendorf tubes and centrifuged at 13000 rpm for 10 min and sterile-filtered (0,45 nm). Lastly, 30 µl of chloroform were added.

## Phage assay

The strain MD5 was infected with the supernatants (phage lysates) from the TM OD600 measurements. An overnight culture of MD5 was prepared (2 ml LB + 20 µl 20 % maltose). The ONC is centrifuged and resuspended in 1 ml $MgSO_4$. 100 µl of the MD5 cells are mixed with 3 ml R-Top agar (Table 7) in a glass eprouvette and poured on top of a regular LB agar plate. Serial dilutions of the phage lysate with TMG buffer (Table 8)are prepared. The phage lysates dilutions were spotted on the top agar (5 µl). After drying the plates were incubated at 37°C overnight. The next day the plaques were counted, and the pfu/ml was calculated.

**Table 7 R-Top agar recipe used in this study**

| R-Top Agar | | Final volume |
|---|---|---|
| Peptone | 10 g | 1000 ml |
| Yeast Extract | 1 g | |
| NaCl | 8 g | |
| Agar | 8 g | |
| After autoclaving add | | |
| 1 M $CaCl_2$ | 2 ml | |
| 20 % Glucose | 5 ml | |
| 1 M $MgSO_4$ | 30 ml | |

**Table 8 TMG Buffer used in this study**

| TMG Buffer (pH 7.4) | | Final volume |
|---|---|---|
| Tris | 1.21 g | 1000 ml |
| $MgSO_4x7H_2O$ | 1.2 g | |
| Gelatine* | 0.1 g | |

*A gelatine solution of 1 g in 10 ml $H_2O$ is made by stirring and heating the combined ingredients. After that 1 ml of this solution is added to 1000 ml of TMG Buffer.

# Results & Discussion

## Tilimycin induces phage release

Tilimycin is a genotoxic enterotoxin that is produced by *K. oxytoca.* This species is known to colonize the human gut as an opportunistic pathogen. Other pathogenic species have been shown to trigger prophage induction with their produced toxins, e.g., colibactin [19]. We hypothesize that if tilimycin causes a DNA damage SOS stress response in *E. coli* it results in prophage activation in vitro and in vivo. Therefore, we aim to establish a system using phage λ that can be used to test the hypothesis in the mouse model. To accomplish this, the *E. coli* MD strains optimized for the murine gut, which we received from Marianne De Paepe *et al.* [15] had to be modified to carry an ampicillin resistance, to allow a co-cultivation with *K. oxytoca* in the mouse. For this modification, the λ RED homologous recombination system was chosen. Since all Lambda RED vectors carried one of the resistance genes already present in the used strains, we aimed to generate a pKD46 plasmid with a tetracycline resistance instead of the wild type ampicillin resistance

## Cloning of pKD46-tet

For this project, pKD46 was used as a vector (Figure 8). This vector has a restriction site for PvuI in the *bla* gene that encodes the ampicillin resistance, therefore PvuI was the restriction enzyme of choice. The plasmid has a pSC101 origin, which is low copy. It also is temperature sensitive, which is essential for plasmid eradication after the recombination. The lambda RED genes *exo*, *bet* and *gam* can be induced by arabinose.

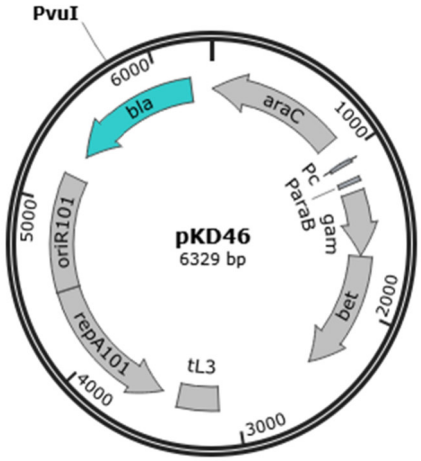


*Figure 8 Vector pKD46 including restriction site for PvuI*

The plasmid has the *bla* gene which encodes an ampicillin resistance and a pSC101 origin, which is low copy. The plasmid also contains the λ RED genes *exo*, *bet,* and *gam* which can be induced by arabinose.

For the insert, the *tetRA* cassette was chosen. The cassette was amplified via PCR from the plasmid pAR183 using primers 7 and 8 which contain PvuI restriction sites on the overhangs (Figure 9).

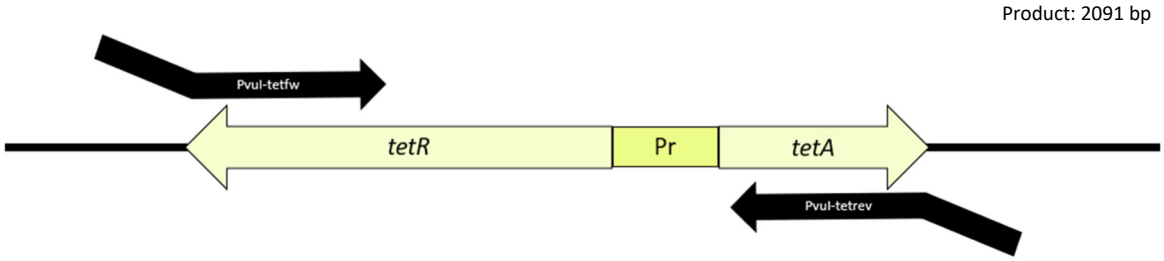


*Figure 9 In silico amplification of tetRA*

The cassette consists of the *tetR* gene and the *tetA* gene which are connected by a promoter sequence. The primers used have overhangs with the sequence for the restriction enzyme PvuI and bind to the ends of the resistance cassette.

For the amplification via PCR 6 reactions were used to gain enough product (Figure 10). The bands were expected to be 2091 bp and all reactions showed a band at that size. The 6 reactions were pooled and purified. The final yield of purified *tetRA* was 3765 ng.

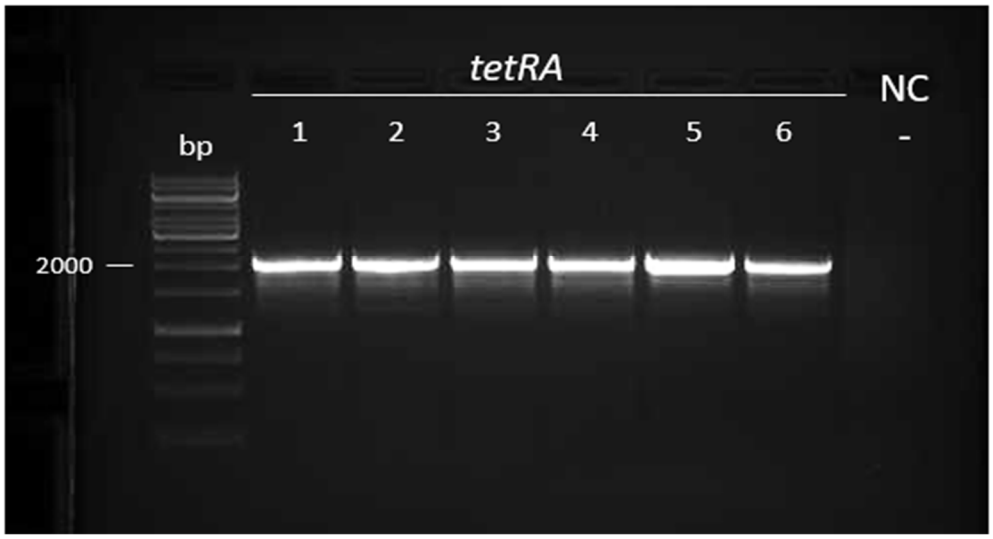


*Figure 10 Amplified tetRA cassette*

The *tetRA* cassette was amplified from pAR183 via PCR. The used ladder is Generuler 1 kb and 17 % of PCR reactions are loaded on the agarose gel. As a negative control (NC-) $ddH_2O$ was used. The 6 reactions were pooled and purified which resulted in a final yield of 3765 ng of purified product.

For the restriction digest the vector as well as the insert were cut with PvuI and applied to the gel (Figure 11). In addition to PvuI, the insert reactions were treated with DpnI to digest the template plasmid. A control of the uncut pKD46 vector was applied to the gel. The bands were

cut out of the gel, pooled and purified. The purified vector yielded 1016 ng of product and the purified insert yielded 826 ng.

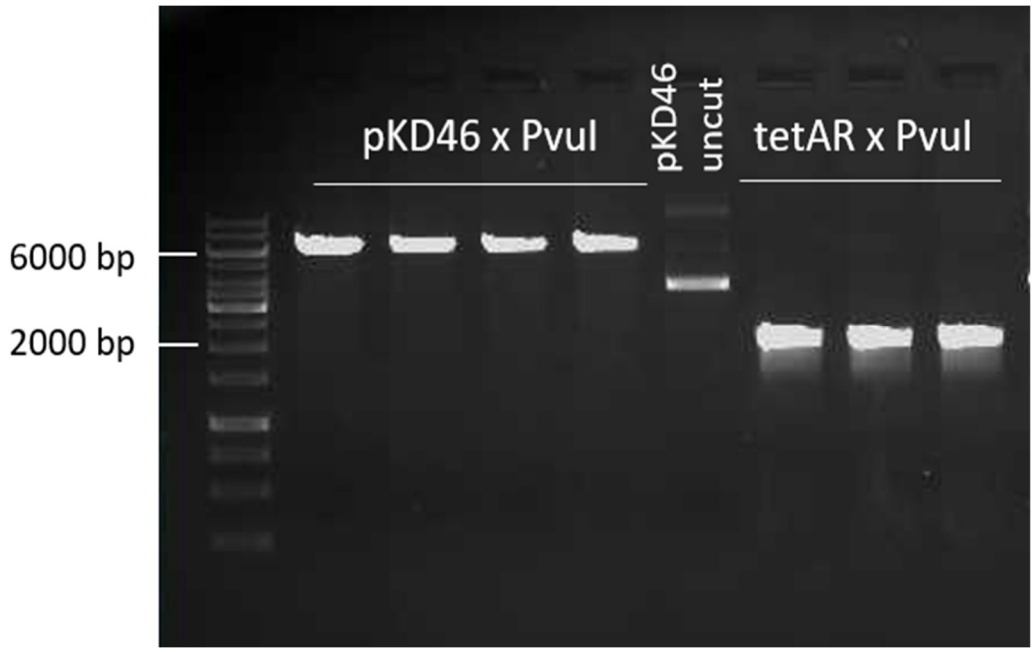


*Figure 11 Restriction digest of pKD46 and tetRA with PvuI*

The reactions containing the insert were additionally treated with DpnI to digest the template plasmid from the PCR amplification. The used ladder is Generuler 1 kb and 100 % of restriction digests are loaded. As a control, the uncut vector was applied to the agarose gel as well. The bands were excised from the gel, pooled, and purified which resulted in a final yield of 1016 ng of vector DNA and 816 ng of insert DNA.

After purification, the vector and insert were ligated. For the ligation, 100 ng of the vector pKD46 and 133 ng of the insert *tetRA* were used.

Only one restriction enzyme (PvuI) was used to cut the vector and insert for this project and therefore there were two possible orientations in which the *tet* cassette could occur. Since the generation of this plasmid took a few attempts, the presence as well as the orientation of the *tetRA* cassette on the plasmid after the ligation reaction was checked by PCR using primers 13 and 14 to detect *tetAR* orientation and primers 13 and 15 to check for *tetRA* orientation. As a template 2 µl of the desalted ligation reaction were used. The primers were chosen to bind on the vector within or outside the remaining *bla* gene and inside the *tet* cassette (Figure 12).

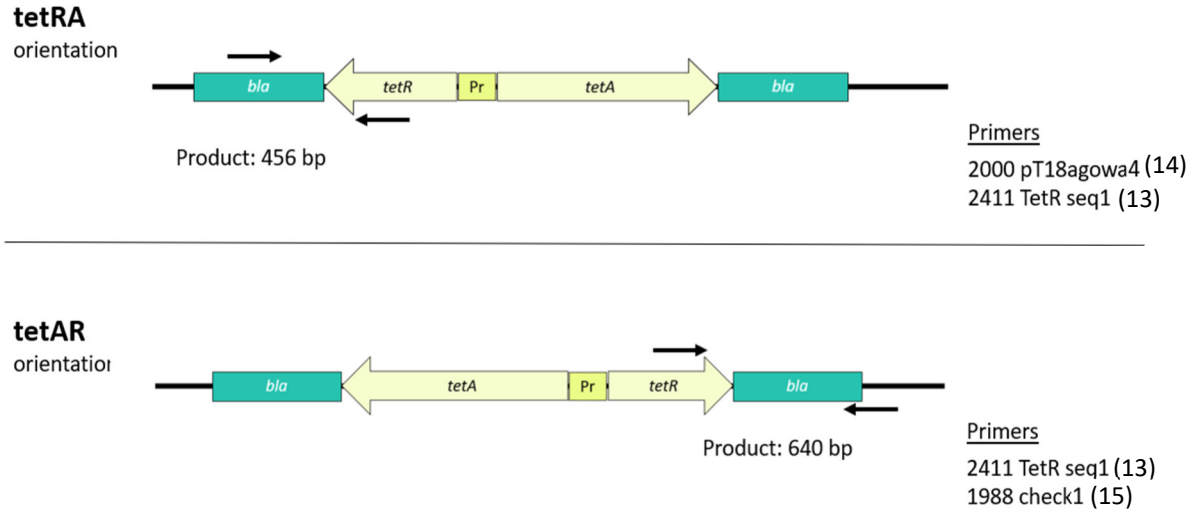


*Figure 12 Tet cassette orientation primers*

Since only one restriction enzyme was used (PvuI), there were two possibilities considering the integration of the tet cassette into the vector. First the *tetRA* and second the *tetAR* orientation. The primers to screen for either direction of the cassette were chosen to bind on the vector as well as the *tet* cassette, so the presence of the correct product and the definite orientation can be confirmed.

The agarose gel showed that only *tetRA* orientation was present after ligation with a band at 456 bp. In general, the ligation worked and the presence of the ligation product pKD46-tet could be confirmed, since one of the chosen primers was binding the *tetRA* cassette and the other one was binding the vector (Figure 13). Next the ligation product was used to transform *E. coli* DH5α cells.

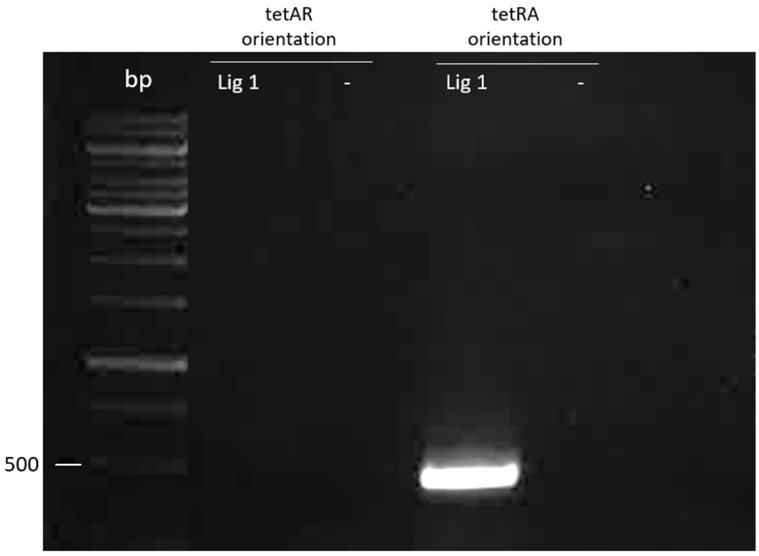


*Figure 13 Detection of ligation product pKD46-tet with tetRA orientation*

The orientation of the *tet* cassette in the ligation product was determined via PCR. The primers 13 and 14 were used to screen for *tetAR* orientation and primers 13 and 15 were used to screen for *tetRA* orientation. Only *tetRA* orientation could be detected in the ligation reaction, but the band confirmed the presence of the ligation product pKD46-tet, since the primers were binding the cassette as well as the vector. As a template 2 µl of the desalted ligation reaction were used and 100 % of the PCR reaction are loaded. The ladder is Generuler 1 kb and for the negative control (NC–) dd$H_2O$ was used.

In previous transformation attempts, pAR183 was used as the positive control, however, the transformation efficiency was very low (5,2 x $10^3$) and first, we suspected that the competent cells were the problem. Adding pKD46 as a positive control showed that the competent cells were not the problem (1,9 x $10^6$). However, since the original pKD46 has an ampicillin resistance we still wanted to have a positive control with tetracycline resistance, like in the cloning product. The template plasmid pAR183 turned out to be an unsuitable candidate for a positive control since it has an R1 backbone, is very big (~97 kb), and therefore has a low transformation efficiency in general. After switching to pBlue_A_TetRA_mono as a tetracycline-resistant positive control the transformation effenciency was in an acceptable range (2 x $10^5$). Another possible factor that lowered the transformation efficiency in general is that tetracycline was not added to the medium during regeneration of the transformation mix. This resulted in no expression of the TetA pump before plating the cells and therefore fewer viable cells on the tetracycline agar plates.

The finished cloning product contains the *tetRA* cassette which interrupts the *bla* cassette on the plasmid (Figure 14). This disrupts the ampicillin resistance and introduces the tetracycline resistance into the plasmid.


*Figure 14 Interrupted bla cassette and integrated tetRA cassette*

The *tetRA* cassette is inserted into the *bla* gene, which disrupts the ampicillin resistance and introduces the tetracycline resistance into the plasmid.

To verify the correct integration of the cassette in the pKD46 plasmid, a colony PCR of the clones received from the transformation was performed. The primers 13 and 15 were used. As another control, the clones that were retrieved from agar plates containing tetracycline, were plated out on ampicillin agar plates and did not show any growth. The first lane on the gel shows a flaw due to insufficiently melted agarose in the gel. For the other clones, the presence of the *tetRA* could be confirmed since they show the expected band size of 456 bp (Figure 15). Clone 3 was chosen to continue working with.

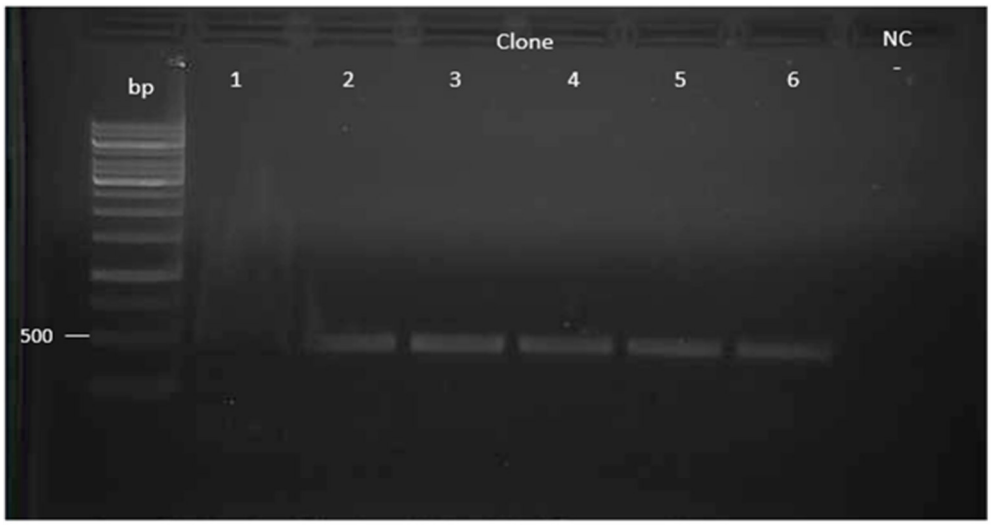


*Figure 15 Detection of positive pKD46-tet clones*

A colony PCR of 6 clones from the transformation was performed using primers 13 and 15. The first two lanes show a smear on the gel which might be due to insufficiently melted agarose. The other clones al clearly showed the correct band for a positive clone. Clone 3 was chosen for the following steps. The ladder is Generuler 1 kb and 33 % of the PCR reaction were loaded. For the negative control (NC–) dd$H_2O$ was used.

The finished pKD46-tet plasmid was then used for a lambda RED recombination, where ampicillin resistance was the gene of interest that was being introduced into a strain, therefore the traditional pKD46, which carries an ampicillin resistance could not be used.

This cloning project did not show the anticipated results right away so parallel to cloning with the first method, we started looking for different cloning strategies. One option to facilitate cloning is using a different tetracycline resistance gene. The *tetRA* gene is a cassette that contains a tetracycline efflux MFS transporter and a transcriptional regulator gene. A possibility to facilitate cloning and generate a smaller plasmid that will be easier to work with is using one tetracycline resistance gene like the one on pBR322 (Figure 16). This gene only consists of 1191 bp whereas the *tetRA* cassette has a size of 2100 bp. Literature searches of the same cloning project showed successful results for this approach and so the primers from Yao *et al.* [90], primers 16 and 17, were used to amplify the tetracycline resistance via PCR from pBR322 (Figure 16). They also used PvuI to digest the vector and the insert, so the cloning strategy is the same as previously, however the insert is changed.

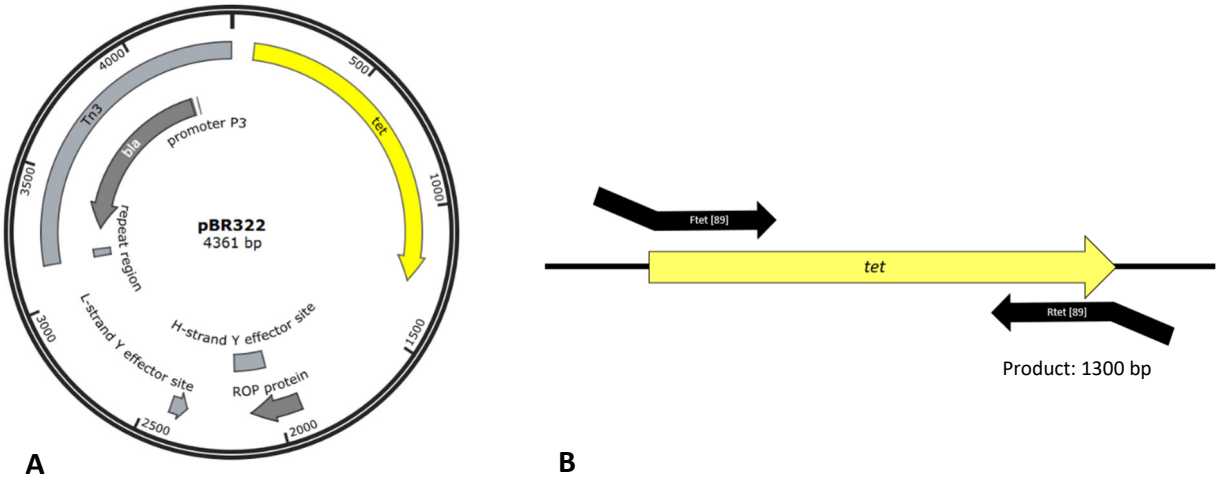


*Figure 16 Alternative cloning strategy with pBR322*

The cloning strategy is the same as previously, but the insert is swapped out for a smaller, less complex tetracycline resistance gene. **A** The tetracycline resistance gene on pBR322 is a single gene and not part of a cassette. **B** Primers 16 and 17 [89] were used to amplify the tetracycline resistance gene. The primers have overhangs with the sequence for the restriction enzyme PvuI.

However, the reaction did not show sharp bands at 1300 bp in the agarose control gel as expected and since the primers have worked for Yao *et al.* [90] the primers could not have been the problem. After checking the whole process, the template plasmid preparation turned out to be the issue. The strain that was carrying pBR322 was *E. coli* XL1 which is tetracycline resistant. The plasmid preparation did not work because tetracycline was used as the antibiotic to keep the strain from losing the plasmid, but the strain did not need the plasmid since the resistance was on the genome and therefore the yield and quality of purified plasmid was low. The agarose gel clearly shows a smear beneath the bands and many clouds at the bottom of the gel, which indicate unbound primers, even though only 17 % of the reaction were loaded (Figure 17).

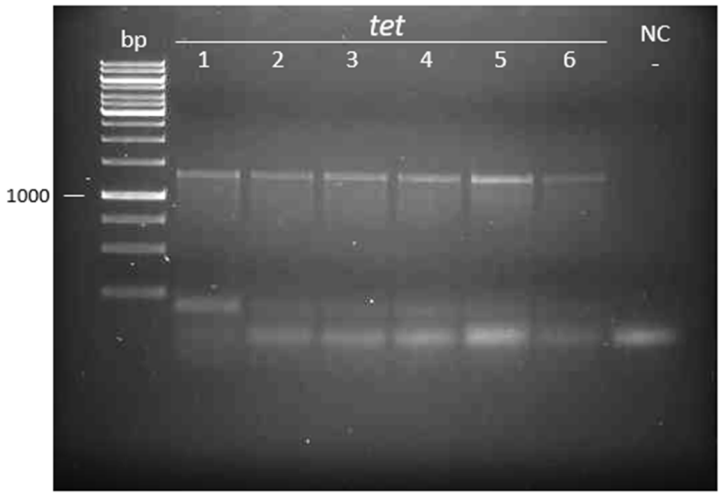


*Figure 17 Low quality PCR tet amplification*

The PCR-amplified tetracycline gene showed smeared bands on the control gel and a lot of unbound primers at the bottom of the gel. The ladder is Generuler 1 kb and 17 % of the PCR reaction were loaded. For the negative control (NC–) dd$H_2O$ was used.

Since we were able to clone the desired product pKD46-tet using *tetRA* as an insert, this strategy was no further pursued.

## Introduction of ampicillin resistance into MD strains

The aim of this cloning project was to introduce an ampicillin resistance to *E. coli* MD strains by inserting the *bla* gene into the *stfR* or the *hsdR* gene depending on the respective genotype. For example, the strain MD5 has the kanamycin resistance placed into the *hsdR* gene and therefore we would use the *stfR* gene for the introduction of the ampicillin resistance. An overview of the mentioned strains and their genotypes can be viewed in Table 9.

**Table 9 MD strains and relevant Genotype**

| Strain | Genotype |
|---|---|
| MD5 | MG1655 ΔfliC ΔompF hsdR::KanR |
| MD6 | MG1655 ΔfliC ΔompF stfR::cat (λ ble) |
| MD47 | MG1655 ΔfliC ΔompF lamB::KanR |
| MD56 | MG1655 ΔfliC ΔompF lamB::FRT stfR::cat (λ ble) |
| MD74 | MG1655 ΔfliC ΔompF lamB::FRT stfR::cat (λ ble $cI^{ind-}$) |

The resistance was introduced into the strains by homologous recombination into the respective genes. The following primer design strategy was used for the homologous recombination. A sequence of 50 bp which is homologous to the target gene was used for the overhangs in both forward and reverse primer respectively (Figure 18). As a representative for both genes, the concept is pictured for *stfR* throughout the entire in silico cloning strategy. The two genes *stfR* and *hsdR* were chosen since the two genes already had antibiotic resistances inserted [15].


*Figure 18 Primer design for λ RED recombination*

For a lambda RED recombination in *E. coli* there needs to be a 50 bp homologous overhang to the target gene on the insert for them to successfully recombine. The figure shows this concept for the *stfR* gene as a representative for both genes relevant for this study.

The insert for this project consists of the *bla* cassette that encodes an ampicillin resistance (AmpR). As a template, the plasmid pBluescript-II-KS(-) was used. The insert was amplified via PCR using the designed primers (9 and 10 for *stfR,* 11 and 22 for *hsdR*) containing the homologous 50 bp overhangs (Figure 19).

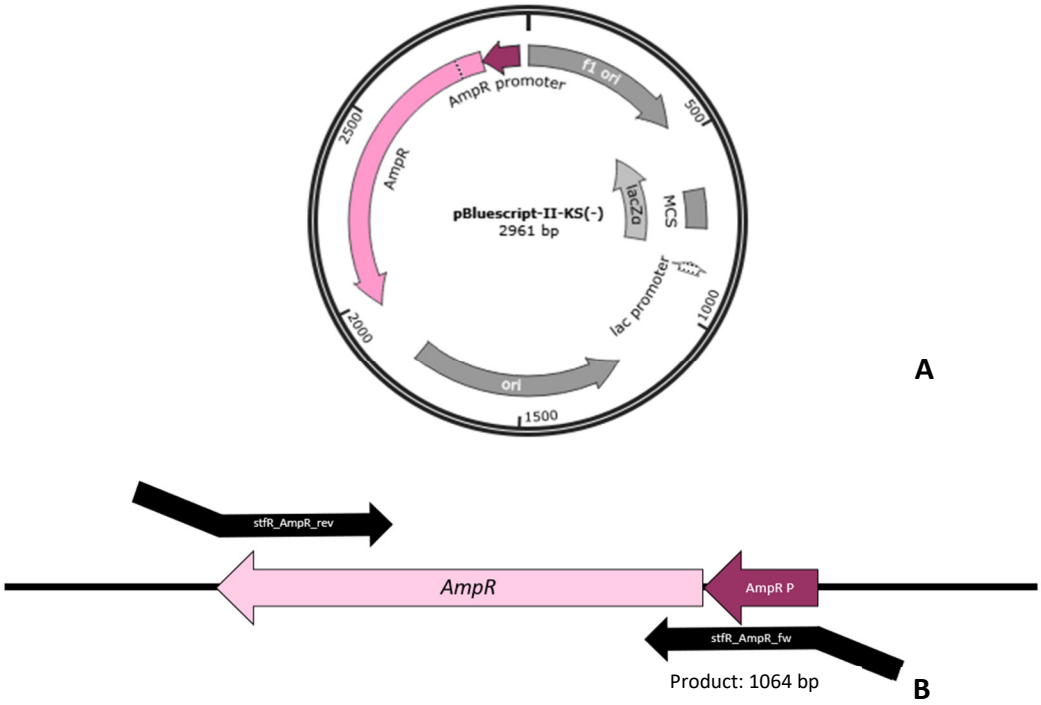


*Figure 19 Insert amplification from pBluescript-II-KS(-)*

For this cloning an ampicillin resistance is introduced into the genome of *E. coli* MD strains. As a representative for both genes, the *stfR* version is depicted. **A** The ampicillin resistance was amplified from the template pBluescript-II-KS(-). **B** The used primers contain the 50 bp homologous overhangs that are crucial for the recombination with the bacterial genome. The primers for *stfR* are 9 and 10 and for *hsdR* 11 and 12.

To avoid template plasmid contamination in the final λ RED recombination clones, the pBluescript-II-KS(-) was linearized using the restriction enzyme SacI. Since the PCR amplification of the ampicillin resistance gene with the overhangs of the respective genes yielded a small amount of product 16 reactions were made for each gene variation (Figure 20). They all showed a band at 1064 bp as expected. The respective reactions were pooled and purified which yielded 3748 ng of AmpR-*stfR* and 2756 ng of AmpR-*hsdR.*

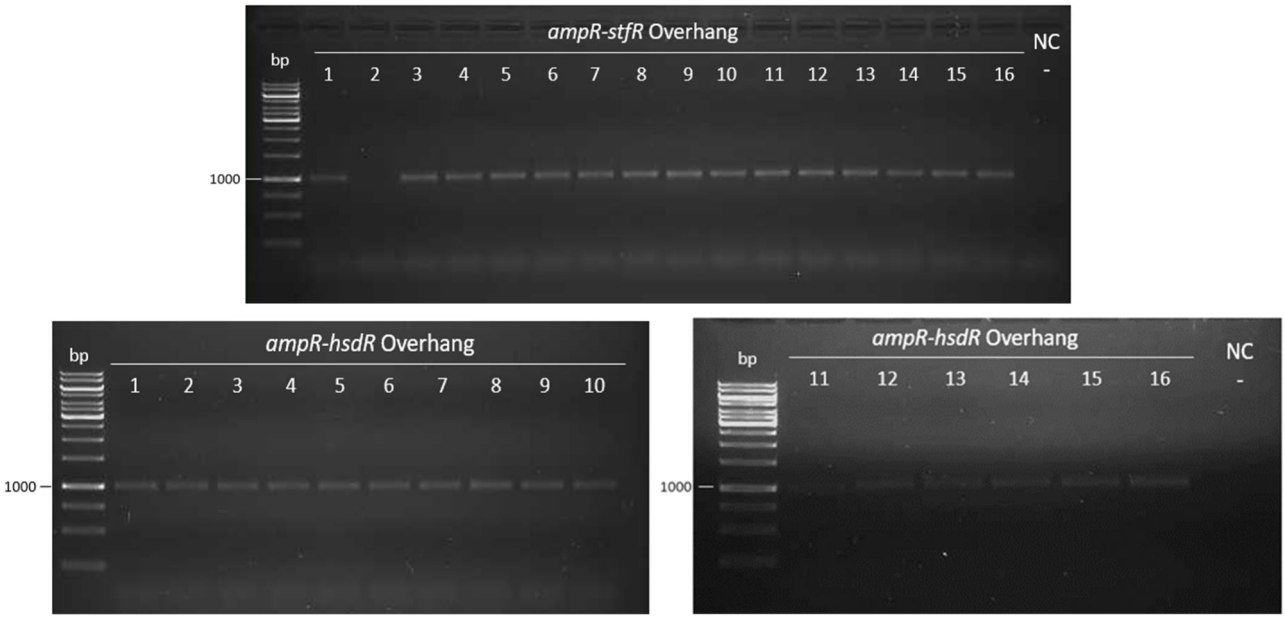


*Figure 20 Amplification of the insert with homologous overhangs*

The amplification of the inserts was done in 16 reactions to gain enough product to perform the lambda RED recombination even after further treating the product. The respective reactions were pooled and purified which yielded 3748 ng of AmpR-*stfR* and 2756 ng of AmpR-*hsdR*. As a template, pBluescript-II-KS(-) linearized with SacI was used. The ladder is Generuler 1 kb and 10 % of each PCR reaction were loaded. For the negative control (NC–) dd$H_2O$ was used.

The purified PCR products were then treated with DpnI to digest the remainder of the template plasmid to avoid template contamination in the final lambda recombination clones. For AmpR-*stfR*-overhang two reactions with 1405 ng DNA and one reaction with 937 ng DNA were performed. For AmpR-*hsdR*-overhang two reactions with 1033 ng DNA and one reaction with 689 ng DNA were performed. The restriction digest reactions were loaded on a gel and then purified and pooled respectively (Figure 21). The purification resulted in 1424 ng of AmpR-*stfR*-overhang and 944 ng of AmpR-*hsdR*-overhang.

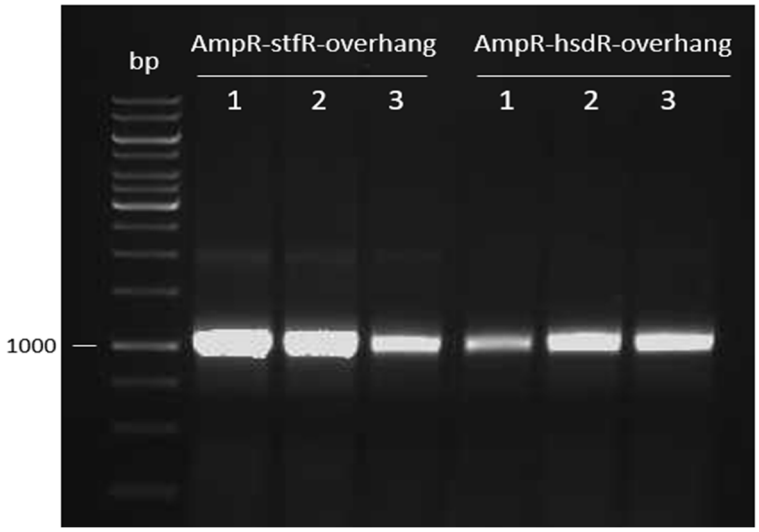


*Figure 21 DpnI digested PCR product with homologous overhangs*

To eliminate any residue of the template plasmid, the amplified insert PCR products were digested with DpnI. For AmpR-*hsdR*-overhang two reactions with 1033 ng DNA and one reaction with 689 ng DNA were performed. The bands were excised, pooled, and purified. After the gel purification, 1424 ng of AmpR-*stfR*-overhang and 944 ng of AmpR-*hsdR*-overhang remained.

The next step is the homologous recombination via the RED system which switches the 50 bp homologous regions from the gene on the chromosome for the ones on the PCR product and places the flanked resistance gene inside the target gene which results in an ampicillin-resistant strain (Figure 22). For this, the MD strains that we want to alter (Table 9) were transformed with the previously constructed pKD46-tet since the plasmid contains all the relevant genes for the lambda RED recombination. For the transformation, 356 ng (AmpR-*stfR*-overhang) and 236 ng (AmpR-*hsdR*-overhang) of PCR product were used.

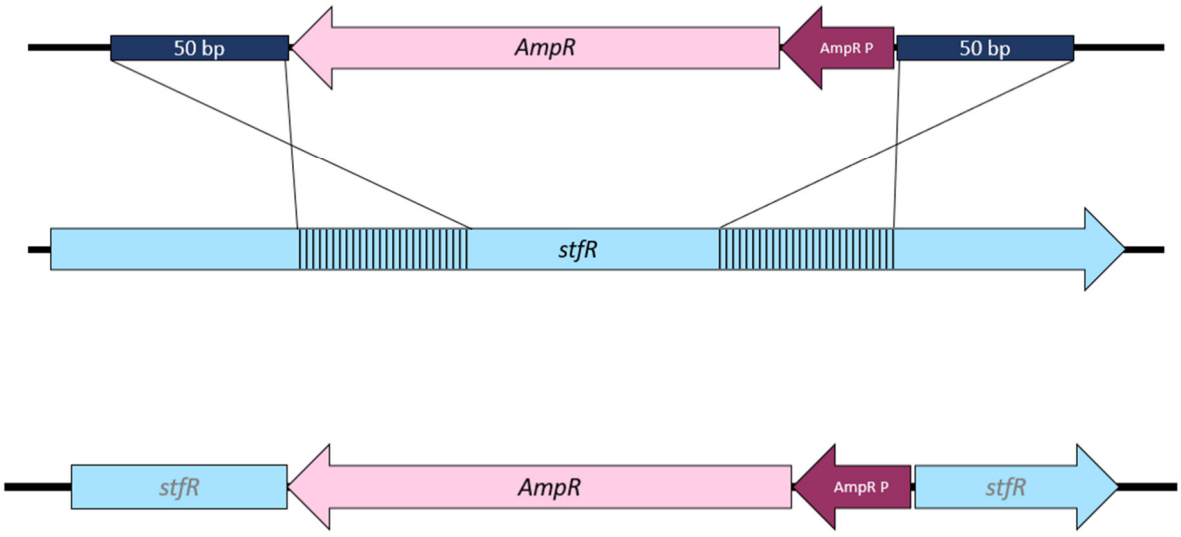


*Figure 22 Homologous recombination*

The 50 bp regions on the PCR product that are homologous to the target gene flank the ampicillin resistance. In the recombination process the homologous regions on the chromosome switch with the ones on the PCR product and thereby integrate the ampicillin resistance into the gene on the chromosome and simultaneously knock-out said gene while making the strain resistant to ampicillin.

As previously mentioned SacI was used to linearize the template plasmid and the amplified insert was purified via agarose gel. Before that, the preparation was simply done by purifying the PCR product that was amplified from an uncut vector. A λ RED recombination was performed, and the clones were growing on ampicillin plates, but the correct position of the resistance on the genome could not be confirmed via control PCR so we suspected a potential contamination with the template plasmid. Primers 18 and 19 are both binding *lacZ*, which can only be found on the template plasmid pBluescript-II-KS(-) and not in the MD strains. A PCR using those primers was performed to determine whether the ampicillin resistance in the clones was caused by contamination with template plasmid. The agarose gel shows that the PCR of the template plasmid results in a product at 250 bp (Figure 23). The colonies obtained from the RED transformation that were tested (1-8) showed the same band at 250 bp as the plasmid, whereas the MD56 wild type did not have any PCR product. This leads to the conclusion that the colonies are most likely contaminated with the ampicillin resistance template plasmid and therefore grow on ampicillin plates. Since all inserts for the different MD strains were prepared in the same way, only MD56 colonies were used to test for template plasmid contamination. After verifying that the colonies were indeed contaminated with template plasmid, the new approach of insert preparation including template linearization and gel purification was used.

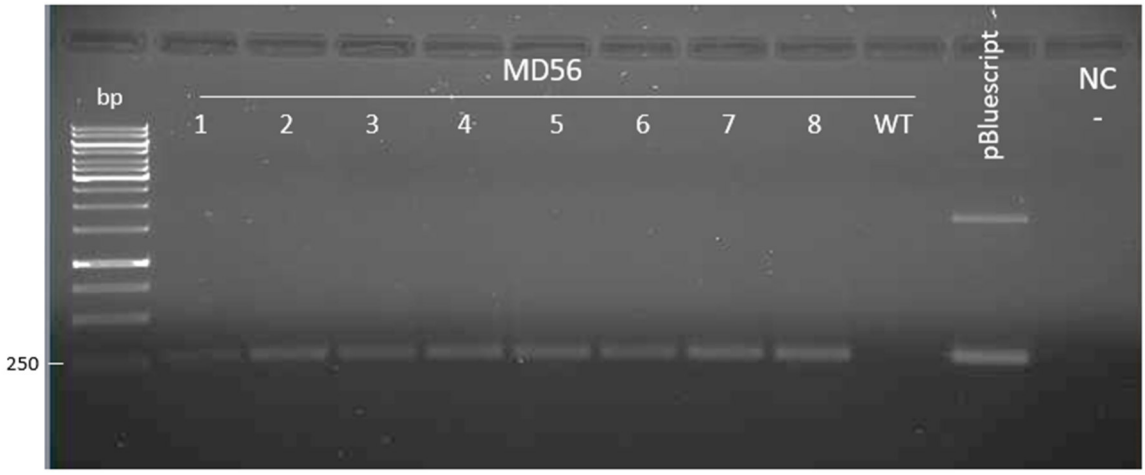


*Figure 23 Detection of template plasmid in lambda RED recombination clones*

As a representative for all MD strains MD56 was tested for template plasmid contamination via PCR. The primers 18 and 19 that bind the *lacZ* gene on the plasmid were used. All clones show bands identical to the plasmid. The wild type version of MD56 was used as a negative control to ensure that no PCR product was amplified from the genome. The ladder is 1 KB Generuler and 66 % of the PCR product are loaded. For the negative control (NC–) dd$H_2O$ was used.

After executing the new template preparation strategy another lambda RED recombination was performed and representative MD5 was tested for plasmid contamination via colony PCR using primers 18 and 19. The control agarose gel showed that there was no plasmid contamination in the six tested clones (Figure 24). As a control, the template plasmid

pBluescript-II-KS(-) was used. The negative control seems to have a slight band at 250 bp but this is most likely a contamination caused by the application on the gel.

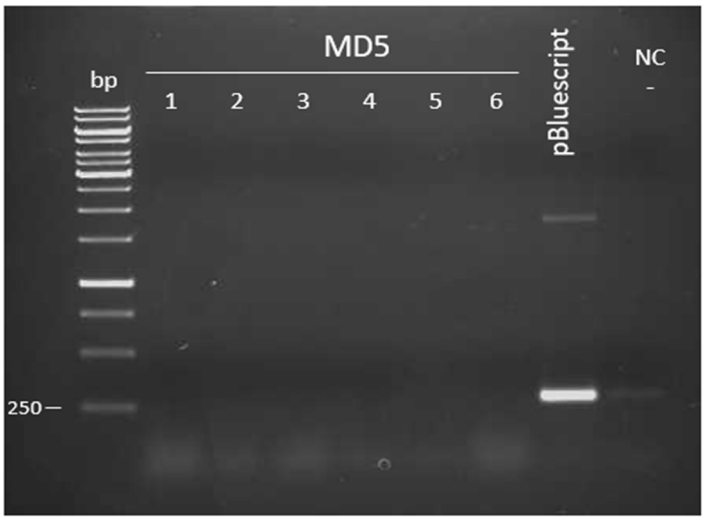


*Figure 24 No detection of template plasmid in lambda RED recombination clones*

The template plasmid pBluescript-II-KS(-) could not be detected in the 6 tested colonies but was used as a control for the PCR. Primers 18 and 19 were used for colony PCR. The negative control has a slight band probably due to a gel application contamination. The ladder is 1 KB Generuler and 100 % of the PCR product are loaded. For the negative control (NC–) dd$H_2O$ was used.

Even after eliminating the template plasmid contamination, there were clones on the ampicillin LB plates, in which the correct position of the ampicillin could not be confirmed. For the first attempt to confirm the insertion of the ampicillin resistance into the target gene two primers outside the homologous region were chosen, for *stfR* primers 21 and 22 (Figure 25).


*Figure 25 Primers for ampicillin resistant clone detection in stfR*

Primers 21 and 22 bind in the *stfR* gene outside of the homologous region chosen for the recombination. A positive clone yields a band at 1114 bp and the wild type yields a band at 399 bp.

The control PCR results in a 399 bp band in the wild type gene and in a 1114 bp band if the ampicillin resistance including the promoter is inserted into the *stfR* gene. The *stfR* gene was the target for resistance integration in the strains MD5 and MD47. Multiple clones were tested via colony PCR, eight for each strain are shown below (Figure 26). As a negative control, a wild type colony of MD47 was tested as well. All tested colonies showed the wild type band (399

bp) on the gel meaning the ampicillin resistance was not inserted at the right position into the target gene.

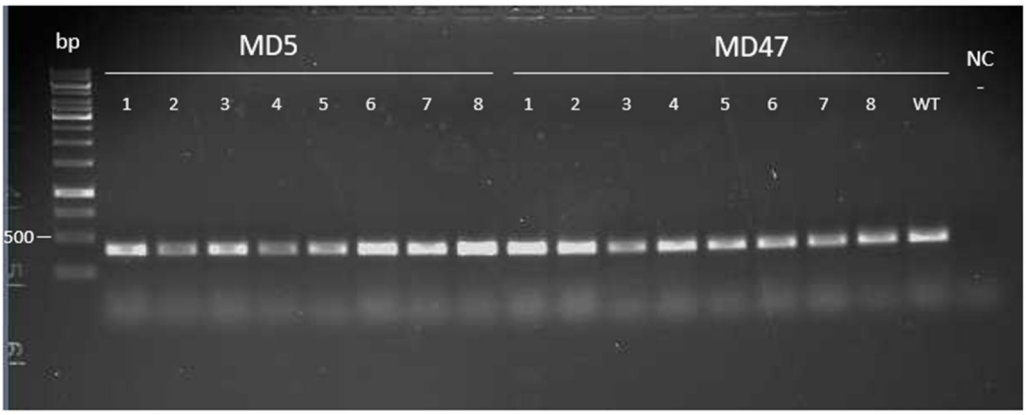


*Figure 26 Screening for correct ampicillin resistant clones (stfR)*

A colony PCR was performed to identify clones with the ampicillin resistance including the promoter at the correct position in the *stfR* gene. The product with an inserted resistance would be at 1114 bp and at 399 bp for the wild type. For MD5 and MD47 each 8 clones were tested, and all of them showed the wild type gene. As a negative control, the wild type of MD47 was done as well. The ladder is 1 KB Generuler and 66 % of the PCR product are loaded. For the negative control (NC–) dd$H_2O$ was used.

To test the insertion of the ampicillin resistance into the *hsdR* gene the same approach as in the *stfR* gene was used at first. The primers were chosen to bind outside the homologous region that was used for the lambda RED recombination (Figure 27). For this, the primers 23 and 24 were used.

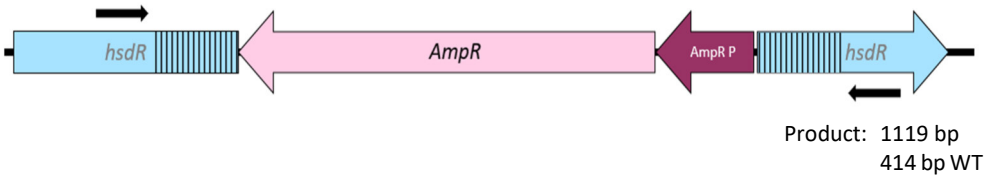


*Figure 27 Primers for ampicillin resistant clone detection in hsdR*

Primers 23 and 24 bind in the *hsdR* gene outside of the homologous region chosen for the recombination. A positive clone yields a band at 1119 bp and the wild type yields a band at 414 bp.

The PCR yields a product of 1119 bp if the ampicillin resistance is correctly inserted into the target gene and a product of 414 bp if *hsdR* is present in its wild type form. The strains MD6, MD56, and MD74 were the ones with *hsdR* as the target gene. Figure 28 shows that eight clones of each strain were tested via colony PCR. All clones show the wild type gene at 414 bp. As a control, a wild type colony of MD74 was amplified as well. There is only a slight band at the correct size which might have been due to an application error on the agarose gel.

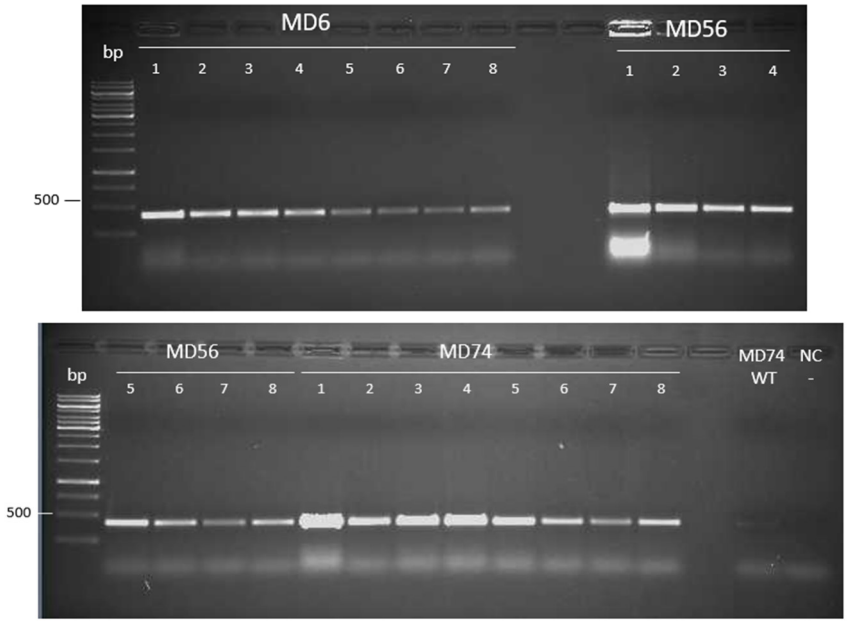


*Figure 28 Screening for correct ampicillin resistant clones (hsdR)*

A colony PCR was performed to identify clones with the ampicillin resistance including the promoter at the correct position in the *hsdR* gene. The product with an inserted resistance would be at 1119 bp and at 414 bp for wild type. For MD6, MD56 and MD74 each 8 clones were tested, and all of them showed the wild type gene. As a negative control, the wild type of MD74 was done as well. It showed a very light band. The ladder is 1 KB Generuler and 100 % of the PCR product are loaded. For the negative control (NC–) dd$H_2O$ was used.

Since there were concerns that the PCR product of a positive clone might be too large a different approach was developed. For this strategy, one primer was binding in the *hsdR* gene outside of the homologous region used for the recombination again, but the other primer was binding in the ampicillin resistance gene (Figure 29). This results in a much smaller product however there is no control to see if the PCR worked or not. For this reaction, the primers 20 and 23 were used.

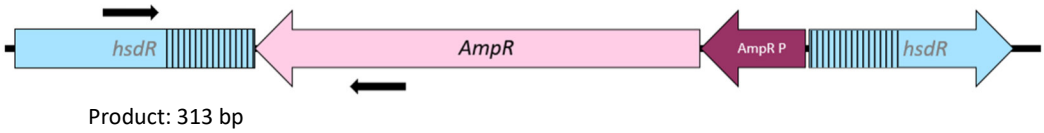


*Figure 29 Alternative primers for ampicillin resistant clone detection in hsdR*

Primer 23 binds in the *hsdR* gene outside of the homologous region chosen for the recombination and primer 20 binds in the ampicillin resistance gene. A positive clone yields a band at 313 bp and the wild type yields no product.

If a clone carries the correctly inserted ampicillin resistance in the *hsdR* gene the PCR results in a product of 313 bp. If the wild type gene is present, there will be no band at all. Once again, recombination with the strains MD6, MD56, and MD74 was performed, and eight colonies of

each strain were tested via colony PCR. All tested clones showed no band which means the ampicillin resistance was not inserted at the correct location (Figure 30). As a control, a wild type colony of MD74 was tested via PCR as well and as expected it did not yield any product.

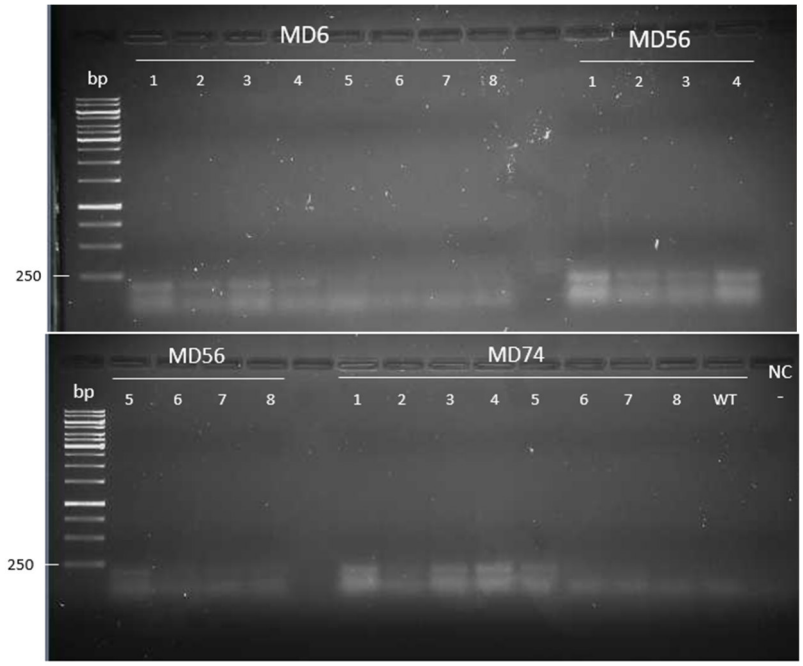


*Figure 30 Alternative screening for correct ampicillin resistant clones (hsdR)*

A colony PCR was performed to identify clones with the ampicillin resistance including the promoter at the correct position in the *hsdR* gene. The product with an inserted resistance would be at 313 bp for wild type. For MD6, MD56, and MD74 each 8 clones were tested, all of them showed no band which indicates the wild type gene. As a negative control, the wild type of MD74 was done as well. The ladder is 1 KB Generuler and 100 % of the PCR product are loaded. For the negative control (NC–) dd$H_2O$ was used.

It was not possible to obtain any correct ampicillin-resistant clones using this cloning strategy. But since colonies were growing on LB ampicillin agar plates the recombination must have occurred somewhere. There is a high possibility that the recombination occurred on the plasmid since the original pKD46 plasmid was carrying an ampicillin resistance. We did not remove the sequence for that resistance but rather just did a restriction cut in the middle of the gene and inserted the tetracycline resistance there which means the sequence for the ampicillin resistance is still present. The linear fragment that also carries the ampicillin resistance, therefore, could recombine with the two homologous ampicillin regions that were flanking the tetracycline resistance cassette. Since the sequence for the beta-lactamase gene consists of 860 bp it is a longer sequence with more homology and therefore most likely has a higher probability to recombine than the 50 bp homologous regions that are flanking it.

An alternative strategy to create a pKD46 plasmid carrying a tetracycline resistance is therefore needed. One option to obtain said plasmid is Gibson Assembly [91]. For this, the section of the vector plasmid pKD46 without the ampicillin resistance would be amplified using primers with a distinct overhang sequence. The insert fragment must be amplified with primers providing the same overhangs. Then different enzymes in the same buffer connect the vector and insert to form a finished plasmid. An exonuclease leaves single-stranded 3' overhangs that enable the annealing of the components that have complementary overhangs. A polymerase repairs the gaps left in the annealed region and a DNA ligase eliminated nicks in the connected DNA strands. This method would avoid the presence of residues of the *bla* gene and eliminate the potential risk of homologous recombination of the ampicillin resistance.

## Tilimycin induced phage release influences growth in *E. coli*

*K. oxytoca* AHC6 wild type (Tox+) and a toxin-deficient mutation (Tox-) were cultured and the supernatants were harvested. The supernatants were used to treat MD strains that carry phage lambda (MD6, MD56, MD74). The MD strains are *E. coli* MG1655 Δ*fliC* Δ*ompF* that were additionally modified by De Paepe *et al* [15]. The three strains that were tested all carried phage λ and had genetic variations, which are a *lamB* deletion for MD56 and a *lamb* deletion plus λ $cI^{ind-}$ mutation for MD74.

The MD6 cells were incubated with the supernatants described above as well as 85 µM tilimycin. As a negative control LB medium was used. The growth curves for both supernatants are almost identical and there is no difference between toxin-carrying and non-toxin-carrying treatment. In general, those growth curves differ from the negative control which is fresh LB because the supernatants were harvested from the *K. oxytoca* cultures, which already metabolized a big part of the nutrients in the medium. On top of that *K. oxytoca* was cultured in CASO medium, however, LB is the preferred medium to grow *E. coli.* This means that the *E. coli* MD6 cells from this assay must grow under minimal nutrient conditions and therefore the difference in the growth curves can be explained. The 85 µM tilimycin treatment at first showed a similar curve to the negative control with LB but after four hours at an OD600 of 1.2 the curve starts to flatten and the remaining four hours the OD600 only increases minimally compared to the other growth curves (Figure 31).

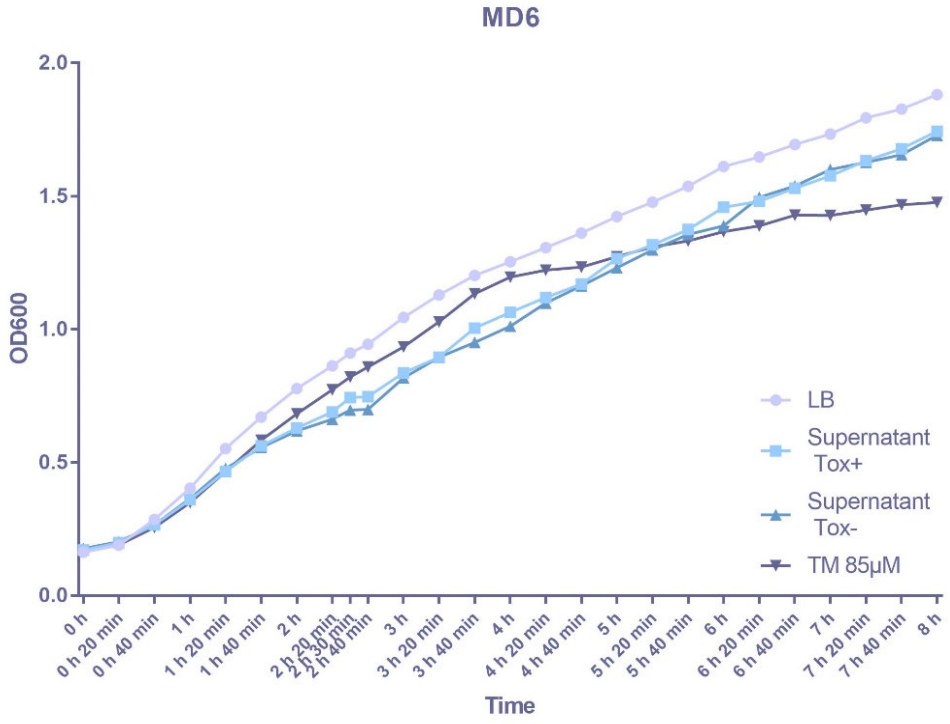


*Figure 31 Tilimycin reduces growth in MD6*

*E. coli* MD6 cells were treated with toxin and non-toxin containing supernatants from *K. oxytoca* cultures. In addition, an 85 µM treatment and a negative control with LB were done. The tilimycin treatment showed a flattened growth rate after 4 hours. The supernatant rates differed from the negative control because of the lack of nutrients compared to fresh LB medium. (n=2)

MD56 has a *lamB* deletion and is otherwise genetically identical to MD6. The phage receptor *lamB* deletion prevents free phage from infecting the cells and has a higher relevancy for the susceptible strain MD47. Using the strains with the *lamB* deletion in an assay enables a determination of how much free phage derives from spontaneous induction in lysogenic bacteria as opposed to phage deriving from reproduction in susceptible bacteria without the genetic modification. The OD600 measurements of MD56 show similar results to MD6. The cells that received the supernatants grew similarly regardless of the toxin presence and yet again they don't grow as well as the LB control because of the reduced nutrients. The cells that were treated with tilimycin showed the same pattern as before. After four hours at an OD600 of about 1.2, the growth curve flattened for the remainder of the eight hours (Figure 32).

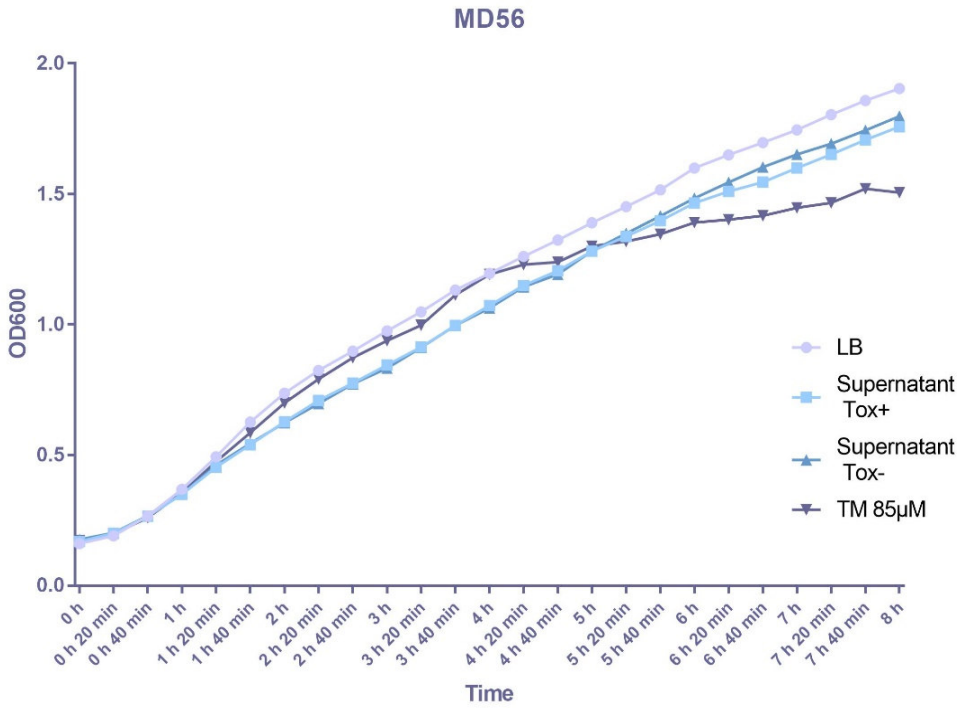


*Figure 32 Tilimycin reduces growth in MD56*

*E. coli* MD56 cells were treated with toxin and non-toxin-containing supernatants from *K. oxytoca* cultures. In addition, an 85 µM treatment and a negative control with LB were done. The tilimycin treatment showed a flattened growth rate after 4 hours. The supernatant rates differed from the negative control because of the lack of nutrients compared to fresh LB medium. (n=2)

MD74 is different compared to the previous two strains because it doesn't carry a wild type phage λ but a non-inducible phage. This means the phage λ has $cI^{ind-}$ mutation. A phage release in this strain can only occur randomly and spontaneously and cannot be induced. The supernatant-treated cells again have a slightly flatter growing curve than the LB control due to the nutrient-deficient medium. However, the tilimycin treated cells behave differently than in the other strains. The growth curve does not show the distinct flattening after four hours like in MD5 and MD56. The TM treated cells' growth curve starts differentiating from the LB control at around 5 hours to a flatter curve (Figure 33). This shows that a concentration of 85 µM TM does influence the growth of *E. coli* cells.

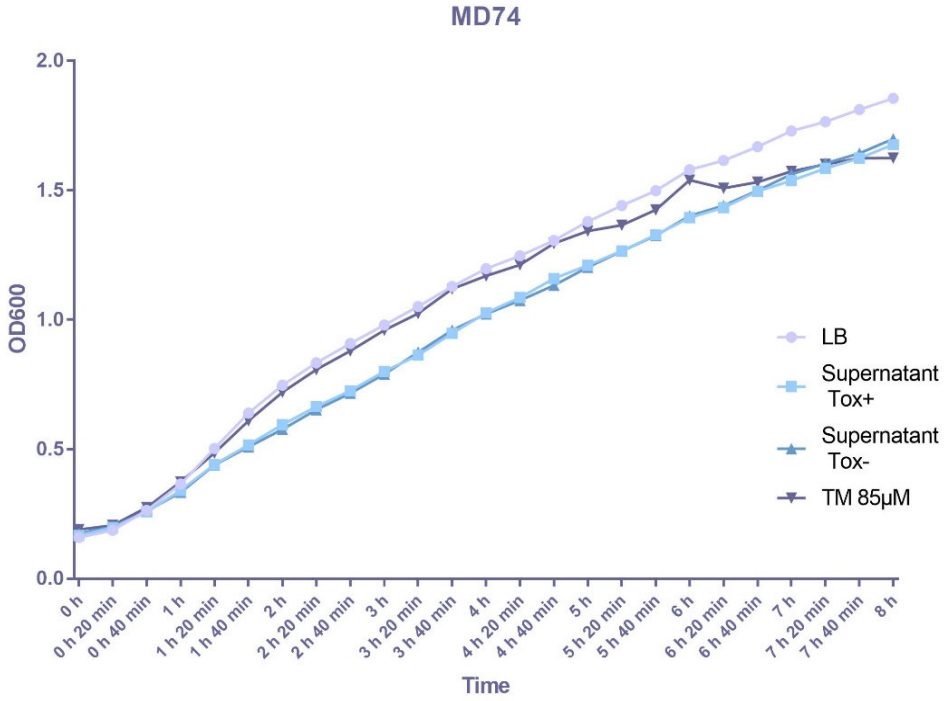


*Figure 33 Tilimycin reduces growth in MD74*

*E. coli* MD74 cells were treated with toxin and non-toxin-containing supernatants from *K. oxytoca* cultures. In addition, an 85 µM treatment and a negative control with LB were done. The tilimycin treatment showed a flattened growth rate after 5 hours. The supernatant rates differed from the negative control because of the lack of nutrients compared to fresh LB medium. (n=2)

Since the control strain MD74 carrying a non-inducible λ strain shows a different growth curve than the strains carrying wild type λ there is a possibility that TM did not only act bacteriocidic but also triggered prophage induction which resulted in phage release and therefore a flattened growth curve. To visualize the differences in the growth curves the three strains' 85 µM TM-treated growth curves were combined in one graph (Figure 34). The two strains carrying the wild type phage λ have a virtually identical curve and the MD74 strain carrying a non-inducible strain has a distinctly steeper growth curve and a higher OD600 after 8 hours of growth. To determine the amount of free phage released to the medium a phage assay was performed.

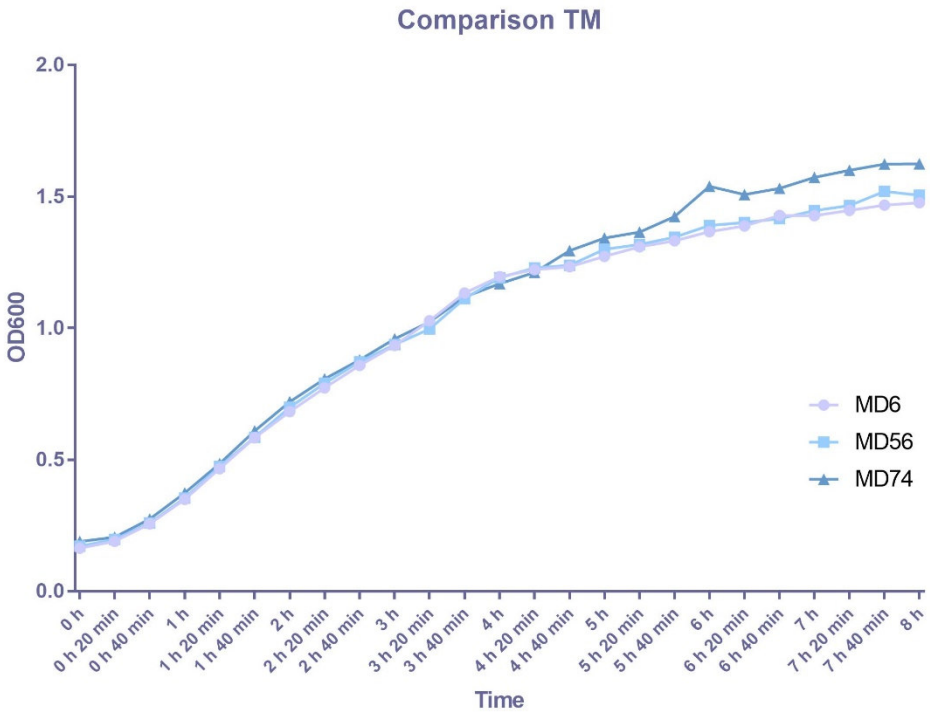


*Figure 34 Tilimycin has less impact on MD74 carrying non-inducible phage*

The growth curves of MD6, MD56, and MD74 are compared in one graph. The curves of MD6 and MD56, which carry a wild type phage, are flatter compared to MD74 which has a non-inducible phage λ.

To gain further insight into the state of the cells after the incubation time of 8 hours, the cells would have to be viewed under a microscope to determine whether a morphology change of the cells could have interfered with the OD600 measurements. The cells should also be plated after or at different points within the incubation time to gain insight into the viability of the cells.

The reason why the supernatants were used initially was to determine if a reaction that occurred with pure 85 µM tilimycin could be recreated with the supernatant of a toxin-producing *K. oxytoca* strain to mimic this encounter in a co-cultivation or later in the murine gut. So, an important step is to measure the tilimycin concentration in the supernatants to determine whether there really is no impact on the cells at the concentration of the supernatant or whether TM cannot be detected in the supernatant. Since tilimycin adheres to plastic surfaces, it is important to minimize the use of plastic in the preparation of the supernatants. For the centrifugation step however, plastic 50 ml Greiner tubes had to be used.

Since *K. oxytoca* cells, in general, don't pellet easily the cells were centrifuged longer to receive fewer residual cells in the supernatant. There is a possibility that this centrifugation step was too long and a great amount of the tilimycin in the supernatant adhered to the plastic wall of the Greiner tube. In that case, the experiment would have to be repeated with fresh supernatants to see the actual reaction of the cells to the toxin-positive supernatant.

## Tilimycin treated cells suggest higher phage count

To determine whether the growth curves of the MD strains are in relation to the prophage activation, a phage assay was performed. The phage lysates were prepared from the cultures of the growth assay. The lysates were then spotted onto R-Top agar plates that contained the infectible strain MD5. Below the plaque-forming units per ml (PFU/ml) were calculated (Table 10). If the system is functional TM should have an impact on the phage release in MD6 and MD56 because those strains carry the wild type phage λ strain. MD74 however, which carries the non-inducible λ strain should not be impacted as much since only spontaneous prophage induction should appear. The table shows that compared to the negative control treatment, which is LB medium, all strains had a higher PFU/ml for the TM treatment. The supernatants do not show any pattern and the released phage is probably due to cell stress that is caused by the nutrient deficiency. Notably, the power of the values of MD74 does not vary as much as in MD56 for example. Compared to MD6, MD56 has a higher phage release in general, even with the negative control LB medium treatment. These numbers suggest that the system could work with the expected results however the values from the spot assay provide just a vague hint. Another important factor that was not included in this assay is the viable cells per ml. There are differences in growth and most likely cell lysis happening, so to gain reliable information on the TM effect on this system the assay must be repeated, and the data need to be normalized to the viable cells per ml.

**Table 10 Phage count (PFU/ml) from spot-on phage assay,** 5 µl of dilutions of the phage lysate with TMG buffer were spotted onto top agar mixed with infectible strain MD5.

| | MD6 | MD56 | MD74 |
|---|---|---|---|
| LB medium | 0 | $5.5x10^7$ | 0 |
| $Tx^-$ supernatant | $1.0x10^3$ | $2.4x10^7$ | $4.0x10^3$ |
| $Tx^+$ supernatant | $2.1x10^4$ | $8.0x10^6$ | $2.0x10^3$ |
| Tilimycin 85 µM | $6.5x10^4$ | $2.3x10^8$ | $6.0x10^3$ |

To receive more accurate PFU/ml values the assay should be repeated as a common phage assay, where the phage lysate is mixed with the infectible strain and the R-Top agar so that the plaques are distributed throughout the agar plate. Since the supernatant-treated phage lysates showed no distinguishable results, as already mentioned, the TM concentration should be measured to determine whether the concentration is too low to impact the phage release

in the same way the 85 µM TM did or if there is no toxin at all. In any case, the experiment could as well just be repeated with fresh supernatant to see if the results are inconclusive again.

To see whether the TM-caused effects transfer to the murine model the resistance genes must successfully be introduced into the *E. coli* MD strains so that the system can be tested in vivo using similar phage assay methods to this study. *E. coli* and *K. oxytoca* can also be co-cultivated to avoid the supernatant treatment. In another step, the system can be transferred into the murine model to test the reaction of the prophage activity in vivo. For this, the mouse gut will have to be cleared from its natural microbiome using beta-lactam antibiotics, like in previous studies [66]. After that, the mouse gut can be co-colonized with toxin-producing *K. oxytoca* as well as the different *E. coli* MD strains. In that case, *K. oxytoca* of course will be the toxin-producing party and provide the tilimycin. MD6 carries the wild type phage λ and when prophage activation is initiated, the strain will release free phage. One option is to use the stool to produce a phage lysate and do phage assays as previously described. Another possibility is to co-cultivate another strain in the mouse gut which is an infectible or susceptible strain. In combination with MD6, most likely MD5 will be used. Since the strains carry different antibiotic resistances, the murine stool can be suspended and plated. In this case, we gain knowledge on how many bacteria of the donor strain remain that were not subjected to prophage activation but since phage λ also carries a unique antibiotic resistance we can also tell at which percentage the infectible strains were infected. The lamb mutation strains, MD56 and MD47, can be used to determine the difference in how much free phage occurs and how much is derived from multiplication in infectible bacteria. MD74 like previously will act as a negative control, as the phage it carries has a $cI^{ind-}$ mutation, making it non-inducible. As another negative control for this whole system, non-toxin-producing *K. oxytoca* is co-cultivated with the *E. coli* MD strains. This system has been used previously by Kienesberger *et al*. [80] where they showed the mutagenic nature of TM.

## PAI promoter identification in *K. oxytoca*

Toxin-producing *K. oxytoca* contains a gene cluster that has been discovered to be a pathogenicity island. The PAI consists of two operons, the *NRPS* operon that contains the genes *npsA* and *npsB,* and the *aroX* operon that contains five genes including *aroX.* The two operons are connected by a distinct sequence. We hypothesize that the region connecting the two operons contains promoter sequences for *aroX* (PraroX) *and npsA* (PrnpsA) The aim is to test this theory by cloning the promoter region of the PAI of *K. oxytoca* upstream of *gfp* in both orientations and to transform *K. oxytoca* with the finished cloning product (Figure 35). Furthermore, we wanted to see if the activity of the promoter region relied on being in a *K. oxytoca* strain. To gain this knowledge, different strains of *E. coli* were transformed with the vectors pAR181_gfpmut3b_PrnpsA as well as pAR181_gfpmut3b_PraroX.

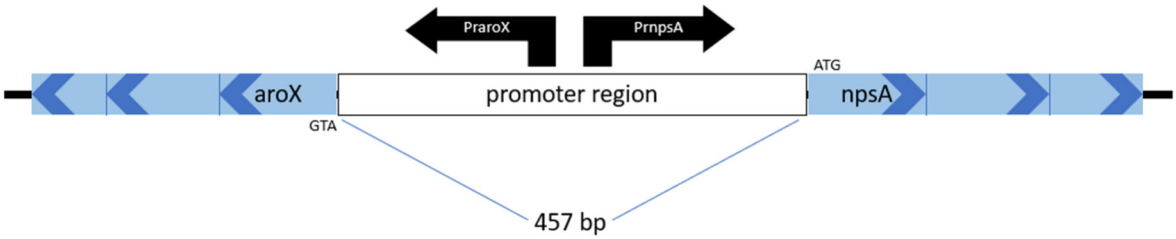


*Figure 35 Promoter region of PAI of K. oxytoca*

The potential promoter region is 457 bp long and is flanked by the *aroX* and *npsA* genes. The promoter region is suspected to contain two promoters one being PraroX, which is facing toward the *aroX* gene, and one being PrnpsA which is facing towards the *npsA* gene.

## Cloning of pAR181_gfpmut3b_PrnpsA & PraroX

For the cloning project, the PAI promoter region of *K. oxytoca* AHC6 was amplified via PCR in both *npsA* and *aroX* directions using primer 1 and 2 and primer 3 and 4 respectively. The primers have overhangs that encode restriction sites for the enzymes SacI and SphI (Figure 36).


*Figure 36 In silico of Amplification of the promoter region of PAI of K. oxytoca*

The primers were designed to bind to the expected promoter region with a restriction enzyme sequence on the overhangs. The two restriction enzymes SphI and SacI were chosen interchangeably so that when ligated with the vector, there would be one plasmid with either orientation of the promoter region.

To ensure a sufficient amount of PCR product four reactions using the two primer sets to amplify the promoter in both orientations were performed. All reactions showed the expected band size of 475 bp (Figure 37). The respective reactions were then pooled and purified. The purification yielded a total amount of 2824 ng of PrnpsA and 2456 ng of PraroX.

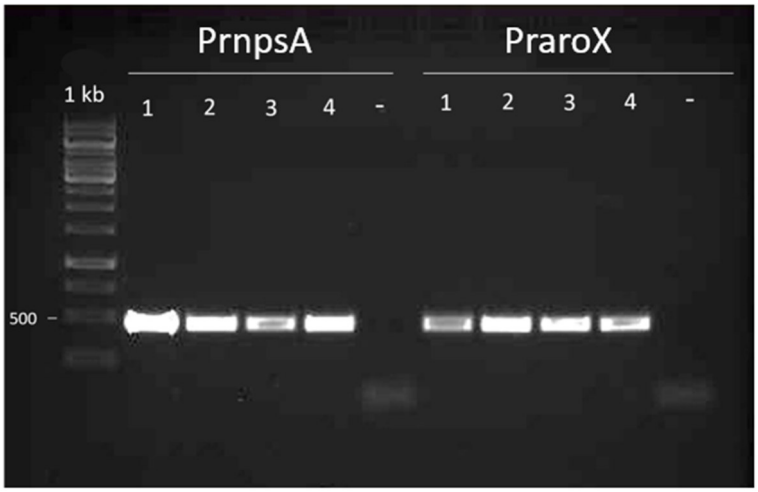


*Figure 37 Amplification of npsA and aroX promoter region*

To generate enough product 4 reactions with each primer set were performed to amplify both orientations of the promoter region. As a template chromosomal *K. oxytoca* DNA was used. The ladder is Generuler 1 kb and 17 % of the PCR reaction was loaded. For the negative control (NC–) dd$H_2O$ was used.

The vector used was pAR181_gfpmut3b which is a pACYC derivate and has a p15A origin and is, therefore, low-copy (10 copies). The resistance marker on the plasmid is chloramphenicol and the restriction enzymes used for the cloning are SacI and SphI. The plasmid carries the promoter of the *rnB* gene, which is a highly transcribed gene, therefore the promoter is strong (Figure 38).

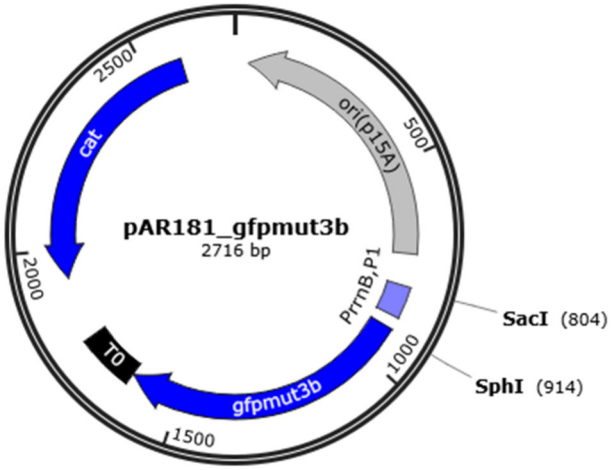


*Figure 38 The vector plasmid pAR181_gfpmut3b*

The vector map shows the two restriction sites, SacI and SphI, that are relevant for the project. The vector has a chloramphenicol resistance and a low copy p15 origin. The wild type promoter on the plasmid is PrrnB which is strong.

The amplified promoter regions as well as the vector pAR181_gfpmut3b, which originally carries the *rnB* promoter upstream of the *gfp* gene, were cut using both enzymes SacI and SphI. In addition, cut controls with only one of the enzymes were made. The controls showed that the enzymes did not cut the entirety of the used DNA but since the bands at the correct size were excised from the gel and purified, it was not necessary to repeat the cuts (Figure 39). After purification, there were 328 ng of vector DNA, 608 ng of PrnpsA, and 608 ng of PraroX.


*Figure 39 Restriction digest of pAR181_gfpmut3b, PrnpsA and PraroX with SacI and SphI*

There are two restriction reactions with both SacI and SphI for the vector as well as the two promoter orientation inserts. In addition, one reaction of each restriction enzyme cutting the vector separately was performed. The bands show that the enzymes did not cut the vector entirely. The uncut vector was added to the gel as well. The bands were excised at the correct sizes and purified which yielded 328 ng of vector DNA, 608 ng DNA of PrnpsA, and 608 ng of PraroX.

The vector was dephosphorylated and subsequently ligated with the purified inserts. After that, a transformation of *E. coli* DH5α with the ligation products was conducted. In addition, a positive control with the original form of the vector (PrrnB) and a negative control with water were performed. To confirm the position of the insert at the correct site a colony PCR using primers 5 and 6 of various clones was performed, including controls with the original vector that shows a smaller band than the finished cloning product and a negative control with water (Figure 40). Since the first 11 tested colonies with the insert PraroX didn't yield a positive clone, more colonies were tested. So finally, the clones PrnpsA 2 and 6 and PraroX 14 and 16 were sequenced using primer 5 and 6 as well and they showed 100 % homology to the template DNA. This means that the plasmids containing PrnpsA 2 equals PrnpsA 6 and both will be referred to only as pAR181_gfpmut3b_PrnpsA and the plasmids containing PraroX 14 equals PraroX16 and both will be referred to only as pAR181_gfpmut3b_PraroX.

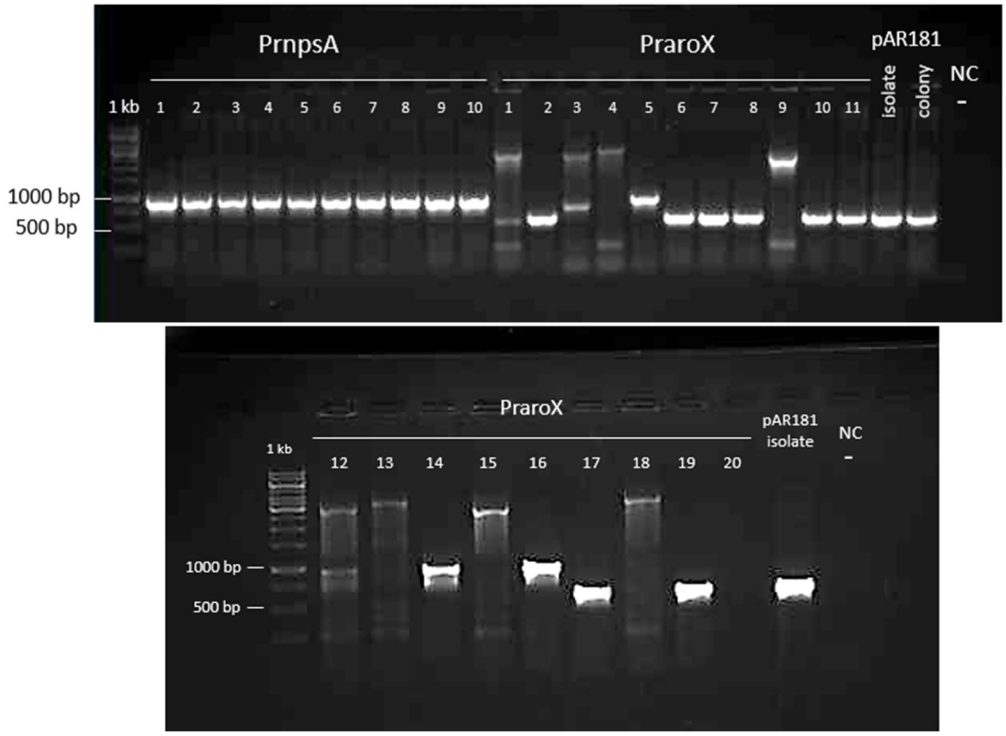


*Figure 40 Identification of positive clones that carry the insert*

To detect a clone carrying the correct product, 10 PrnpsA clones and 19 PraroX clones were screened. PrnpsA 2 and 6 and PraroX 14 and 16 were identified as potentially correct clones. As a control to show the wild type band size, the same PCR was performed with wild type pAR181_gfpmut3b from both a colony and an isolate. The ladder is Generuler 1 kb and 67 % of the PCR reaction were loaded. For the negative control (NC–) $ddH_2O$ was used.

Figure 41 shows the order of genetic elements on the original vector as well as the finished cloning product with the promoter regions in either direction upstream of the *gfpmut3b* gene.

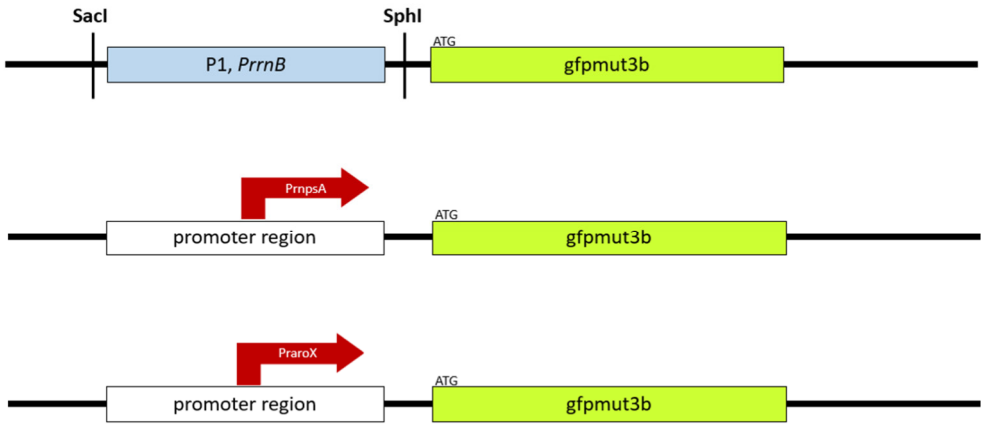


*Figure 41 Finished cloning product compared to original vector*

The original *rnB* promoter upstream of the *gfpmut3b* gene is replaced by the promoter region in *npsA* orientation and *aroX* orientation. This way GFP acts as a reporter of the respective promoter activity.

The finished plasmids were used to transform different strains to study the behavior of the promoter regions in various hosts and determine whether the claimed promoter region indeed shows promoter activity.

## PAI Sequence shows Fluorescence signal in *E. coli* DH5α

Since *E. coli* DH5α is a strain that is commonly used for cloning, the cloning products, which were generated with that strain, were first tested in DH5α. The constructed plasmids pAR181_gfpmut3b_PrnpsA and pAR181_gfpmut3b_PraroX as well as pAR181_gfpmut3b (PrrnB) as a GFP positive control and pBAD33 as a negative control, as it carries a chloramphenicol resistance, were compared in a GFP assay. Since we did not know how strong the promoter activity will be and how long the assay must run to obtain fluorescence signals, the measurements were done for 160 minutes at first. If the PAI sequence contains promoter sequences, the assay will show fluorescence signals.

The growth curves indicate that after 160 minutes the cells carrying the promoter plasmids have a slight disadvantage compared to the glow control and the negative control, which is pBAD33 in this case (Figure 42). The fluorescence data only shows signals for the glow control (PrrnB) at first glance but after removing the glow control from the graph very low signals for both promoter orientations as well as the negative control become visible. Initially, the promoter plasmids seem to show a higher fluorescence signal than the negative control however after 160 minutes all three treatments show the same intensity. To identify whether the plasmids containing the PAI sequence glow or if it is just a background signal like in the wild type the fluorescence signal must be traced for a longer timeframe. Even though the assay was only measuring for less than 3 hours, the OD600 data suggests that the growth of the cells containing the pAR181 plasmid may be inhibited. Previous results within the Zechner group with similar results showed to be successful by switching to a different host strain for the promoter plasmid measurements. Since earlier similar experiments showed signals in *E. coli* MG1655 but not in DH5α, MG1655 was chosen as the next host to test the promoter activity via GFP assay. In addition to changing the host strain, the time of the assay was adjusted to a running time of 8 h 40 min. In addition, pACYC184 was chosen as a new negative control, to use a similar plasmid to pAR181_gfpmut3b. Since pAR181 is a pACYC derivate pACYC184 was used. To test whether the hypothesis that if the PAI sequence contains promoter sequences, it will result in fluorescence signals, proves true further assays must be performed.

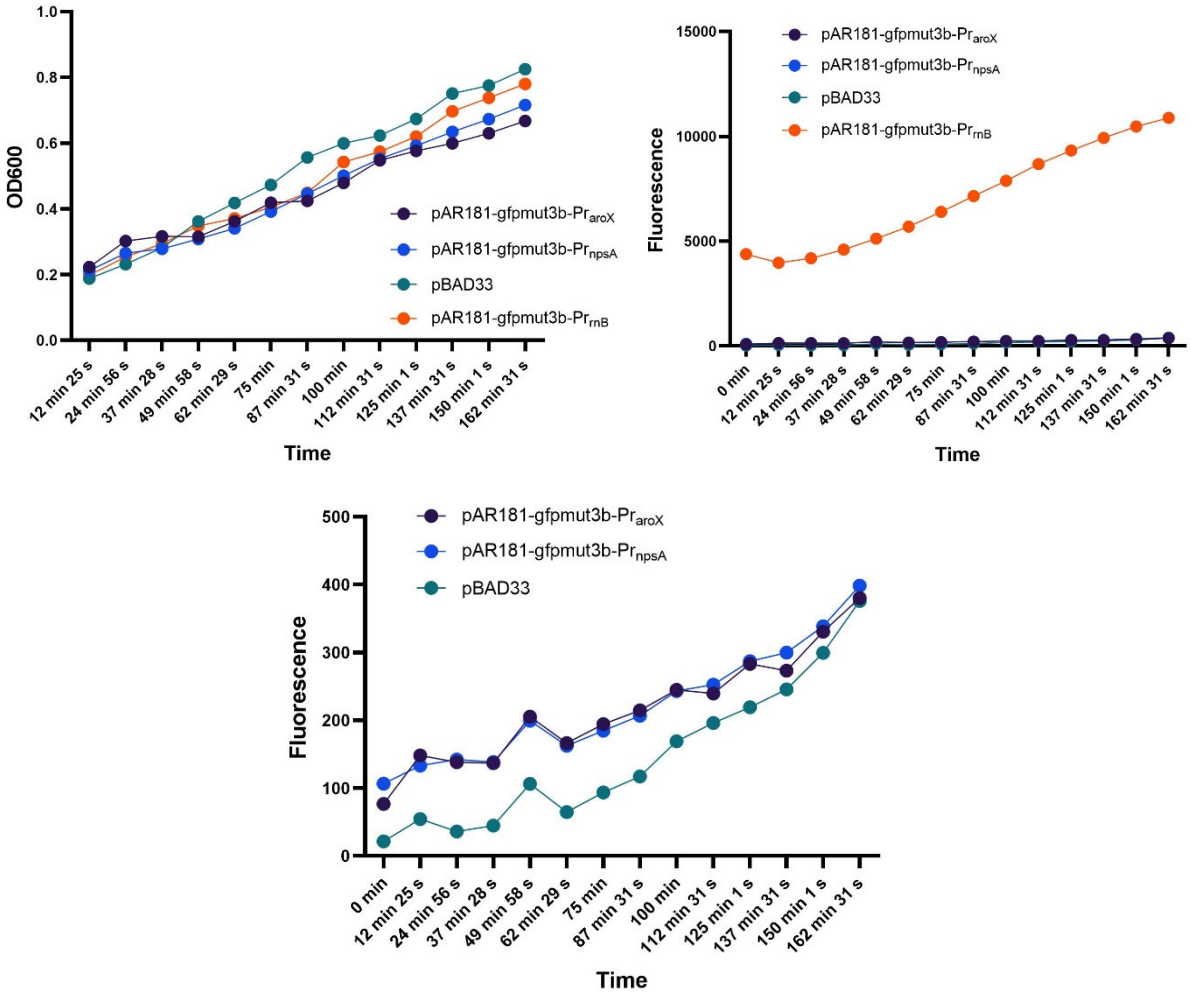


*Figure 42 Fluorescence signal in DH5 alpha*

The pAR181_gfpmut3b plasmids in the variation of PraroX, PrnpsA, and PrrnB (positive control) were compared in *E. coli* DH5α. As a negative control, the strain carrying pBAD33 was used, since it carries a chloramphenicol resistance like the other plasmids. The OD600 data shows that the cells containing the promoter plasmids have a slight disadvantage in growth. The positive control glows at a much higher rate than the other plasmids. After removing the glow control the data shows that after the first 130 min of the assay the promoter plasmids seem to have a higher fluorescence signal than the negative control, however after 160 min they have the same fluorescence intensity. (n=4)

## PAI Sequence shows Fluorescence signal in *E. coli* MG1655

*E. coli* MG1655 cells were transformed with the constructed plasmids pAR181_gfpmut3b_PrnpsA and pAR181_gfpmut3b_PraroX as well as pAR181_gfpmut3b (PrrnB) as a GFP positive control and pACYC184 as a negative control, as it forms the backbone of pAR181 and has a chloramphenicol resistance. If the PAI sequence contains a promoter sequence, the assay will show fluorescence signals.

The OD600 shows a disadvantage in growth for the strain carrying the positive control (Figure 43). The negative control grows at the same growth rate as the cells carrying the promoter plasmid with the PrnpsA orientation. The PraroX version of the plasmid has a slight growth advantage. The fluorescence levels of the positive control are out of proportion high compared to the other strains. Even though GFP is not toxic to the cell, the extreme production of the protein might cause the cells to slow down on growth because many of the cell's resources go towards building GFP. This would explain the reduced growth compared to the other strains. If the fluorescence values of the positive control are removed from the chart, the plasmids containing both promoter orientations show a higher signal than the negative control which does not carry any *gfp* gene at all. There is no noticeable difference in signal intensity between the two promoter orientations after 8 hours. In general, this proves that there is promoter activity in this DNA sequence of the PAI and that it can be active outside of *Klebsiella spp.* So, there is most likely no essential factor that needs to induce the promoter activity that is specific to *K. oxytoca*. One thing that can be observed is that the promoter has a very low signal which is implying low activity, meaning it is a weak promoter. This makes sense because it is connected to the toxin-producing operon, which does not need to be always transcribed in high frequencies, especially compared to the positive control, the *rnB* gene, which is a ribosomal gene that encodes components of the ribosome. The promoter of this gene is highly active, especially in the exponential stage of cell growth. If toxins would be produced at this rate, the producing bacteria would probably be damaged by their own pollutants especially since tilimycin has genotoxic properties, which might affect the producing bacteria's own DNA. The data from this assay clearly shows fluorescence signals for both orientations of the PAI region which means the hypothesis that the sequence contains a promoter sequence could be confirmed.

The next step for this study was to test the plasmids containing the PAI sequence in its strain of origin, *K. oxytoca.* We wanted to see if there would receive different signals from the GFP assay compared to the measurements with *E. coli* as a host.

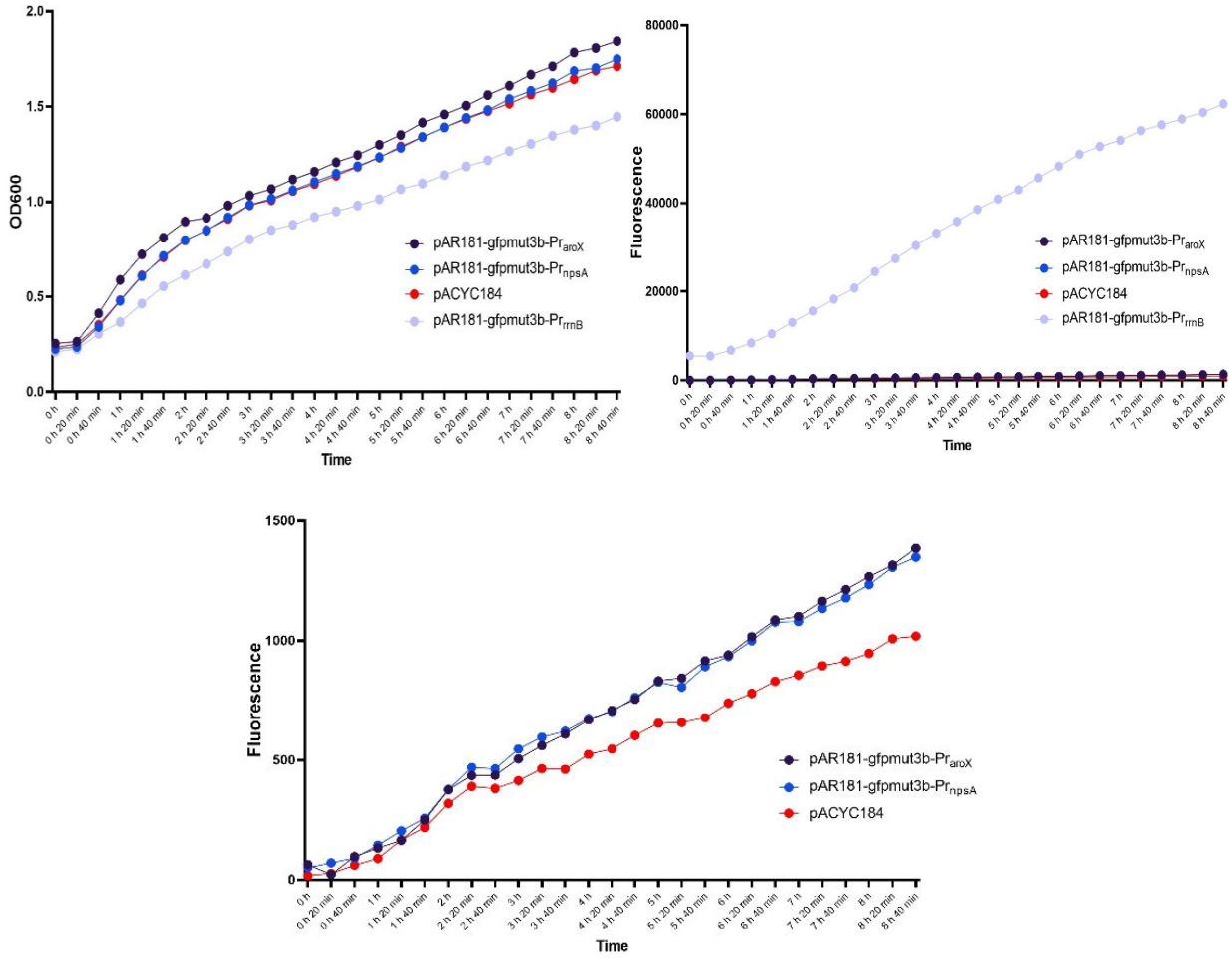


*Figure 43 Fluorescence activity in E. coli MG1655*

The pAR181_gfpmut3b plasmids in the variation of PraroX, PrnpsA, and PrrnB (positive control) were compared in *E. coli* MG1655. As a negative control, cells carrying pACYC184 were used. The OD600 shows that the cells containing the negative control grow at the same rate as the plasmid with PrnpsA orientation. The PraroX shows slight advantages in growth and the positive control grows at a slower rate. The fluorescence signal for the positive control is extensively high compared to the promoter plasmids and the negative control. After removing the positive control, the data shows that the promoter plasmids in both orientations result in a fluorescence signal that is distinguishable from the negative control. Both orientations show the same intensity of the signal. (n=2)

## Glucose does not increase Fluorescence Signal in *Klebsiella oxytoca* AHC6

After testing the promoter plasmids in *E. coli*, *K. oxytoca* AHC6 was transformed. Once again, the plasmids with the promoter in *npsA* and *aroX* directions upstream of *gfp* as well as PrrnB as a positive control and pACYC184 as a negative control were used. Since previous internal studies suggested that glucose might induce toxin production, an assay comparing glucose-treated cells to untreated cells was performed. It can be hypothesized that if glucose is present, it will result in a higher fluorescence signal.

The OD600 results show that the glucose does not affect the growth of the cells overall, however, the cells containing the negative control plasmid (pACYC184) showed reduced growth for both with and without glucose compared to the cells containing the remaining plasmids (Figure 44). This might be due to the differences of the negative control plasmid pACYC184 compared to pAR181_gfpmut3b. The promoter plasmids and the negative controls all grow at a similar rate regardless of the treatment. The fluorescence data shows that the positive control glows at the same rate and is not influenced by the glucose treatment. Removing the glow control from the graph reveals that the glucose treatment does not have any effect on the fluorescence signal emitted from the cells, as treated and untreated cells behave similarly. We can assume that glucose in the used concentration (0.25 g/L) does not enhance the promoter activity of the PAI promoters.

In general, the fluorescence data showed activity for both promoter orientations, however, the ParoX gave a higher signal than PnpsA. This would mean that ParoX is a slightly stronger promoter than PnpsA. This is different compared to the data in *E. coli* where, after the same amount of time, both promoter orientations showed the same signal. However, just like in *E. coli*, the overall signals are very low compared to the positive control PrrnB. This means that even in *K. oxytoca* the promoters are weak which is probably due to their origin as PAI promoters. Since tilimycin has DNA-damaging properties, the cells will most likely try to keep the toxin concentration at a minimum to avoid damaging their own DNA. Upon further review of the records, a calculation error was discovered and 0.25 g/L instead of the intended 2.5 g/L was used. This means that to determine the influence of glucose on the promoter region of the PAI of *K. oxytoca* this assay will have to be repeated with the planned concentration of glucose. This experiment could not prove the hypothesis that if glucose is present, it will result in higher fluorescence levels, but this only applies to a concentration of 0.25 g/L.

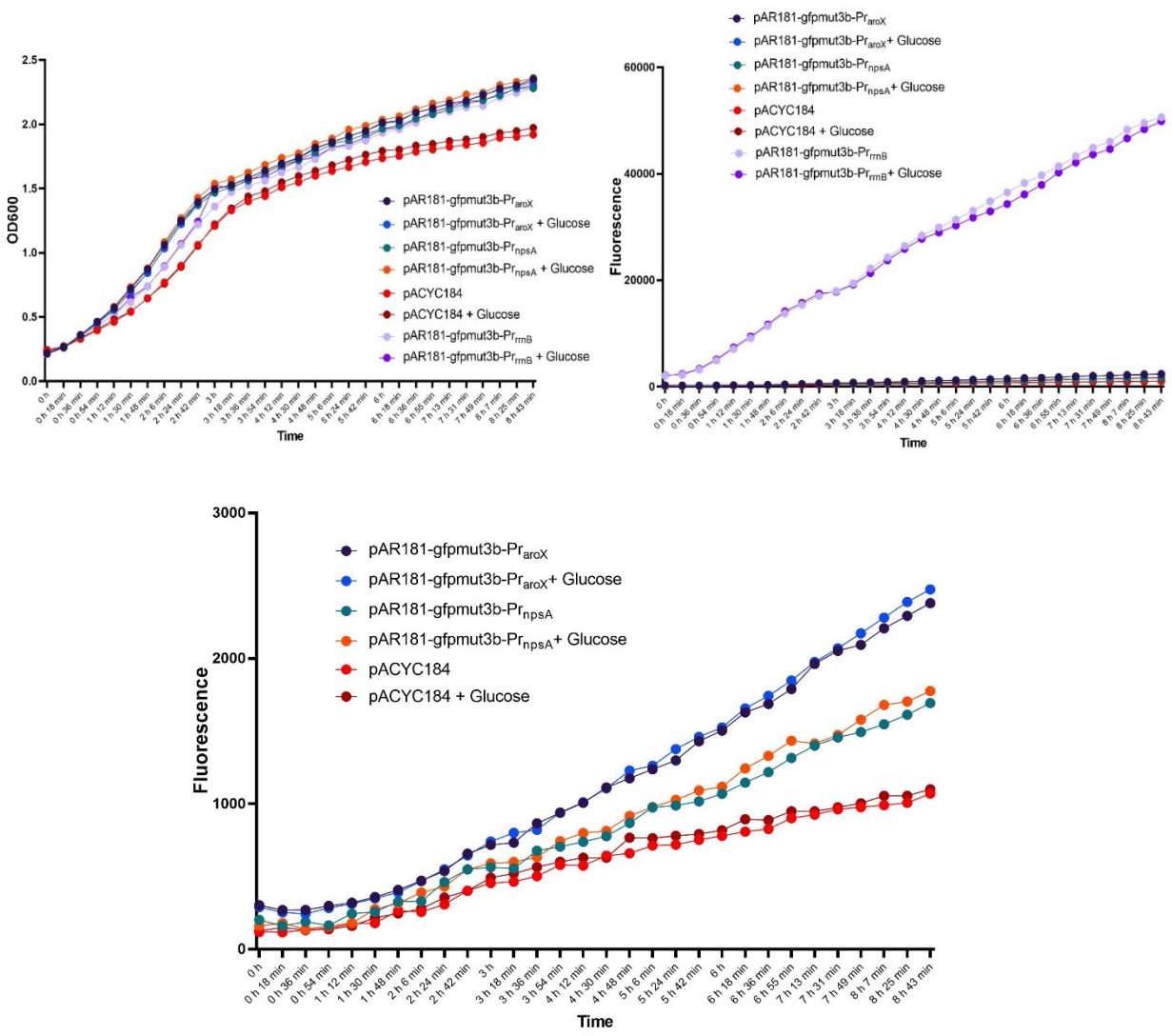


*Figure 44 Glucose (0,25 g/L) does not influence fluorescence signal in AHC6*

The pAR181_gfpmut3b plasmids in the variation of PraroX, PrnpsA, and PrrnB (positive control) were compared in *K. oxytoca* AHC6 with and without glucose present. As a negative control, cells carrying pACYC184 were used. The OD600 data suggests that glucose does not influence the growth of cells. However, the negative control shows reduced growth regardless of glucose treatment compared to the other curves. Fluorescence is not influenced by glucose and all treatments show the same signals with and without glucose. The plasmid containing the *aroX* orientation of the promoter region shows a higher fluorescence signal than the *npsA* orientation. (n=2)

## Tilivalline does not Influence Fluorescence Signal

Since *K. oxytoca* produces tilimycin which then spontaneously reacts to tilivalline in the presence of indole, we questioned whether the aromatic compound that causes an autofluorescence of tilivalline can interfere with the measured data of the GFP assay. We hypothesize that if tilivalline is present, it will result in a higher fluorescence signal.

To clarify whether the presence of TV has any influence on the data, a *K. oxytoca* AHC6 strain with a *tnaA* deletion was used. This gene encodes a tryptophanase that catalyzes the reaction of $H_2O$ and L-tryptophan to indole, $NH_4^+$, and pyruvate. The strain with the *tnaA* deletion cannot produce indole which means TM cannot react to TV spontaneously and therefore an autofluorescence caused by TV will not interfere with the GFP measurements. Once again both AHC6 wild type and *ΔtnaA* strain were transformed with the pAR181 plasmids with both promoter orientations, the pAR181_gfpmut3b plasmid with *rnB* promoter as a positive control and pACYC184 as a negative control.

The OD600 values show that AHC6 wild type negative control grows at a lower rate compared to the other strain and plasmid pairings (Figure 45). The *ΔtnaA* negative control, however, seems to grow at the same rate or even a slightly higher rate as the strains containing the promoter and positive control plasmids. The fluorescence signals for the positive control do not vary with the different strains. After removing the positive control, the fluorescence data shows that both wild type and *ΔtnaA* strains containing the promoter plasmids emit the same signal. This means that the absence of indole and TV does not show a difference in fluorescence signal intensity. As previously observed the presence of pAR181_gfpmut3b_PraroX results in higher fluorescence levels in the cells than pAR181_gfpmut3b_PrnpsA. The *ΔtnaA* negative control shows a higher fluorescence signal than the wild type containing the same plasmid. The reason for this might be that the OD600 of the *ΔtnaA* strain was higher than the wild type. The additional material and higher cell density may result in higher fluorescence values. The performed assay did not confirm the hypothesis that the presence of tilivalline results in higher fluorescence levels because the signal values were equally high with and without TV.

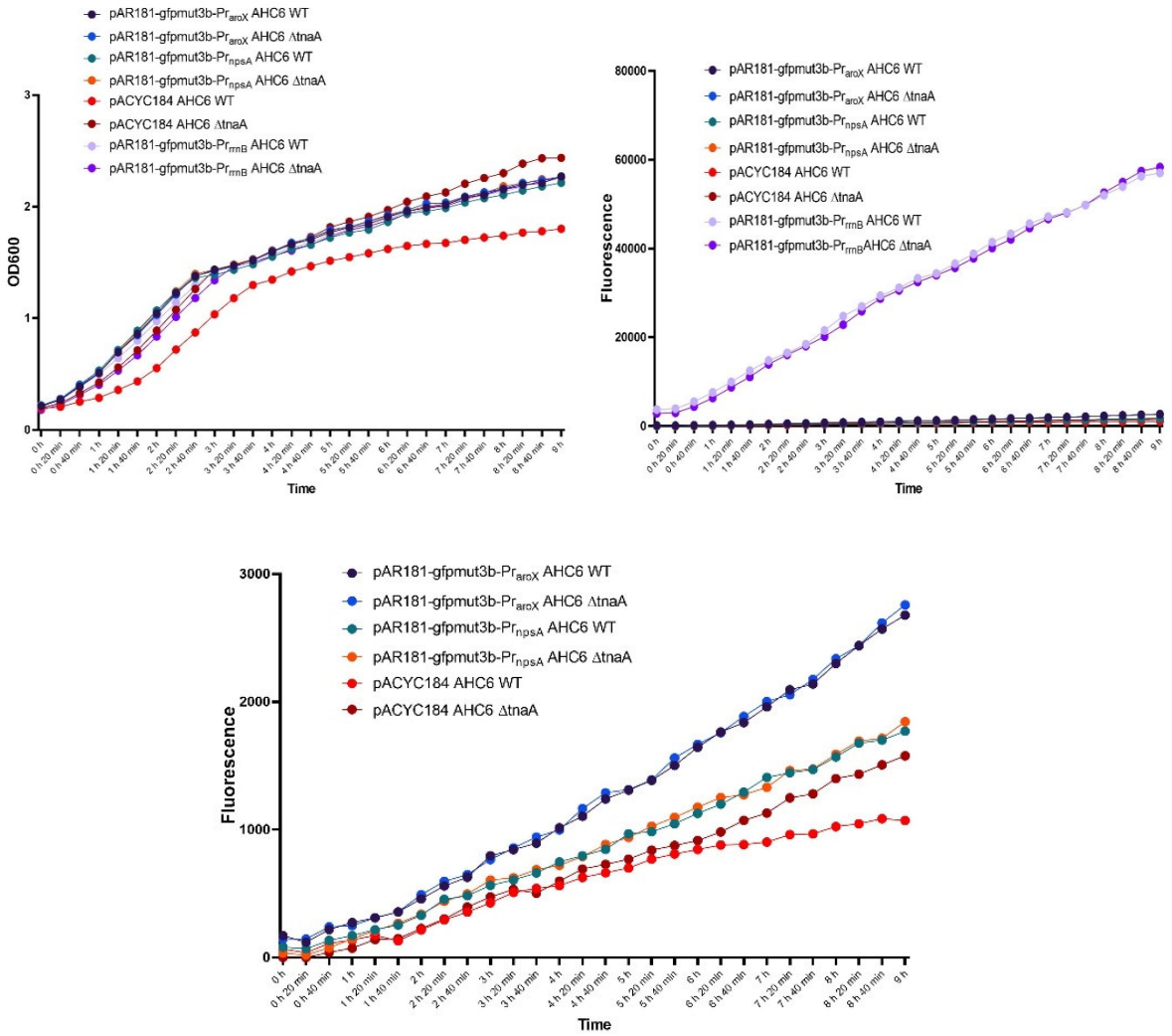


*Figure 45 Fluorescence signals in K. oxytoca AHC6 wild type do not differ from signals in AHC6 ΔtnaA*

The pAR181_gfpmut3b plasmids in the variation of PraroX, PrnpsA, and PrrnB (positive control) were compared in *K. oxytoca* AHC6 wild type and a *tnaA* deletion. As a negative control, cells carrying pACYC184 were used. The OD600 data shows that all strain and plasmid combinations grow at a similar rate, except AHC6 wild type carrying pACYC184, which shows reduced growth. The fluorescence signals for the positive controls in both strains show the same levels of fluorescence. The promoter plasmids in *aroX* and *npsA* orientations show identical fluorescence signals in both strains but differ from each other. The negative control has higher fluorescence levels in the *ΔtnaA* strain which might be due to the higher cell density in the *ΔtnaA* strain. Again, the PraroX plasmid shows higher fluorescence levels than the PrnpsA plasmid which means that the *aroX* promoter has a higher promoter activity. (n=2)

## Longer incubation time shows higher fluorescence signal

The values of fluorescence measurements were always relatively low, and the design of the assay had limitations in the form of culture volume. To receive different insights, we planned to measure the fluorescence levels of a greater culture volume (5 ml) after a longer period of time. For this, media was inoculated with *K. oxytoca* AHC6 strains containing pAR181 with PraroX and PrnpsA as well as the positive control (PrrnB) and pACYC184 as a negative control. After 20 hours 1 ml of the cultures was used for a measurement in the omega plate reader (Figure 46). The OD600 measurements show that, like previously, the negative control grew at a slightly lower rate. The graph including the positive control shows a very high fluorescence signal for pAR181 just like before. However, the fluorescence signals for the promoter plasmids can be seen. For a better visual of the fluorescence data, the positive control was removed. The fluorescence values show that the strains with the promoter plasmids are glowing as they showed higher signals than the negative control pACYC184. As previous data already suggested the *aroX* promoter orientation shows a higher glow than the *npsA* orientation. The PraroX signal is almost three times as high as the negative control and the PrnpsA signal is almost twice as high as the negative control signal. This means that the *aroX* promoter shows a higher level of activity compared to the *npsA* promoter. To gain further knowledge about the viability of the bacterial cultures, the suspensions can be plated and observed under a microscope. To receive further information on the growth of the bacteria and fluorescence signal and therefore promoter activity over a 20-hour time frame, a new assay must be designed. Since the omega plate reader is limited to small-volume cultures, the assay needs a different approach. One possibility would be growing the plasmids in *K. oxytoca* AHC6 in 50 ml of CASO and manually taking 1 ml of the culture every other hour and measuring it in the omega plate reader to be able to create a graph with extended data.

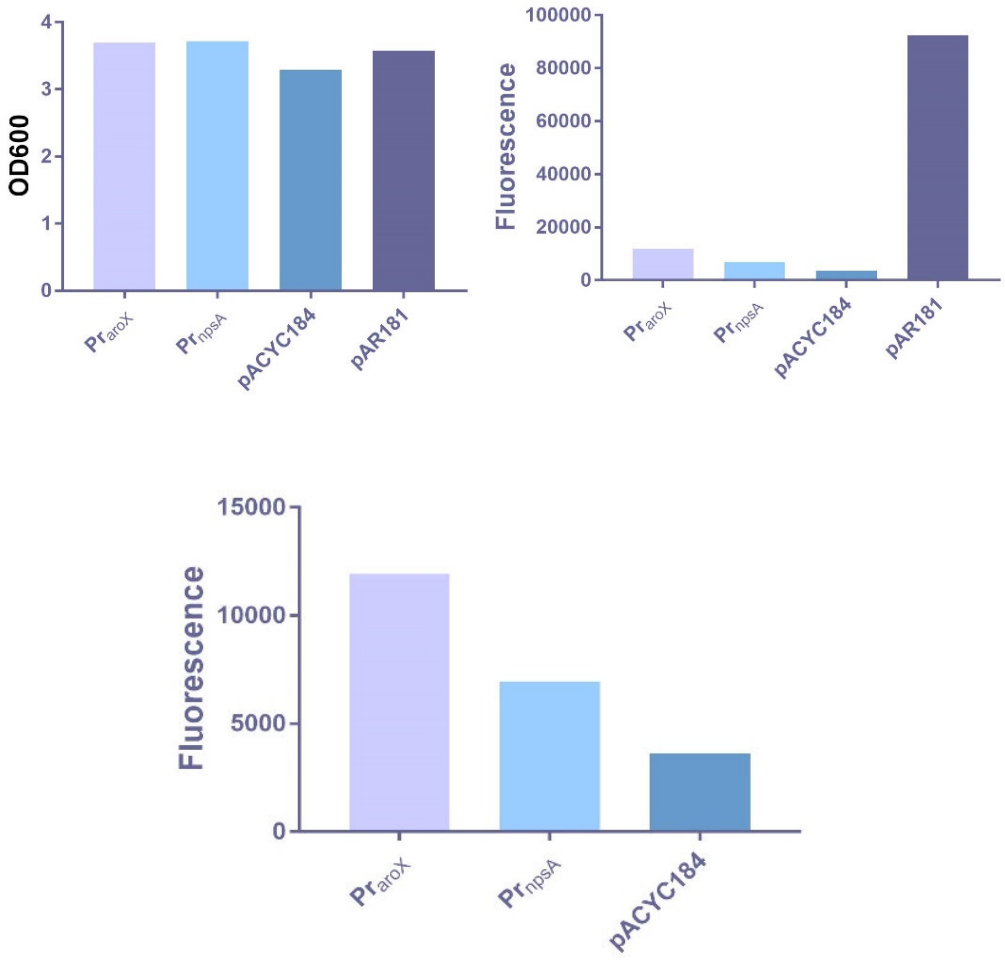


*Figure 46 Increased Fluorescence signals after 20 hrs*

The pAR181_gfpmut3b plasmids in the variation of PraroX, PrnpsA, and PrrnB (positive control) were compared in *K. oxytoca* AHC6 after 20 hours of incubation. As a negative control, the strain carrying pACYC184 was used. The OD600 data shows that the negative control grew slightly less compared to the cells carrying the other plasmid variations. The fluorescence levels for the positive control were high but the signals of the promoter plasmids can be seen. The positive control data was removed to display the promoter plasmids' data better. Compared to the negative control the fluorescence signal of the plasmid carrying PraroX was three times as high as the negative control and the signal of PrnpsA was twice as high as the negative control's signal. (n=2)

With these experiments, we gained insight into the activity of the PAI sequence connecting the *aroX* and the *npsA* gene. The identified region on the operon appears to have promoter activity and contains two promoters, one in *aroX* orientation and one in *npsA* orientation. To gain further information on under which conditions the promoter is on and how long it is active or rather when it is turned off again, other systems, for example, a luciferase reporter system, must be used. A luciferase reporter system can provide information on when the promoter is turned off again since the luciferase enzyme is unstable and therefore can only be detected when the promoter is on, as opposed to GFP which is stable and accumulates in the cells even if the promoter is not active anymore. Knowledge on when and under which conditions the promoter is off and therefore when the toxin production is off, can be used for future therapeutic approaches in patients with AAHC.

The promoter shows different intensities of activity in *E. coli* strains compared to *K. oxytoca.* Both promoter orientations show an identical fluorescence signal in *E. coli* MG1655 but a vastly higher signal for *aroX* orientation in *K. oxytoca* AHC6. This leads to the assumption that *K. oxytoca* has some properties that regulate the PAI promoter and therefore the toxin production. Further research should focus on identifying said factors. In this study we expected glucose to have an enhancing effect on the promoter, however, the assays with the used concentration did not show an increased signal. Repeating the assay with different glucose concentrations might influence the fluorescence signal intensity caused by the promoters.

The gene cluster that is relevant for the biosynthesis of enterotoxins is not unique to *K. oxytoca* but also appears in other closely related species like *Klebsiella pasteurii*, *Klebsiella michiganensis,* and *Klebsiella grimontii.* Standard identification methods can not differentiate between these species, and they are usually combined and referred to as the *K. oxytoca* species complex [92]. For this study, the PAI of *K. oxytoca* AHC6 only was examined. For further research, the gene clusters of other toxin-producing *Klebsiellae* should be studied to see if they show similar results and if the promoter regions in these strains exhibit the same activity or if the promoter strength varies from strain to strain.

The knowledge about the promoter region of the PAI of *K. oxytoca* is essential since it could provide information in future studies on how which substances inhibit and which substances enhance the transcription of the toxin-relevant genes *aroX* and *npsA* in *K. oxytoca.* Since 70 % of healthy infants are colonized with *K. oxytoca* that act as pathobionts that can produce toxins and therefore can be an enormous threat [92]. Having knowledge on how to influence toxin production via the promoters could change the amount of cytotoxins that babies must face by simply adding or removing certain factors from the diet. Studies have shown that the toxin tilimycin is genotoxic and generates stem cell mutations in the colon, which further encourages keeping the doses in affected individuals to a minimum [93].

# Conclusion

This study consisted of two separate projects. One aim of this study was, to establish a system to observe the impact of the genotoxic tilimycin on prophage induction in vitro as well as in vivo in the mouse model. To obtain this *E. coli* MD strains carrying phage λ, strains without λ (infectible cells), and a strain with a non-inducible phage (negative control) were used [15]. The strains needed to have an ampicillin resistance introduced so that they can be co-cultivated with the ampicillin-resistant *K. oxytoca* in the mouse model later. The strategy included introducing the resistance via λ RED recombination into the strains. Since all the λ RED recombination plasmids had resistances that were unsuitable for this project, we decided to generate a tetracycline-resistant pKD46. The vector for this project was pKD46 and the insert was a tetracycline cassette consisting of *tetA* and *tetR.* PvuI was the used restriction enzyme for this cloning. Upon initial issues with the ligation process of this cloning project, the ligation reaction was checked for the correct product via PCR, and after the transformation, the finished product could be detected.

Since only one restriction enzyme was used the cassette could be inserted in either direction and therefore it was crucial to do two sets of PCRs with primers for each orientation of the cassette. The generated pKD46-tet was used to perform the λ RED recombination with an ampicillin resistance with homologous ends. However correct clones could not be obtained, even though things like template plasmid contaminations were considered and eliminated. Alternative strategies to integrate the ampicillin resistance were discussed. Since there were ampicillin-resistant colonies after the recombination but the resistance could not be detected at the correct position, the resistance must have recombined somewhere else.

We suspected that the pKD46-tet plasmid was the problem. The ampicillin resistance on pKD46 was cut by PvuI and the tetracycline resistance cassette was added to interrupt the *bla* gene. This means that the entire sequence of the ampicillin resistance still is on the plasmid, however, it is split by the Tet cassette. The insert used for this cloning is the ampicillin resistance. The plasmid pKD46 is a low-copy plasmid, however, there is only one chromosome in the bacterial cell. This means that the ampicillin resistance is more likely to recombine with one of the plasmids than the desired gene on the chromosome. Another factor to potentially promote the integration into the plasmid is that the ampicillin resistance is split into two parts by the *tet* cassette, one being 444 bp and one being 417 bp. The overhang that was designed for the recombination of the ampicillin resistance into the genome only consists of 50 bp, so the recombination with a 400 bp homology is probably favored.

To combat this issue starting with a new cloning strategy is probably the best solution. The easiest option to eliminate the possibility of integration into the plasmid is generating a new pKD46-tet plasmid via Gibson Assembly [91]. With this method, the part of the vector that is needed, without the ampicillin resistance, is amplified as well as the tetracycline insert. Both

need to have primers with complementary overhangs. The two elements then get ligated according to the manual and a pKD46-plasmid without *bla* residues is generated.

The mentioned *E. coli* MD strains could not be made ampicillin resistant, but they were still tested in assays for which the ampicillin resistance was not necessary. The MD strains carrying the phages (MD6, MD56, MD74) were analyzed for their OD600 with different treatments. The treatments included supernatants from cultures of wild type *K. oxytoca* AHC6 (toxin-producing) and a toxin-deficient mutation, as well as 85 µM tilimycin and LB medium. The assays showed that the supernatant treatments produced identical results and that the TM treatment resulted in reduced growth, especially in the two strains carrying inducible phage strains. MD74 carrying the non-inducible strain showed a less reduced growth curve for the TM treatment, which might be due to fewer phages being activated and destroying their host cells. To determine the viability of the bacteria, they must be plated after the assay and viewed under the microscope.

It is unclear whether the toxin-positive supernatant did not imitate the results generated by TM 85 µM because the toxin concentrations were too low or because there was no toxin in the treatment at all. To determine this, the supernatant TM concentrations must be measured. One possibility is that during the preparation process, the toxin-positive supernatant had too much contact with plastic, to which TM attaches, resulting in a reduced concentration. The growth curves of the supernatant-treated cells were slightly reduced compared to the LB medium negative control, which was probably due to a reduced nutrient supply because it was used by *K. oxytoca* when it was growing in the medium, which was later used to prepare the supernatant. As an alternative to the supernatant treatment, the MD strains can be co-cultivated with toxin-producing and non-producing *K. oxytoca* AHC6 strains in vitro.

To determine whether the TM-treated cells released more phage, phage lysates were harvested and prepared from the OD600 assay cultures. To get an overview only spot-on phage assays with MD5 as the infected strain were performed and the results suggested that the TM treatment resulted in a higher PFU/ml value. To get a clearer PFU/ml value the assay should be repeated but instead of spotting the lysate onto the R-TOP agar, it should be mixed in with the R-TOP agar and the infectible strain. The results we got from this study suggested that TM at the used concentration might result in prophage activation however, in negative controls other factors like lack of nutrients caused prophage activation as well. To definitively identify TM as a prophage activating agent the experiments must be repeated and further experiments have to be performed.

The second aim of this study was to determine whether the region between the AROX operon and the NPRS operon on the PAI of *K. oxytoca* has promoter activity. To achieve this the potential promoter region was cloned upstream of *gfp.* In assays comparing the promoter

plasmids to a positive and a negative control, we tried to see whether the region caused a fluorescence signal, which would mean that the region contains an active promoter. After performing the assays with different strains carrying the plasmids, we concluded that since the promoter plasmids resulted in a fluorescence signal, the region is, in fact, a promoter sequence. However, the promoter regions showed differently strong signals in *E. coli* compared to *K. oxytoca.*

While the two orientations produced an identical level of fluorescence signal in *E. coli*, the *aroX* orientation showed a higher signal than the *npsA* orientation in *K. oxytoca.* This might be due to regulation factors that interfere with the promoter in its strain of origin but are not present in other strains like *E. coli.* An important step for future research is identifying the regulation factors so that they can be used as a tool to reduce toxin production in AAHC patients. Another interesting experiment would be to transform other *Klebsiella spp.* strains with the plasmids carrying the *K. oxytoca* promoters to see whether the fluorescence signal strength is the same or if there are additional factors or even fewer factors that regulate the expression of the toxin operons via the promoter. Another important study for the future is, as previously mentioned, cloning the promoter region of different toxin-producing *Klebsiella spp.* to determine whether those promoter regions behave the same in assays or if they show different signals.

# References


1 R. W. Hendrix, “Bacteriophage genomics,” *Curr Opin Microbiol,* vol. 6(5), pp. 506-511, 2003, doi:10.1016/j.mib.2003.09.004.

2 P Simmonds and P. Aiewsakun, “Virus classification - where do you draw the line?” *Arch Virol*, vol 163(8), pp. 2037-2046, 2018, doi:10.1007/s00705-018-3938-z.

3 S. M. Doore and B. A. Fane, “The microviridae: Diversity, assembly, and experimental evolution,” *Virology,* vol 491, pp 45-55, 2016, doi:10.1016/j.virol.2016.01.020.

4 H. W. Ackermann, D. Prangishvili, “Prokaryote viruses studied by electron microscopy.” *Arch Virol,* vol 157, pp. 1843–1849, 2012, doi:10.1007/s00705-012-1383-y.

5 G. Lima-Mendez *et al.*, “Prophinder: a computational tool for prophage prediction in prokaryotic genomes,” *Bioinformatics*, vol 24(6), pp 863–865, 2008, doi:10.1093/bioinformatics/btn043.

6 D. E. Fouts, “Phage_Finder: automated identification and classification of prophage regions in complete bacterial genome sequences,” *Nucl. Acids Res*, vol. 34(20), pp. 5839-5851, 2006, doi:10.1093/nar/gkl732.

7 A. M. Nanda, K. Thormann, J. Frunzke, “Impact of Spontaneous Prophage Induction on the Fitness of Bacterial Populations and Host-Microbe Interactions,” *J Bacteriol*, vol. 197(3), pp. 410-419, 2015, doi:10.1128/JB.02230-14.

8 E. F. Boyd, “Bacteriophage-encoded bacterial virulence factors and phage-pathogenicity island interactions,” *Adv Virus Res,* vol. 82, pp. 91-118, 2012, doi:10.1016/B978-0-12-394621-8.00014-5.

9 E. Lederberg, “Lysogenicity in *E. coli* K-12,” Genetics, vol. 36, p. 560, 1951.

10 S. R. Casjens and R.W. Hendrix, “Bacteriophage lambda: Early pioneer and still relevant,” *Virology*, vol.479-480, pp. 310-330, 2015, doi:10.1016/j.virol.2015.02.010.

11 R. W. Hendrix and R. L. Duda, “Bacteriophage lambda PaPa: not the mother of all lambda phages,” *Science,* vol. 258(5085), pp. 1145-1148, 1992, doi:10.1126/science.1439823.

12 A. Mathieu, M. Dion, Deng, L. *et al.* “Virulent coliphages in 1-year-old children fecal samples are fewer, but more infectious than temperate coliphages,” *Nat Commun,* vol. 11(1), 378, 2020, doi:10.1038/s41467-019-14042-z.

13 J. Lossouarn *et al.*, “*Enterococcus faecalis* Countermeasures Defeat a Virulent *Picovirinae* Bacteriophage,” *Viruses,* vol. 11(1), 48, 2019, doi:10.3390/v11010048

14 S. Alexeeva *et al.*, “Spontaneously induced prophages are abundant in a naturally evolved bacterial starter culture and deliver competitive advantage to the host,” *BMC Microbiol*, vol. 18(1), 120, 2018, doi:10.1186/s12866-018-1229-1.

15 M. De Paepe *et al.*, “Carriage of λ Latent Virus Is Costly for Its Bacterial Host due to Frequent Reactivation in Monoxenic Mouse Intestine,” *PLoS Genet*, vol. 12(2), e. 1005861, 2016, doi:10.1371/journal.pgen.1005861.

16 A. G. Clooney *et al.*, “Whole-Virome analysis Sheds Light on Viral Dark Matter in Inflammatory Bowel Disease,” *Cell Host Microbe*, vol. 26(6), pp. 764-778, 2019, doi:10.1016/j.chom.2019.10.009.

17 L. J. V. Piddock and R. Wise, “Induction of the SOS response in *Escherichia coli* by 4-quinolone antimicrobial agents,” *FEMS Microbiology Letters*, vol. 41(3), pp. 289–294, 1987, doi:10.1111/j.1574-6968.1987.tb02213.x

18 F. S. Gimble and R. T. Sauer, “λ Repressor mutants that are better substrates for RecA-mediated cleavage,” *J Mol Biol.*, vol. 206(1), pp. 29-39, 1989, doi:10.1016/0022-2836(89)90521-4.

19 J. E. Silpe *et al.*, “The bacterial toxin colibactin triggers prophage induction,” *Nature*, vol. 603, pp. 315–320, 2022, doi:10.1038/s41586-022-04444-3.

20 J. P. Nougayrède, S. Homburg, F. Taieb, “*Escherichia coli* induces DNA double-strand breaks in eukaryotic cells,” *Science*, vol. 313(5788), pp. 848-85, 2006, doi:10.1126/science.1127059.

21 E. Tacconelli, E. Carrara, A. Savoldi *et al.*, “Discovery, research, and development of new antibiotics: the WHO priority list of antibiotic resistant bacteria and tuberculosis,” *Lancet Infect Dis,* vol. 18(3), pp. 318-327, 2018, doi:10.1016/S1473-3099(17)30753-3.

22 “Review on Antimicrobial Resistance,” commissioned by UK Prime Minister, 2016, https://amr-review.org/

23 B. Burrowes *et al.*, “Bacteriophage therapy: potential uses in the control of antibiotic-resistant pathogens,” *Expert Rev Anti Infect Ther*, vol. 9(9), pp. 775-785, 2011, doi:10.1586/eri.11.90.

24 W. H. Manwaring, “Deleterious Effects of ‘Bacterophage’ Therapy,” *Cal West Med*, vol. 43(3), p. 182, 1935.

25 C. L. Pasricha and A. J. H. deMonte, “Bact. Alkalescens in Infection of the Urinary Tract and Bacteriophage Therapy,” *Ind Med Gaz,* vol. 76(7), pp. 414-416, 1941.

26 K. E. Kortright *et al.,* “Phage Therapy: A Renewed Approach to Combat Antibiotic-Resistant Bacteria,” *Cell Host Microbe*, vol. 25(2), pp. 219-232, 2019, doi:10.1016/j.chom.2019.01.014.

27 Y. Choi *et. al*., "Identification and characterization of a novel flagellum-dependent Salmonella-infecting bacteriophage, iEPS5," *Appl Environ Microbiol,* vol. 79(16), pp. 4829-4837, 2013, doi:10.1128/AEM.00706-13.

28 H. Furukawa and S. Mizushima, "Roles of cell surface components of *Escherichia coli* K-12 in bacteriophage T4 infection: interaction of tail core with phospholipids," *J Bacteriol,* vol. 150(2), pp. 916-924, 1982, doi:10.1128/jb.150.2.916-924.1982.

29 L. Mindich, J. F. Sinclair, J. Cohen, "The morphogenesis of bacteriophage phi6: particles formed by nonsense mutants," *Virology,* vol. 75(1), pp. 224-231, 1976, doi:10.1016/0042-6822(76)90021-0.

30 B. K. Chan *et al.,* "Phage selection restores antibiotic sensitivity in MDR Pseudomonas aeruginosa," *Sci Rep,* vol. 26(6), 26717, 2016, doi:10.1038/srep26717.

31 H. W. Smith and M. B. Huggins, "Successful treatment of experimental *Escherichia coli* infections in mice using phage: its general superiority over antibiotics," *J Gen Microbiol,* vol. 128(2), pp. 307-318, 1982, doi:10.1099/00221287-128-2-307.

32 H. W. Smith and M. B. Huggins, "Effectiveness of phages in treating experimental *Escherichia coli* diarrhoea in calves, piglets and lambs," *J Gen Microbiol*, vol. 129(8), pp. 2659-2675, 1983, doi:10.1099/00221287-129-8-2659.

33 H. W. Smith, M. B. Huggins, K. M. Shaw, "Factors influencing the survival and multiplication of bacteriophages in calves and in their environment," *J Gen Microbiol,* vol. 133(5), pp. 1127-1135, 1987, doi:10.1099/00221287-133-5-1127.

34 P. Kudrin *et al.,* "Subinhibitory Concentrations of Bacteriostatic Antibiotics Induce *relA*-Dependent and *relA*-Independent Tolerance to β-Lactams," *Antimicrob Agents Chemother,* vol. 61(4), e02173-16, 2017, doi:10.1128/AAC.02173-16.

35 C. M. Theriot and V. B. Young, "Interactions Between the Gastrointestinal Microbiome and *Clostridium difficile*," *Annu Rev Microbiol,* vol. 69, pp. 445-461, 2015, doi:10.1146/annurev-micro-091014-104115.

36 C. Loc-Carrillo and S. T. Abedon, "Pros and cons of phage therapy," *Bacterophage,* vol. 1(2), pp 111-114, 2011, doi:10.4161/bact.1.2.14590.

37 S. E. Luria and M. Delbrück, "Mutations of Bacteria from Virus Sensitivity to Virus Resistance," *Genetics,* vol. 28(6), pp. 491-511, 1943, doi:10.1093/genetics/28.6.491.

38 B. K. Chan *et al.,* "Phage treatment of an aortic graft infected with *Pseudomonas aeruginosa," Evol Med Public Health,* vol. 2018(1), pp 60-66, 2018, doi:10.1093/emph/eoy005.

39 S. E. Darch *et al,* "Phage Inhibit Pathogen Dissemination by Targeting Bacterial Migrants in a Chronic Infection Model," *mBio,* vol. 8(2), e00240-17, 2017, doi:10.1128/mBio.00240-17.

40 D. R. Roach *et al,* "Synergy between the Host Immune System and Bacteriophage Is Essential for Successful Phage Therapy against an Acute Respiratory Pathogen," *Cell Host Microbe,* vol. 22(1), pp. 38-47, 2017, doi:10.1016/j.chom.2017.06.018.

41 M. S. Bedi, V. Verma, S. Chhibber, "Amoxicillin and specific bacteriophage can be used together for eradication of biofilm *Klebsiella pneumoniae* B5055," *World J Microb Biot,* vol. 25, pp. 1145-1151, doi:10.1007/s11274-009-9991-8.

42 P. J. Turnbaugh et al., "The human microbiome project," *Nature,* vol. 449(7164), pp. 804-810, 2007, doi:10.1038/nature06244.

43 J. C. Thonard and H. W. Scherp, "Inhibition of a collagenase by the human gingival microbiota," *J Bacteriol*, vol. 76(4), pp. 355-358, 1958, doi:10.1128/jb.76.4.355-358.1958.

44 P. Lepage *et al.,* "A metagenomic insight into our gut's microbiome," *Gut,* vol. 62(1), pp. 146-158, 2013, doi:10.1136/gutjnl-2011-301805.

45 J. Penders *et al.,* "Factors Influencing the Composition of the Intestinal Microbiota in Early Infancy," *Pediatrics,* vol. 118(2), pp. 511-521, 2006, doi:10.1542/peds.2005-2824.

46 S. Wei *et al*., "Short- and long-term impacts of azithromycin treatment on the gut microbiota in children: A double-blind, randomized, placebo-controlled trial," *EBioMedicine*, vol. 38, pp. 265-272, 2018, doi:10.1016/j.ebiom.2018.11.035.

47 M. A. M. Rogers and D. M. Aronoff, "The influence of non-steroidal anti-inflammatory drugs on the gut microbiome," *Clin Microbiol Infect*, vol. 22(2), 178.e1-178.e9, 2016, doi:10.1016/j.cmi.2015.10.003.

48 D. E. Freedberg *et al.,* "Proton Pump Inhibitors Alter Specific Taxa in the Human Gastrointestinal Microbiome: A Crossover Trial," *Gastroenterology,* vol. 149(4), pp. 883-885, 2015, doi:10.1053/j.gastro.2015.06.043.

49 J. M. Deleemans *et al.,* "The Chemo-Gut Pilot Study: Associations between Gut Microbiota, Gastrointestinal Symptoms, and Psychosocial Health Outcomes in a Cross-Sectional Sample of Young Adult Cancer Survivors," *Curr Oncol,* vol. 29(5), pp. 2973-2994, 2022, doi:10.3390/curroncol29050243

50 J. Qin *et al.*, "A human gut microbial gene catalogue established by metagenomic sequencing," *Nature,* vol. 464(7285), pp. 59-65, 2010, doi:10.1038/nature08821.

51 T.R. Abrahamsson *et al.,* "Low gut microbiota diversity in early infancy precedes asthma at school age," *Clin Exp Allergy*, vol. 44(6), pp. 842-850, 2014, doi:10.1111/cea.12253.

52 A. Trompette *et al.,* "Gut microbiota metabolism of dietary fiber influences allergic airway disease and hematopoiesis," *Nat Med,* vol. 20(2), pp. 159-166, 2014, doi:10.1038/nm.3444.

53 T. G. Dinan and J. F. Cryan, “Gut Feelings on Parkinson’s and Depression,” *Cerebrum,* vol. 2017, pp. 04-17, 2017.

54 C. Kong *et al.,* “Probiotics improve gut microbiota dysbiosis in obese mice fed a high-fat or high-sucrose diet,” *Nutrition,* vol. 60, pp. 175-184, 2019, doi:10.1016/j.nut.2018.10.002.

55 D. Abraham *et al.*, “Exercise and probiotics attenuate the development of Alzheimer's disease in transgenic mice: Role of microbiome,” *Exp Gerontol*, vol. 115, pp. 122-131, 2019, doi:10.1016/j.exger.2018.12.005.

56 K. Matsuoka, “Fecal microbiota transplantation for ulcerative colitis,” *Immunol Med,* vol. 44(1), pp. 30-34, 2021, doi:10.1080/25785826.2020.1792040.

57 M. T. Madigan, “Brock Biology of Microorganisms,” San Francisco: Benjamin Cummings, 13th Edition, xviii 1043, 77 p, 2012

58 R. Podschun and U. Ullmann, “Klebsiella spp. as nosocomial pathogens: epidemiology, taxonomy, typing methods, and pathogenicity factors,” *Clin Microbiol Rev*, vol. 11(4), pp. 589-603, 1998, doi:10.1128/CMR.11.4.589.

59 R. Podschun, I. Penner, U. Ullmann, “Interaction of Klebsiella capsule type 7 with human polymorphonuclear leucocytes,” *Microb Pathog,* vol. 13(5), pp. 371-379, 1992, doi:10.1016/0882-4010(92)90080-8.

60 A. Ghasemian *et al*., “The association of surface adhesin genes and the biofilm formation among *Klebsiella oxytoca* clinical isolates,” *New Microbes New Infect*, vol. 27, pp. 36-39, 2018, doi:10.1016/j.nmni.2018.07.001.

61 D. M. Livermore, “beta-Lactamases in laboratory and clinical resistance,” *Clin Microbiol Rev,* vol. 8(4), pp. 557-584, 1995, doi:10.1128/CMR.8.4.557.

62 J. G. Bartlett, “Antibiotic-associated diarrhea,” *N Engl J Med,* vol 346(5), pp. 334-339, 2002, doi:10.1056/NEJMcp011603.

63 C. Högenauer *et al.*, “Klebsiella oxytoca as a causative organism of antibiotic-associated hemorrhagic colitis,” *N Engl J Med*, vol. 355(23), pp. 2418-2425, 2006, doi:10.1056/NEJMoa054765.

64 M. M. Joainig *et al.*, “Cytotoxic effects of Klebsiella oxytoca strains isolated from patients with antibiotic-associated hemorrhagic colitis or other diseases caused by infections and from healthy subjects,” *J Clin Microbiol*, vol. 48(3), pp. 817-824, 2010, doi:10.1128/JCM.01741-09.

65 G. Schneditz *et al.*, “Enterotoxicity of a nonribosomal peptide causes antibiotic-associated colitis,” *Proc Natl Acad Sci USA,* vol. 111(36), pp. 13181-13186, 2014, doi:10.1073/pnas.1403274111.

66 K. Unterhauser *et al., "Klebsiella oxytoca* enterotoxins tilimycin and tilivalline have distinct host DNA-damaging and microtubule-stabilizing activities," *Proc Natl Acad Sci USA*, vol. 116(9), pp. 3774-3783, 2019, doi:10.1073/pnas.1819154116.

67 E. Dornisch *et al.,* "Biosynthesis of the Enterotoxic Pyrrolobenzodiazepine Natural Product Tilivalline," *Angew Chem Int Ed Engl*, vol. 56(46), pp. 14753-14757, 2017, doi:10.1002/anie.201707737.

68 E. M. Alexander *et al.,* "Biosynthesis, Mechanism of Action and Inhibition of the Enterotoxin Tilimycin Produced by the Opportunistic Pathogen *Klebsiella oxytoca*," *ACS Infect Dis*, vol 6(7), pp. 1976-1997, 2020, doi: 10.1021/acsinfecdis.0c00326

69 I. Zollner-Schwetz *et al.,* "Role of Klebsiella oxytoca in antibiotic-associated diarrhea," *Clin Infect Dis*, vol. 49(9), pp. e74-e78, 2008, doi:10.1086/592074.

70 M. Obladen, "Necrotizing enterocolitis--150 years of fruitless search for the cause.," *Neonatology*, vol. 96(4), pp. 203-210, 2009, doi:10.1159/000215590.

71 S. C. Fitzgibbons *et al.*, "Mortality of necrotizing enterocolitis expressed by birth weight categories," *J Pediatr Surg*, vol. 44(6), pp. 1072-1076, 2009, doi:10.1016/j.jpedsurg.2009.02.013.

72 A. D. Bedrick, "Necrotizing enterocolitis: neurodevelopmental 'risky business'," *J Perinatol*, vol. 24(9), pp. 531-533, 2004, doi:10.1038/sj.jp.7211158.

73 S. R. Hintz *et al.*, "Neurodevelopmental and growth outcomes of extremely low birth weight infants after necrotizing enterocolitis," *Pediatrics*, vol. 115(3), pp. 696-703, 2005, doi:10.1542/peds.2004-0569.

74 C. M. Cotton *et al.,* "Prolonged duration of initial empirical antibiotic treatment is associated with increased rates of necrotizing enterocolitis and death for extremely low birth weight infants," *Pediatrics,* vol. 123(1), pp. 58-66, 2009, doi:10.1542/peds.2007-3423.

75 S. Sullivan *et al., "*An exclusively human milk-based diet is associated with a lower rate of necrotizing enterocolitis than a diet of human milk and bovine milk-based products." *The Journal of pediatrics, vol. 156(4), pp. 562-567, 2010,* doi:10.1016/j.jpeds.2009.10.040.

76 K. Alfaleh, J. Anabrees, T. Al-Kharfi, "Probiotics for prevention of necrotizing enterocolitis in preterm infants," *Cochrane Database Syst Rev*, vol. 3, CD005496, 2011, doi:10.1002/14651858.CD005496.pub3.

77 S. Paveglio *et al.,* "Cytotoxin-producing *Klebsiella oxytoca* in the preterm gut and its association with necrotizing enterocolitis," *Emerg Microbes Infect*, vol. 9(1), pp. 1321-1329, 2020, doi:10.1080/22221751.2020.1773743.

78 J. Jacob *et al.,* "Etiologies of NICU deaths," *Pediatrics,* vol. 135(1), pp. e59-e65, 2015, doi:10.1542/peds.2014-2967.

79 K. M. Hermann and L. M. Weaver, "THE SHIKIMATE PATHWAY," *Annu Rev Plant Physiol Plant Mol Biol,* vol. 50, pp. 473-503, 1999, doi:10.1146/annurev.arplant.50.1.473.

80 S. Kienesberger *et al., "*Enterotoxin tilimycin from gut-resident Klebsiella promotes mutational evolution and antibiotic resistance in mice," *Nat Microbiol*, vol. 7(11), pp. 1834-1848, 2022, doi:10.1038/s41564-022-01260-3.

81 Y. Shao *et al., "*Stunted microbiota and opportunistic pathogen colonization in caesarean-section birth," *Nature*, vol. 574(7776), pp. 117-121, 2019, doi:10.1038/s41586-019-1560-1.

82 National Human Genome Research Institute, "Gene Expression," https://www.genome.gov/genetics-glossary/Gene-Expression.

83 National Human Genome Research Institute, "Gene Regulation," https://www.genome.gov/genetics-glossary/Gene-Regulation

84 F. Jacob, D. Perrin, C. Sanchez, J. Monod, "[Operon: a group of genes with the expression coordinated by an operator]," *Hebd Seances Acad Sci*, vol. 250, pp. 1727-1729, 1960.

85 J. H. Miller *et al.,* "The promoter-operator region of the lac operon of Escherichia coli," *J Mol Biol*, vol. 38(3), pp. 413-420, 1968, doi:10.1016/0022-2836(68)90395-1.

86 Y. Wang *et al.*, "A successful hybrid deep learning model aiming at promoter identification," *BMC Bioinformatics,* vol. 23(1), pp. 206, 2022, doi:10.1186/s12859-022-04735-6.

87 H. Hutter, "Fluorescent Reporter Methods," *Methods Mol Biol,* vol. 351, pp. 155-173, 2006, doi:10.1385/1-59745-151-7:155.

88 G. Miksch *et al.,* "A rapid reporter system using GFP as a reporter protein for identification and screening of synthetic stationary-phase promoters in Escherichia coli," *Appl Microbiol Biotechnol*, vol. 70(2), pp. 229-236, 2006, doi:10.1007/s00253-005-0060-4.

89 A. Cosic *et al.,* "Variation in Accessory Genes Within the *Klebsiella oxytoca* Species Complex Delineates Monophyletic Members and Simplifies Coherent Genotyping," *Front Microbiol,* vol. 12, 692453, 2021, doi:10.3389/fmicb.2021.692453.

90 J. Yao *et al.,* "Genetic Features of blandm-1 and Characterization of the Corresponding Knockout Mutant of Enterobacter cloacae Produced by Red Homologous Recombination," *Jundishapur J Microbiol*, vol. 13(4), 2020, doi:10.5812/jjm.101645.

91 G. Assembly, E. Protocol, and N. E. Biolabs, "Gibson Assembly® Protocol (E5510) V.2," pp. 1–6, 2022.

92 T. M. Greimel *et al., "*Toxin-Producing Klebsiella oxytoca in Healthy Infants: Commensal or Pathobiont?," *J Pediatr Gastroenterol Nutr*, vol. 74(1), e1-e7, 2022, doi:10.1097/MPG.0000000000003299.

93 L. Pöltl *et al.*, "Microbiota-derived genotoxin tilimycin generates colonic stem cell mutations," *Cell Rep*, vol. 42(3), 112199, 2023, doi:10.1016/j.celrep.2023.112199.

# Figures

# Tables